

# Technische Universität München

Lehrstuhl für Bodenkunde

Carbon sequestration and soil organic matter composition affected by altered soil  
aggregate dynamics due to land-use changes

Carsten Werner Müller

Vollständiger Abdruck der von der Fakultät Wissenschaftszentrum Weihenstephan  
für Ernährung, Landwirtschaft und Umwelt der Technischen Universität München zur  
Erlangung des akademischen Grades eines

Doktors der Naturwissenschaften

genehmigten Dissertation.

Vorsitzender: Univ.-Prof. Dr. A. Göttlein

Prüfer der Dissertation:

1. Univ.-Prof. Dr. I. Kögel-Knabner

2. apl. Prof. Dr. H. Papen

(Albert-Ludwigs-Universität Freiburg)

Die Dissertation wurde am 15.04.2009 bei der Technischen Universität München  
eingereicht und durch die Fakultät Wissenschaftszentrum Weihenstephan für  
Ernährung, Landnutzung und Umwelt am 22.07.2009 angenommen.

## Summary

Besides climate, mineralogy and pedogenesis, land-use and management strongly influence the humus level in soils. The large terrestrial carbon (C) pool gains therefore a lot of interest as it is sensitive to changing land-use and associated management regimes. How much organic C is stored in a soil and for how long this C remains in the soil depends on C input, pool sizes and their stability.

In the present work the impact of altered soil aggregation due to land-use change on soil organic matter (SOM) dynamics was studied. The main objectives were to study (i) short term effects on SOM bioavailability due to tillage (physical soil disruption), (ii) the re-development of SOM depth gradients after soil homogenisation (e.g. ploughing) and (iii) the long term effects of changing historic land-use on SOM dynamics. In order to meet these objectives three studies were conducted at different scales. The studies were chosen to span from short term (<20 days) to long term (>50 years) effects of land-use changes. The work also accounted for variable spatial scales ranging from laboratory scale up to field scale. By combining a laboratory experiment, a lysimeter study and a field study it was possible to obtain an understanding for ongoing processes due to land-use changes on SOM dynamics.

By the first experiment, short term effects of aggregate disruption due to land-use were studied on a small scale (laboratory). To imitate and study the influence of aggregate disruption (e. g. due to tillage or freezing-thawing cycles) on SOM bioavailability, incubation experiments were conducted with ultrasonically disrupted bulk soils. Bulk soil material was taken from the Ap horizon of a Leptic Cambisol (eutric) under agricultural use. The obtained material was incubated in triplicate for 18 days at 20°C and constant water content. Additionally it was studied how the prior removal of water extractable OM (WEOM) influences soil organic C (SOC) mineralisation. Before and after the incubation experiments, the quality of salt (10 mM K<sub>2</sub>SO<sub>4</sub>) extractable OM (SEOM) was analyzed by UV-absorbance, solid state <sup>13</sup>C-CPMAS NMR spectroscopy and the analysis of neutral sugars.

Physical disruption had a clear effect on the amount and composition of extractable SEOM and WEOM, which tends to be less accessible in intact soil material. Plant derived sugars were dominating the OM which was additionally released after aggregate disruption. The increase in CO<sub>2</sub> released by heterotrophic respiration due

to aggregate disruption was in the range of +27% and +38% compared to intact soils. An increased mineralisation of the soluble OM parts during these short-term incubation experiments was demonstrated by the higher decomposition degrees of SEOM after incubation. Increased CO<sub>2</sub> release after aggregate disruption under field conditions as due to freezing-thawing cycles or tillage can to some extent be explained by the mineralisation of additional bioavailable labile dissolved OM (DOM) fractions.

The second experiment was conducted to study medium term effects of land-use changes at a medium scale. The development of depth gradients of SOM composition and distribution within 4 years after soil disturbance and homogenization was studied in a lysimeter experiment with juvenile beech trees (*Fagus sylvatica* L.). By this approach it was possible to imitate the ploughing and concomitant planting of trees as it is common for newly established forests. The use of lysimeters with homogenised soil in eight replicates enabled an experiment unbiased by field scale heterogeneities. Four months before the final harvest of the lysimeters, <sup>15</sup>N labelled beech litter was applied on top of the soils to study the fate of nitrogen (N) on a short term. The sampling scheme applied to the given dense soil layers (0–2 cm, 2–5 cm, 5–10 cm and 10–20 cm) was crucial to study the subtle reformation of SOM properties with depth in the artificially filled lysimeters. Due to the combination of physical SOM fractionation with the application of <sup>15</sup>N-labelled beech litter and <sup>13</sup>C-CPMAS NMR spectroscopy a detailed view was obtained on vertical differentiation of SOM properties.

Four years after soil disturbance a significant decrease of the mass of particulate OM (POM) could be found from the 0–2 cm to the 10–20 cm layer. A clear depth distribution was also shown for C and N stored within the SOM fractions related to bulk soil. The mineral fractions <63 μm clearly dominated C storage (between 47% (0–2 cm) to 60% (5–10 cm) of bulk soil C) and N storage (between 68% (0–2 cm) to 86% (5–10 cm) of bulk soil N). A drastic increase in aliphatic C structures concomitant to decreasing O/N-alkyl C was detected with depth. The increase in aliphaticity was also demonstrated from free POM (fPOM) to occluded POM (oPOM). Only a slight depth gradient was observed for natural <sup>13</sup>C abundance in SOM fractions. A clear vertical incorporation of <sup>15</sup>N from the applied labelled beech litter into POM fractions was found, probably resulting from faunal and fungal incorporation. A significant reformation process of a SOM depth profile was clearly

achieved within a very short time after soil homogenisation. A clear incorporation of  $^{15}\text{N}$  (4.01‰ vs. air) by fungal hyphae and rhizomorphs (*Xerocomus*) down to 60 cm showed the importance of fungi for the vertical incorporation of litter derived OM into soils. One important finding of this study is that especially in soils with reforming SOM depth gradients after land-use changes selective sampling of whole soil horizons can bias predictions of C and N dynamics as it overlooks a potential development of gradients of SOM properties on smaller scales. Furthermore, the results implicate a heterogeneous vertical C sequestration achieved by different C amounts of SOM fractions in ploughed topsoil.

The third experiment was conducted at field scale and included land-use changes which were older than 50 years. Historic alterations in land-use from forest to grassland and cropland to forest were used to determine impacts on C stocks and distribution and SOM characteristics in Haplic Cambisols. A continuous Norway spruce (*Picea abies* L. Karst.) forest (F-F), a former cropland afforested in 1930 (C-F) and a grassland deforested in 1953 (F-G) were used for the study. To account for the natural heterogeneity of the field site, soil samples were taken at 9 soil pits per site. From all 9 soil pits C and N stocks, bulk density, pH and cation exchange capacity (CEC) were analysed in order to obtain statistical significant data sets. Additionally, SOM fractions of A and Bw horizons were separated by physical means from one central soil pit per pedon. To unravel differences of SOM composition, SOM fractions were analysed by  $^{13}\text{C}$ -CPMAS NMR spectroscopy and radiocarbon analysis.

For the mineral soils, differences in total C stocks between the sites were low (F-F = 8.3 kg m<sup>-2</sup>; C-F = 7.3 kg m<sup>-2</sup>; F-G = 8.2 kg m<sup>-2</sup>). Due to the C stored within the organic horizons larger total C stocks (+25%) were found under continuous forest compared to grassland. The lower contents of free POM under grassland pointed to a faster SOM turnover. High alkyl / O/N-alkyl C ratios of fPOM fractions indicated higher decomposition stages under forest (1.16) in relation to former cropland (0.48). Historic management, such as burning of tree residues was still identifiable in the subsoil by the aryl C rich composition and  $^{14}\text{C}$  activity of oPOM fractions. The high potential of longer lasting C stabilisation within fractions of slower turnover was indicated by the larger amounts of clay-bound C per square meter found under continuous forest in contrast to grassland.

Overall, the results of this study showed effects of land-use changes on different temporal and spatial scales. The influence of soil homogenisation and aggregate disruption as due to tillage reached from accelerated SOC mineralisation on a short term to the development of heterogeneous vertical SOC sequestration within the ploughed layer. Nevertheless, also decades or even centuries afterwards, land-use changes are still reflected in the distribution and composition of SOM. These differences result in ongoing SOM redistribution within bulk soils but also between differently stabilised SOM fractions. Furthermore, land-use changes are visible in clear differences of the chemical SOM composition of SOM fractions e.g. alkyl / O/N-alkyl C ratios.

## Zusammenfassung

Neben Klima, Mineralogie und Pedogenese haben Landnutzung und Bewirtschaftung einen entscheidenden Einfluss auf die Höhe der Humusvorräte in Böden. Der Boden als größter terrestrischer Kohlenstoffspeicher ist somit in besonderer Weise anfällig gegenüber Veränderung in der Bewirtschaftung. Wie viel und wie lang Kohlenstoff (C) im Boden verbleibt hängt zudem entscheidend von der Größe des jeweiligen C Pools und dessen Persistenz ab.

In der vorliegenden Arbeit wurde der Einfluss sich ändernder Landnutzung und der damit einhergehenden Prozesse auf die Dynamik der organischen Bodensubstanz (OBS) und somit der C Stabilisierung innerhalb verschiedener Bodenpools untersucht. Das besondere Augenmerk der Arbeit lag dabei auf (i) kurzfristigen Effekten durch Aggregatzerstörung (z.B. durch Pflügen oder Gefrier-Tau Zyklen) auf die Bioverfügbarkeit der OBS, (ii) Wiedereinstellung von Tiefengradienten der OBS nach Homogenisierung des Bodens (z.B. durch Pflügen) und (iii) Langzeitauswirkungen historischer Bewirtschaftung auf die Dynamik der OBS. Um diese Ziele zu erreichen, wurden Untersuchungen auf verschiedenen räumlichen und zeitlichen Skalen durchgeführt. Die Einzeluntersuchungen reichten von kurzfristigen (<20 Tage) bis hin zu langfristigen (>50 Jahre) Effekten veränderter Bewirtschaftung auf Qualität und Menge der OBS. Die räumlichen Skalen umfassten dabei Laborversuche bis hin zu Feldversuchen. Die Arbeit teilt sich dabei in drei Teile die vom Inkubationsversuch über einen Grosslysimeterversuch bis hin zur Freilanduntersuchung reichen. Auf allen untersuchten Skalen lag das besondere Augenmerk beim Einfluss der Landnutzung auf an die Bodenaggregation gekoppelte OBS Dynamik.

Im ersten Experiment wurden kurzfristige Prozesse nach Aggregatzerstörung auf der Laborebene untersucht. Um den Einfluss der Aggregatzerstörung auf die Bioverfügbarkeit der OBS zu simulieren, wurde Boden mittels Ultraschall dispergiert. Für dieses Laborexperiment wurde Gesamtboden eines Ap Horizontes einer Braunerde unter Ackernutzung verwendet. Das Probenmaterial wurde für 18 Tage bei 20°C und konstantem Wassergehalt inkubiert. Zusätzlich wurde die Auswirkung der vorherigen Entfernung Wasser-extrahierbarer OBS aus ultraschallbehandeltem Boden auf die Kohlenstoff Mineralisierung untersucht. Vor und nach den Inkubationsversuchen wurde die Qualität der Salz-extrahierbaren OBS

(10 mM K<sub>2</sub>SO<sub>4</sub>) mittels UV-Absorption, <sup>13</sup>C-CPMAS NMR Spektroskopie und der Analyse von Neutralzuckern untersucht.

Die Physikalische Zerstörung der Bodenstruktur zeigte einen klaren Effekt auf die Menge und Zusammensetzung Salz-extrahierbarer OBS. Es konnte deutlich mehr OBS aus dispergierten Bodenproben extrahiert werden. Die zusätzlich durch Aggregatzerstörung gelöste OBS wurde besonders von pflanzenbürtigen Zuckern dominiert. Das in den zwei durchgeführten Inkubationsversuchen zusätzlich durch Aggregatzerstörung frei gesetzte CO<sub>2</sub> lag dabei +27% und +38% über der CO<sub>2</sub> Freisetzung der intakten Bodenproben. Höhere Zersetzungsgrade der extrahierbaren OBS nach den Inkubationsversuchen weisen dabei auf eine verstärkte Mineralisierung der löslichen OBS Pools hin. Somit kann die erhöhte CO<sub>2</sub> Freisetzung nach Aggregatzerstörung unter Feldbedingungen (z. B. durch Bodenbearbeitung oder Gefrier-Tau Zyklen) zu einem gewissen Teil der Mineralisierung zusätzlich bioverfügbarer gelöster OBS zugeschrieben werden.

In der zweiten Studie der vorliegenden Arbeit wurde auf einer mittleren zeitlichen und räumlichen Skala die Entwicklung von Tiefengradienten der OBS untersucht. Die Verwendung mittels Schüttung gefüllter Grosslysimeter ermöglichte eine statistisch reproduzierbare Untersuchung der mittelfristigen Auswirkungen der Bodenhomogenisierung (z.B. Pflügen) und Landnutzungsänderung unabhängig von der üblichen Heterogenität in Feldversuchen. Die Lysimeter wurden mit jungen Buchen (*Fagus sylvatica* L.) bepflanzt, wodurch eine Neuaufforstung nach Bodenbearbeitung imitiert werden konnte. Das gewählte dichte Beprobungsschema (0–2 cm, 2–5 cm, 5–10 cm and 10–20 cm) war ausschlaggebend für die Abbildung der feinskaligen Neuformierung von OBS Eigenschaften. Durch das Kombinieren von physikalischer Fraktionierung mit der Applikation <sup>15</sup>N markierter Buchenstreu und der <sup>13</sup>C-CPMAS NMR Spektroskopie war es möglich, ein detailliertes Bild der vertikalen Ausdifferenzierung der OBS zu erhalten. Vier Jahre nach der Bodenbearbeitung war eine signifikante Abnahme des Anteils freien partikulären Materials (POM) mit der Tiefe erkennbar. Eine klare Tiefenverteilung wurde auch für die Kohlenstoff- und Stickstoffanteile der einzelnen OBS Fraktionen bezogen auf den Gesamtboden gefunden. Dabei dominierte die mineralgebundene Fraktion <63 µm klar die Kohlenstoff- (von 47 bis 60% des Gesamtboden-C) und Stickstoffspeicherung (von 68 bis 86% des Gesamtboden-N). Mit der Tiefe fand eine sehr starke relative Anreicherung aliphatischer Verbindungen bei gleichzeitiger Abnahme von

O/N-alkyl C statt. Eine Zunahme aliphatischer Verbindungen wurde auch von der freien partikulären OBS hin zu der in Aggregaten okkludierten partikulären OBS beobachtet. Ein nur gering entwickelter Tiefengradient wurde für  $^{13}\text{C}$  nachgewiesen. Jedoch konnte eine deutliche vertikale Inkorporation des  $^{15}\text{N}$  aus der markierten Buchenstreu beobachtet werden. Es wurde gezeigt, dass der Eintrag des  $^{15}\text{N}$  Labels in das Aggregatinnere vom Transport durch pilzliche Hyphen maßgeblich beeinflusst wurde.

Innerhalb der vierjährigen Versuchszeit nach Bodenhomogenisierung konnte somit eine deutliche Herausbildung eines OBS Tiefenprofils nachgewiesen werden. In Böden mit sich nach Landnutzungswandel neu formierenden OBS Tiefengradienten kann die horizontweise Beprobung zu Fehleinschätzungen führen. Die Abschätzung der C und N Dynamik kann die Entwicklung von OBS Eigenschaften auf kleineren Skalen deutlich unterschätzen.

In der dritten Studie wurde auf der Feldskala die Auswirkung historischen Landnutzungswandels von Wald zu Grasland und Ackerland zu Wald untersucht. Im Mittelpunkt standen dabei die Kohlenstoffvorräte deren Verteilung und die Eigenschaften der OBS der untersuchten Braunerden. Das Untersuchungsgebiet umfasste einen Fichtenbestand (*Picea abies* L. Karst.) (F-F), ein ehemaliges Ackerland, welches 1930 aufgeforstet wurde (C-F), und ein Grasland welches 1953 durch Rodung entstand (F-G). Die räumliche Heterogenität berücksichtigend wurden 9 Bodengruben je Fläche beprobt. Durch die Untersuchung der C und N Vorräte, Lagerungsdichten, pH Werte und der Kationenaustauschkapazität an allen 9 Bodengruben je Fläche konnten statistisch abgesicherte Datensätze erhoben werden. Zusätzlich wurde der Boden einer zentralen Bodengrube je Fläche physikalisch in einzelne Bodenfraktionen aufgetrennt. Die Bodenfraktionen wurden mittels  $^{13}\text{C}$ -CPMAS NMR Spektroskopie und  $^{14}\text{C}$  Analysen untersucht.

Die Unterschiede der Kohlenstoffvorräte der Mineralböden zwischen den einzelnen Flächen waren gering (F-F =  $8,3 \text{ kg m}^{-2}$ ; C-F =  $7,3 \text{ kg m}^{-2}$ ; F-G =  $8,2 \text{ kg m}^{-2}$ ). Durch den in der Humusaufgabe gespeicherten Kohlenstoff wurden unter Wald höhere Gesamtkohlenstoffvorräte (+25%) als unter Grasland erreicht. Auf Grund höherer Umsätze war der Gehalt freier POM unter Grasland im Vergleich zu den untersuchten Waldböden geringer. Hohe alkyl / O/N-alkyl C Verhältnisse der freien POM unter Wald (1,16) im Vergleich zum ehemaligen Ackerland (0,48) und Grasland



(0,33) zeugten vom höheren Abbaugrad der OBS unter Wald. Historische Nutzungen wie beispielsweise das Verbrennen von Schlagabraum ließ sich immer noch an der Zusammensetzung und  $^{14}\text{C}$  Abundanz der okkludierten POM ablesen. Das hohe Potential lang anhaltender Kohlenstoffspeicherung in Fraktionen mit geringen Umsatzraten, wurde anhand der großen Menge tongebundenen Kohlenstoffs pro Quadratmeter unter Wald im Vergleich zum Grasland sichtbar.

Zusammenfassend stellte die vorliegende Arbeit Effekte veränderter Landnutzung auf die Dynamik der OBS auf verschiedenen räumlichen und zeitlichen Skalen dar. Der Einfluss von Bodenhomogenisierung und Aggregatzerstörung durch Pflügen reichte dabei von der kurzfristig erhöhten Freisetzung und Mineralisierung der OBS bis hin zu vertikalen Unterschieden der C Sequestrierung im Pflughorizont. Darüber hinaus wurde gezeigt, dass auch Jahrzehnte bis Jahrhunderte nach Landnutzungswandel diese noch an der Verteilung und Zusammensetzung der OBS erkennbar sind. Somit konnte eine auch lange nach dem Landnutzungswandel anhaltende Umverteilung der OBS im Gesamtboden als auch in verschiedenen stabilisierten C Pools nachgewiesen werden. Diese langfristigen Veränderungen aufgrund veränderter Bewirtschaftung spiegeln sich auch klar in der chemischen Zusammensetzung verschiedener OBS Fraktionen wieder, z.B. alkyl / O/N alkyl C Verhältnisse.

---

## Table of contents

<b>Summary</b> .....	<b>I</b>
<b>Zusammenfassung</b> .....	<b>V</b>
<b>Table of contents</b> .....	<b>IX</b>
<b>List of Figures</b> .....	<b>XII</b>
<b>List of Tables</b> .....	<b>XV</b>
<b>1. Introduction</b> .....	<b>1</b>
1.1 Importance of soil aggregation for soil organic matter dynamics .....	2
1.2 Soil disruption affects soil organic matter dynamics .....	3
1.3 Organic matter input effects on soil organic matter dynamics .....	5
<b>2. Objectives</b> .....	<b>8</b>
<b>3. Materials and methods</b> .....	<b>10</b>
3.1 Simulating aggregate disruption at laboratory scale.....	10
3.1.1 Soil material.....	10
3.1.2 Soil extraction and experimental design.....	10
3.1.3 Incubation setup.....	14
3.2 Simulating land-use change at lysimeter scale.....	16
3.2.1 Soil material and lysimeter setup.....	16
3.3 Historic land-use change at field scale .....	19
3.3.1 Study area, soil material and sampling scheme.....	19
3.4 Fractionation of bulk soils .....	22
3.4.1 Density fractionation.....	22
3.4.2 Particle size fractionation .....	23
3.5 Determination of physical parameters .....	23
3.5.1 Bulk density.....	23
3.5.2 Particle size distribution and mineralogy .....	23
3.6 Determination of chemical parameters .....	24
3.6.1 Determination of total carbon and nitrogen content .....	24
3.6.2 pH measurements .....	24

---

3.6.3	Determination of cation exchange capacity and base saturation .....	24
3.6.4	Determination of <sup>15</sup> N and <sup>13</sup> C abundance.....	24
3.6.5	Radiocarbon analyses .....	25
3.6.6	Determination of specific UV absorbance .....	25
3.6.7	HF-treatment.....	25
3.6.8	Solid state <sup>13</sup> C CPMAS NMR spectroscopy.....	26
3.6.9	Determination of neutral sugars.....	27
3.7	Data analyses.....	28
3.7.1	Calculation of atom% <sup>15</sup> N excess and normalized carbon stocks .....	28
3.7.2	Test statistics .....	28
<b>4.</b>	<b>Enhanced bioavailability of dissolved organic matter after artificial soil aggregate disruption .....</b>	<b>29</b>
4.1	Sequential extraction of water extractable OM – amount and composition.....	29
4.2	Salt extractable OM – amounts and composition.....	32
4.3	Influence of soil disruption and OM removal on C mineralisation.....	38
4.4	Influence of aggregate disruption on amount and composition of extractable OM.....	41
4.5	Alterations in composition of WEOM during sequential extraction.....	42
4.6	Enhanced mineralisation of former inaccessible OM after aggregate disruption .....	43
<b>5.</b>	<b>Differentiation of vertical soil organic matter distribution and composition four years after soil homogenisation .....</b>	<b>46</b>
5.1	Depth distribution of mass and C and N contents of SOM fractions..	46
5.2	Changing composition of SOM fractions with depth .....	51
5.3	Depth distribution of <sup>13</sup> C and <sup>15</sup> N signatures of SOM fractions.....	53
5.4	Vertical differentiation of SOM 4 years after soil homogenisation .....	55
5.5	Forming of depth gradients of <sup>13</sup> C and <sup>15</sup> N after soil homogenisation.	56

---

<b>6.</b>	<b>Historic land-use effects on soil organic carbon distribution and composition .....</b>	<b>60</b>
6.1	Differences of C and N stocks between land-use systems .....	60
6.2	Distribution and quality of SOM fractions .....	62
6.3	Chemical composition of SOM fractions under different land-use .....	64
6.4	<sup>14</sup> C abundance of SOM fractions from forest and grassland .....	67
6.5	Altered C stocks and distribution due to land-use changes .....	69
6.6	SOM composition affected by historic land-use changes .....	71
<b>7.</b>	<b>Conclusions .....</b>	<b>75</b>
<b>8.</b>	<b>References .....</b>	<b>77</b>
<b>9.</b>	<b>Danksagung (Acknowledgements) .....</b>	<b>91</b>

## List of Figures

- Figure 1 Experimental design of the two incubation experiments. Black vertical arrows indicate the different treatments of the sample sub-sets. Prior and after incubation salt extractable OM was extracted by 10 mM  $K_2SO_4$  from all aliquots. .... 12
- Figure 2 Water extractable organic matter (WEOC) of litter material from an Oi layer of a grassland after shaking (10 min), freezing (4 days) and ultrasonication ( $200 J ml^{-1}$ ). .... 13
- Figure 3 Incubation system setup and gas flow scheme modified according to HEINEMEYER et al. (1989) ..... 15
- Figure 4 Sample tube capped with polyester fibre used for incubation experiments (see p. 29). .... 15
- Figure 5 (A) sealed 1L glass bottles containing sample tubes and (B) an overview of the automated system for soil respiration measurement according to HEINEMEYER et al. (1989). .... 16
- Figure 6 View on the lysimeter station at the Helmholtz Centre Munich with the 8 beech (*Fagus sylvatica* L.) lysimeters in the centre of the picture. .... 18
- Figure 7 View on the top of a single lysimeter after cutting of beech (*Fagus sylvatica* L.) trees while the final harvest in September 2006 with visible mesh and instrumentation for matrix potential measurements. .... 18
- Figure 8 Single soil slice (20 cm thickness) before sampling after cutting of the soil monolith, with steel rings for bulk density determination on top. .... 19
- Figure 9 View from the North over the Eastern Saxon Ore Mountains showing the historic mosaic of different land-use systems. In the background the tertiary volcano “Geisingberg” is visible. White arrow is indicating the study site. .... 20
- Figure 10 The historic land-use site in Saxony. On the left hand site the former cropland (C-F) and from the centre to the background the grassland site (F-G) is visible. .... 20
- Figure 11 Sampling design for the determination of historic land-use effects, main soil pit in the centre and eight additional pits on a circle of 5 m radius. .... 22

Figure 12 $^{13}\text{C}$ -CPMAS NMR spectra with indicated chemical shift regions (fPOM from 0–2 cm layer of the lysimeter study, see page 46). .....	27
Figure 13 Experiment B: Sequentially water extractable organic carbon (WEOC) of untreated bulk soil ( <i>soilB</i> ) and the bulk soil after soil disruption ( <i>soilB+U</i> ) ( $n = 5$ ). Statistical significant differences between the treatments are indicated by $*(p < 0.05)$ .....	30
Figure 14 Experiment B: Specific UV absorbance at 254 nm ( $\text{SUVA}_{254}$ ) of water extractable organic matter from untreated bulk soil ( <i>soilB</i> ) and the bulk soil after soil disruption ( <i>soilB+U</i> ) ( $n = 5$ ). The <i>soilB+U</i> after sequential WEOM extraction was used as <i>soilB-WEOM</i> for experiment B after this extraction procedure. Statistical significant differences between the treatments are indicated by $*(p < 0.05)$ .....	31
Figure 15 Experiment B: $^{13}\text{C}$ CPMAS NMR spectra of the sequentially extracted WEOM (first 3 steps) of untreated bulk soil ( <i>soilB</i> ) and the bulk soil after soil disruption ( <i>soilB+U</i> ). Due to the declining yields of extractable OM only the WEOM of the first 3 steps (out of 5) were measurable.....	31
Figure 16 Experiment A: Respiration rates as mean values with standard deviation ( $n = 3$ ) of the first 5 days of bulk soil ( <i>soil A</i> ), bulk soil after soil disruption ( <i>soilA+U</i> ).....	38
Figure 17 Experiment B: Respiration rates as mean values with standard deviation ( $n = 3$ ) of the first 5 days of bulk soil ( <i>soilB</i> ), bulk soil after soil disruption ( <i>soilB+U</i> ) and bulk soil after soil disruption and subsequent sequential WEOM extraction ( <i>soilB-WEOM</i> ). .....	39
Figure 18 Cumulative $\text{CO}_2\text{-C}$ release per g C within the sample, shown for experiment A as mean values with standard deviation ( $n = 3$ ). .....	40
Figure 19 Cumulative $\text{CO}_2\text{-C}$ release per g C within the sample, shown for experiment B as mean values with standard deviation ( $n = 3$ ). .....	40
Figure 20 Mass distribution of the SOM and particle size fractions from the studied lysimeters. Data points are the mean values of 8 replicates with error bars representing standard deviations. Significant differences of the masses between different soil layers of a single SOM fraction are indicated by letters and $*(p < 0.05)$ , $** (p < 0.01)$ . .....	47

- Figure 21 Carbon to nitrogen ratios of the SOM and particle size fractions from the studied lysimeters. Data points are the mean values of 8 replicates with error bars representing standard deviations. Significant differences of the C/N ratios between different soil layers of a single SOM fraction are indicated by letters and  $^*(p<0.05)$ ,  $^{**}(p<0.01)$ . ..... 47
- Figure 22 Carbon and nitrogen distribution within SOM and particle size fractions related to bulk soil (<6.3 mm) for the four soil layers studied. Data points are the mean of 8 replicates with error bars representing standard deviations. Significant differences of the C- and N-amounts between different soil layers of a single SOM or particle size fraction are indicated by letters and  $^*(p<0.05)$ ,  $^{**}(p<0.01)$ . ..... 49
- Figure 23  $^{13}\text{C}$ -CPMAS NMR spectra of SOM fractions of the soil layers 0–2 cm, 2-5 cm and 5–10 cm from lysimeter 1. .... 51
- Figure 24  $^{15}\text{N}$  abundances expressed as  $\delta$  values vs. air of SOM fractions in control lysimeters and lysimeters treated with  $^{15}\text{N}$ -labelled beech litter. Data points are the mean of 4 replicates with error bars representing standard deviations. Significant differences between  $^{15}\text{N}$  labelled and control lysimeters are shown by  $^*(p<0.05)$ . fSi, fine silt; C, clay. .... 54
- Figure 25 Mass contents of fractions and distribution of organic carbon within soil fractions of bulk soil <2 mm originated from continuous forest (F-F), former cropland (C-F) and grassland (F-G). .... 62
- Figure 26 Distribution of organic carbon within soil fractions of bulk soil <2 mm originated from continuous forest (F-F), former cropland (C-F) and grassland (F-G). .... 63
- Figure 27 Total C stocks within soil fractions normalized on 1 cm thickness of horizon for the continuous forest (F-F), former cropland (C-F) and grassland (F-G). .... 64
- Figure 28  $^{13}\text{C}$ -CPMAS-NMR spectra of the bulk soils and SOM fractions from the A and Bw horizons of continuous forest (F-F), former cropland (C-F) and grassland (F-G). .... 65
- Figure 29  $^{13}\text{C}$ -CPMAS-NMR spectra of the organic layers / horizons as well as grass and root samples from the grassland (F-G) and Norway spruce roots from the Ah horizon under continuous forest (F-F). .... 66

## List of Tables

Table 1 Texture, pH (in water and in 10 mM CaCl <sub>2</sub> ), C/N ratios and C and N contents of the soil material used for the study of enhanced bioavailability of dissolved organic matter after soil disruption. Soils were sampled in April 2006 ( <i>experiment A</i> ) and August 2006 ( <i>experiment B</i> ). .....	10
Table 2 Texture, pH (in 10 mM CaCl <sub>2</sub> ) and bulk density of the upper four soil layers (0–20 cm) of the analysed beech lysimeters at the Helmholtz Centre München given as mean values with standard deviation (n=8).....	17
Table 3 Carbon, nitrogen contents and stocks and C/n ratios of the upper four soil layers (0–20 cm) of the analysed beech lysimeters at the Helmholtz Centre München given as mean values with standard deviation (n=8). .....	17
Table 4 Thickness of horizon, bulk density and texture (n=3) of continuous forest (F-F), former cropland (C-F) and grassland (F-G). Data are given as mean value with standard deviation.....	21
Table 5 pH values in H <sub>2</sub> O and 10 mM CaCl <sub>2</sub> , effective cation exchange capacity (ECEC), potential cation exchange capacity (PCEC) and base saturation (BS) of continuous forest (F-F), former cropland (C-F) and grassland (F-G). Data are given as mean value with standard deviation. ....	21
Table 6 Carbon recovery after treatment with 10% hydrofluoric acid (HF) of bulk soils and clay fractions from continuous forest (F-F), former cropland (C-F) and grassland (F-G). .....	26
Table 7 Salt extractable organic carbon (SEOC) contents, specific UV-absorbance at 254 nm (SUVA <sub>254</sub> ) of the 10 mM K <sub>2</sub> SO <sub>4</sub> solution extracts before (t <sub>0</sub> ) and after (t <sub>x</sub> ) the incubation experiment of soil aliquots and cumulative released CO <sub>2</sub> -C from bulk soil ( <i>soilA</i> , <i>soilB</i> ), bulk soil after soil disruption ( <i>soilA+U</i> , <i>soilB+U</i> ) and bulk soil after soil disruption and subsequent sequential WEOM extraction ( <i>soilB-WEOM</i> ). Statistical significant differences between different treatments are indicated by *( <i>p</i> <0.05). .....	32
Table 8 Integrated chemical shift regions obtained by <sup>13</sup> C CPMAS NMR for the sequentially extracted WEOM of untreated bulk soil ( <i>soilA</i> , <i>soilB</i> ), the bulk soil after soil disruption ( <i>soilA+U</i> , <i>soilB+U</i> ), and the SEOM before (t <sub>0</sub> ) and after (t <sub>x</sub> )	



the incubation experiment of aliquots from the incubated soil materials of experiment A and B.....	34
Table 9 Contents of neutral sugars derived from SEOM extracted by 10mM K <sub>2</sub> SO <sub>4</sub> of experiment A and B (before (t <sub>0</sub> ) and after (t <sub>x</sub> ) the incubation), and in water extractable DOM from the first extraction step. The abbreviation n.d. indicates values below the detection limit. Standard error is given in parentheses. ....	36
Table 10 Normalized yields of neutral sugars in relation to units C in the soil material extracted by 10mM K <sub>2</sub> SO <sub>4</sub> of experiment A and B (before (t <sub>0</sub> ) and after (t <sub>x</sub> ) the incubation), and in water extractable DOM from the first extraction step. n.d. - values below detection limit.....	37
Table 11 Carbon and nitrogen contents of the density (POM) and particle size fractions (sand, silt and clay). Data is given as mean values with standard deviation (n = 8). Significant differences related to the soil layer of C and N contents of a single SOM fraction is indicated by letters and *( <i>p</i> <0.05) and **( <i>p</i> <0.01). ....	50
Table 12 Relative contents of alkyl C, O/N-alkyl C, aryl C, carbonyl C and alkyl / O/N-alkyl C ratios obtained by <sup>13</sup> C-CPMAS NMR spectroscopy of the litter and the fPOM, oPOM, oPOM <sub>small</sub> and clay fractions of the three uppermost soil layers from the studied lysimeters. Data is given as mean value with standard deviation. Significant differences between single fractions according to depth are indicated by letters and *( <i>p</i> <0.05), **( <i>p</i> <0.01), the litter was tested versus the fPOM of the 0-2 cm layer.....	52
Table 13 δ <sup>13</sup> C values (vs. V-PDB) of the three POM fractions (fPOM, oPOM and oPOM <sub>small</sub> ) and the fine silt and clay fractions from the studied lysimeters. Data is given as mean values with standard deviations (n = 8), significant differences between different soil layers of a single SOM or particle size fraction are indicated by letters and *( <i>p</i> <0.05) and **( <i>p</i> <0.01).....	53
Table 14 Atom% <sup>15</sup> N excess of the SOM fractions, calculated as difference between atom% <sup>15</sup> N of SOM fractions from labelled and control lysimeters. Standard error is given in parentheses.....	55

---

Table 15 Carbon, N contents and stocks as mean values (n = 9) with standard deviations from continuous forest (F-F), former cropland (C-F) and grassland (F-G).....	61
Table 16 C/N ratios and relative contents of alkyl C, O/N-alkyl C, aryl C, carbonyl C, alkyl / O/N-alkyl C and aromatic / alkyl C ratios of the bulk soils and the SOM fractions as revealed by <sup>13</sup> C-CPMAS NMR spectroscopy for continuous forest (F-F), former cropland (C-F) and grassland (F-G). ....	68
Table 17 Radiocarbon data of bulk soils and SOM fractions from continuous forest (F-F) and grassland (F-G). For the samples with $\Delta^{14}\text{C}$ values below 0‰ the conventional radiocarbon ages in years before present (1950) are given. ....	69

## 1. Introduction

Soil organic matter (SOM) not only vitally impacts soil functions, but also plays a key role in the global C cycle as soils can act as a source or sink for the important greenhouse gases CO<sub>2</sub> and CH<sub>4</sub> (COLE et al., 1993; HUTCHINSON et al., 2007; JARECKI and LAL, 2003; PAUSTIAN et al., 1997). Besides climate, mineralogy, and pedogenesis, especially land-use strongly influences the humus level in soils (BATJES, 1998; BATJES and SOMBROEK, 1997; BELLAMY et al., 2005; COLE et al., 1993; DAWSON and SMITH, 2007; FONTAINE et al., 2007; HUTCHINSON et al., 2007; INGRAM and FERNANDES, 2001; JARECKI and LAL, 2003; LETTENS et al., 2005; STEWART et al., 2007). After each disturbance due to changing land-use a certain time of constant management is needed to reach a new steady state of C inputs and C mineralisation (BATJES, 1998). In some ecosystems, decades after land-use change C stocks have not reached a level comparable to land-use systems with constant management (COMPTON and BOONE, 2000; LANGLEY-TURNBAUGH and KEIRSTEAD, 2005; WALL and HYTONEN, 2005). But also the distribution and composition of certain SOM fractions is strongly affected by changing land-use (DEGRYZE et al., 2004; GERZABEK et al., 2006; GUGGENBERGER et al., 1995). In contrast to total C stocks, especially more labile SOM fractions tend to be influenced on a decadal timescale (BAISDEN et al., 2002).

Soil OM is a heterogeneous mixture of organic compounds differing in composition and bioavailability. How much organic C is stored in a soil and for how long this C remains in the soil depends on OM input, SOM pool sizes and their stability. The differentiation of SOM pools with different composition and turnover is crucial for the understanding of SOC stabilisation but also SOC destabilisation due to land-use. The physical fractionation of soils is a common tool to separate chemically different soil fractions in terms of pools with different turnover. The concept of this approach is to study the role of soil minerals and aggregation in the processes of SOM turnover and stabilisation (CHRISTENSEN, 2001). By density fractionation it is possible to separate light particulate OM from heavy OM bound on mineral surfaces or associated to oxides. The free particulate organic matter (fPOM) is mostly related to primary litter input, whereas in soil aggregates occluded POM (oPOM) is mainly affected by the aggregate turnover of the particular soils (Six et al., 1999). Using <sup>14</sup>C measurements, BAISDEN et al. (2002) showed that greater than or equal to 90% of fPOM turns over in less than 10 years, indicating fPOM to be a sensitive measure of land-use changes.

Throughout the present work POM fractions are referred to represent light OM which is not firmly associated to soil minerals, which corresponds to the light fraction (LF) defined by SIX et al. (1998).

On the long-term (from decades to centuries), recalcitrance and spatial inaccessibility of SOM are two main factors controlling C stabilisation in soils (VON LÜTZOW et al., 2008). For the process based understanding of long-term C stabilisation it is crucial to evaluate the composition and amount of occluded and mineral associated SOM fractions. Recalcitrance and accessibility in macroaggregates seem to determine the turnover dynamics in fast and intermediate cycling OM pools. But for long-term preservation of organic C, occlusion in microaggregates and interactions with mineral surfaces were found to be the major control (FLESSA et al., 2008; KÖGEL-KNABNER et al., 2008; VON LÜTZOW et al., 2008), as the largest part of SOM is in association with the mineral phase (SANCHEZ et al., 1989).

### 1.1 Importance of soil aggregation for soil organic matter dynamics

Organic matter accumulation in soils and therefore the C stabilisation is known to be enhanced by increasing soil aggregation (ANGERS et al., 1997; BESNARD et al., 1996; ELLIOTT, 1986; FLESSA et al., 2008; GOLCHIN et al., 1995; GOLCHIN et al., 1994; JASTROW, 1996; TISDALL and OADES, 1982). EDWARDS and BREMNER (1967) already postulated the microbial inaccessibility of SOM due to the occlusion in aggregates. This spatial inaccessibility of SOM is an important factor controlling the fate of SOC within aggregated soil structures (VON LÜTZOW et al., 2008). Spatial inaccessibility occurs when organic matter is situated in soils in such a way that it is physically inaccessible to microorganisms and their enzymes, and thus protected from decomposition (KILLHAM et al., 1993; VAN VEEN and KUIKMAN, 1990). It has been suggested that this mechanism is mainly due to small pore diameters (<0.2 µm) (BALESDENT et al., 2000; KILLHAM et al., 1993; STRONG et al., 2004) and therefore a reduced diffusion of oxygen into macro- and especially microaggregates, which leads to a reduced microbial activity within the aggregates (SEXSTONE et al., 1985; SOLLINS et al., 1996). GOEBEL et al. (2005) were able to show an increased C mineralisation due to the enhanced wettability after aggregate disruption, showing a reduced C bioavailability due to the hydrophobic properties of intact soil aggregates.

Already in the late 1960s EDWARDS and BREMNER (1967) proposed the theory of microaggregates (<250  $\mu\text{m}$ ) in soils mainly formed by the binding of clay particles, polyvalent cations (Fe, Al and Ca) and SOM. Later a hierarchy of aggregate formation was proposed by TISDALL and OADES (1982), assuming macroaggregates being formed by the assemblage of microaggregates bound together by organic binding agents (e.g. microbial residues, fungal hyphae and roots). In respect to their higher physical stability, microaggregates offer a greater ability to protect SOM than macroaggregates. This was shown by increased C mineralisation rates for soils where microaggregates were broken apart (BALESDENT et al., 2000; GREGORICH et al., 1989). A predominant incorporation and stabilisation of plant residues within microaggregates was demonstrated for agricultural soils (ANGERS et al., 1997; HELFRICH et al., 2008). The transfer of residue-derived C and N into microaggregates seemed to happen within macroaggregates (HELFRICH et al., 2008). The dynamics of macroaggregates are crucial for the sequestration of C, but do not provide long-term protection of C themselves. The higher potential for SOC stabilisation within smaller aggregate structures was nicely shown by JOHN et al. (2005). The authors demonstrated that the turnover time of organic C in the water-stable aggregates of an Ap horizon increased with decreasing aggregate size from 35 yr (>1000  $\mu\text{m}$ ) to 86 yr (<53  $\mu\text{m}$ ).

The fate of SOC is closely related to the degree and turnover of soil aggregation (PLANTE and MCGILL, 2002; TISDALL and OADES, 1982). Therefore, scenarios regarding the impact of changing land-use and climate on C stabilisation strongly require the understanding of soil aggregate dynamics. Soil aggregation itself is a function of a diverse range of conditions, e.g. clay content, mineralogy, C content, climate and management. Mechanisms resulting in different soil aggregate dynamics range therefore from the sub-micron (e.g. mineralogy and microbial mucilage) to the field scale (e.g. climate and management impacts) (SIX et al., 2004). To study the influence of altered aggregation on SOM dynamics due to changing land-use it is crucial to comprise a range of scales from the aggregate to the field level.

## 1.2 Soil disruption affects soil organic matter dynamics

Besides climate, tillage has strong effects on soil aggregation according to SIX et al. (2004). Tillage affects soil aggregation and the occluded SOM by the physical impact

on the soils structural integrity leading to aggregate disruption and the release of occluded SOM. Tillage has two main goals, the control of soil structure for seedbed preparation and the incorporation of organic residues into the soil. Tillage has impacts on the SOM location from small structural scales ( $\mu\text{m}$  to  $\text{cm}$ ) to profile scales ( $\text{cm}$  to  $\text{dm}$ ). Clear effects of tillage were shown for the turnover of soil aggregates and therefore the dynamics of aggregate related SOM (BALESDENT et al., 2000; GRANDY and ROBERTSON, 2007; JACOBS et al., 2009; OORTS et al., 2007; PLANTE and MCGILL, 2002; SIX et al., 2000). JOHN et al. (2005) demonstrated clear effects of different tillage intensities. Under continuous tillage the most important aggregate size class was 53-250  $\mu\text{m}$ , under conservation tillage 250-1000  $\mu\text{m}$  and without tillage >2000  $\mu\text{m}$  (grassland and forest). In regularly tilled soils the physical soil disruption lead to a relative enrichment of stable microaggregate structures. In agricultural systems which are not regularly tilled the absence of physical disruption also led to a clear increase in the total aggregation of topsoils (SHRESTHA et al., 2007; SIMPSON et al., 2004; SIX et al., 1999; SIX et al., 2000). At the same time the increasing amount of stabilised SOC at the absence of tillage is mostly related to microaggregate structures, due to the higher protective capacity of small aggregates (DOU and HONS, 2006). Tillage also promotes the contact between organic residues and the mineral phase in soils due to the destruction and mixture of soil structural units. The extent of POM occlusion into macroaggregate structures is faster in tilled compared to untilled soils, as shown by higher proportions of oPOM in systems with higher tillage intensities (BALESDENT et al., 2000; PLANTE and MCGILL, 2002). Ecosystems with a high SOM proportion situated in less stable macroaggregates are highly susceptible to SOC loss from disturbance and therefore to the movement of SOC from slow to active pools (GRANDY and ROBERTSON, 2007). Especially the labile C pool of fresh SOM was shown to be influenced by soil homogenisation as it happens due to tillage (GRANDY and ROBERTSON, 2007; OORTS et al., 2007). Ploughing at the conversion of forests or natural grasslands to croplands has a strong disruption effect on macroaggregate structures and the occluded SOM. In a study in northern America, TAN et al. (2007) showed that soils (0–20cm) under forest and no tillage preserved 167% / 94% more light fraction (with higher C contents) than under continuous tillage. In undisturbed soil systems higher SOC amounts are stored within POM fractions. A de-protection of differently stabilised SOM fractions (occluded or mineral associated) to the same extent could be shown on sites with 40 years tillage due to maize cultivation after

forest removal (BALESDENT et al., 1998). Consequently, the SOC mineralisation is accelerated not only in particulate SOM pools but also in mineral bound OM pools due to tillage (VON LÜTZOW et al., 2008).

Additional to tillage also drying-rewetting and freezing-thawing events cause physical disruption of soil (i.e. measured as changes in soil aggregation) and organic tissue (e.g. plant litter or particulate OM) followed by an enhanced C mineralisation (AUSTNES and VESTGARDEN, 2008; DENEFF et al., 2001; LUNDQUIST et al., 1999; SIX et al., 2004). It has been shown that the amount of dissolved organic matter (DOM) increases when soils were subjected to drying-rewetting or freezing-thawing events (AUSTNES and VESTGARDEN, 2008; KALBITZ et al., 2000). Dissolved OM is the most mobile and reactive OM fraction in terrestrial systems, containing a wide range from highly biodegradable to stable recalcitrant C compounds (KALBITZ, 2003; ZSOLNAY, 1996), but very little is known about the relation between altered aggregation, physical disruption and DOC dynamics. Often, soil tillage and its enhancing effect on DOM release is evaluated in the literature as effects of enhanced leaching after incorporation of fresh crop residues and enhanced microbial activity (CHANTIGNY, 2003). It is still under debate if the enhanced CO<sub>2</sub> release after natural and artificial aggregate breakdown, e.g. tillage or freezing-thawing cycles can be due to an enhanced release of fast decomposable SOM or microbial residues (BALESDENT et al., 2000; FIERER and SCHIMEL, 2003; WU and BROOKES, 2005). The close positive relationship between DOC extractability and released CO<sub>2</sub> was demonstrated by MARSCHNER and BREDOW (2002) in a 12 day incubation study. For the studied soils, the authors proposed DOC as the most important substrate for microorganisms and showed a clear depletion during short term incubations. For the evaluation of aggregate disruption effects on the SOM mineralisation and a possible enhanced DOC leaching it is crucial to accomplish short term experiments at the laboratory scale. Only by small scale experiments under defined conditions it is possible to clearly evaluate effects of physical disrupted soil aggregates on very labile SOM fractions as DOC.

### 1.3 Organic matter input effects on soil organic matter dynamics

A main factor controlling the distribution, composition and stabilisation of SOM is the OM input. Carbon stocks in native soils reflect the balance of C inputs and C losses

under native conditions (i.e. productivity, moisture and temperature regimes). The quantity and quality of the OM input are the main drivers of the C cycle and therefore also of the C accumulation in soils (TATE et al., 2000). In soil systems which underwent land-use changes the steady state between C input and mineralisation is disturbed. Changing OM input due to altered land-use and cultivation has therefore a direct influence on the quantity and quality of SOM (ELLERBROCK et al., 2001; GERZABEK et al., 2006; HELFRICH et al., 2006; KAISER et al., 2007; WOCHÉ et al., 2005). The different OM input between different management regimes is reflected by differences in C contents and composition of different functional SOM fractions. JOHN et al. (2005) investigated the effect of land-use (spruce, grassland, wheat and maize) on SOC storage in different soil aggregate and density fractions. The authors found that the type of land-use resulted in a different distribution of litter C over functionally different SOM pools. At the grassland, maize and wheat sites the majority of the SOC (86–91%) was found in the mineral-associated SOM fraction, whereas in the A horizon under spruce the free and occluded POM accounted for 52% of the total SOC content.

But also the differing composition of the OM input of different plant species is reflected in the rates of OM incorporation and SOC formation. DE NEERGAARD and GORISSEN (2004) found a faster incorporation of OM input into SOC under clover compared to rye grass due to the smaller C/N ratios of legumes promoting microbial activity in contrast to the higher C/N ratios of grass. As a result, the OM input also has strong impacts on the microbial abundance and structure. In an incubation experiment with organic residues (wheat straw) of different quality BOSSUYT et al. (2001) showed no difference in aggregation or respired CO<sub>2</sub> between high-quality (C/N: 20) and low-quality (C/N: 108) residues. But the authors could demonstrate a direct influence on the microbial community, with fungal dominated low-quality systems and bacterial dominated high-quality systems. By modelling, it was possible to demonstrate that with decreasing supply of fPOM, decomposers slowly disappeared or became dormant and SOM mineralisation ceased (FONTAINE and BAROT, 2005). The authors demonstrated how absent litter supply in deep soils lead to a lack of SOM mineralisation. The extent of how SOM decomposers are out-competed depends mainly on the C input rate (BRADFORD et al., 2008). This assumption was nicely proven by an incubation experiment by FONTAINE et al. (2007), who studied priming effects on deep soil samples with cellulose amendments. The



authors showed that the primed SOC was mainly old C with a calculated age of  $2,567 \pm 226$  years. From a mechanistic point of view, the energy required for the mineralisation of recalcitrant SOC is higher than the energy supplied by the catabolism of the substrate (FONTAINE et al., 2007). The authors assumed an equalisation of mean residence times of SOC from deep soil and surface soil when the cellulose amendment would be repeated annually. The introduction of fresh litter by deep ploughing would destroy the energetic barrier which is an important pre-condition for SOM stabilisation in deeper soil horizons (FONTAINE et al., 2007). As a result, besides the aggregate disruption the incorporation of fresh OM by deep ploughing at the conversion of land-use systems is accelerating the SOC mineralisation at greater depths.

A common tool to track the incorporation of fresh OM into soils and differently stabilised SOM fractions is the application of plant materials enriched in  $^{13}\text{C}$  and/or  $^{15}\text{N}$  (AITA et al., 1997; HAYNES, 1997; KÖLBL et al., 2006). KÖLBL et al. (2006) showed in an experiment with  $^{15}\text{N}$  labelled mustard litter (*Sinapis alba*) a rapid transfer of the labelled material from the fPOM into fine mineral fractions within the first 5 months after litter application. The importance of fungi for the incorporation of organic compounds from the litter into the soil matrix could also be demonstrated by tracing techniques (SCHIMEL and HÄTTENSCHWILER, 2007). In a tracer study with the application of  $(^{15}\text{NH}_4)_2\text{SO}_4$  and  $^{13}\text{C}$  labelled wheat straw to soil material from an Alfisol, FREY et al. (2003) demonstrated the reciprocal fungal transfer of litter-C into soil and soil-N into the litter layer. The authors were able to demonstrate the transfer of litter derived C into macroaggregates by fungal hyphae.

The application of labelled plant material enables the direct study of the processes involved in the vertical fate of C and N from the litter layer to the mineral soil and variably stabilised SOM fractions.

## 2. Objectives

As stated above, soil C pools differ in their susceptibility to land-use changes. The present study aimed to evaluate the influence of stabilizing and destabilising processes on SOM due to altered management with a focus on aggregate related processes.

An overall objective was to study the impact of land-use change on differently stabilised SOM fractions. To evaluate effects of management alterations at different spatial and temporal scales three experiments were combined within the present work. Thus, the study combined impacts of land-use change on SOM ranging from short term (18 days) to medium term (up to 4 years) and long term (>50 years) and from small laboratory to medium (1 m<sup>2</sup>) and field scale.

By the conduction of laboratory experiments, a lysimeter study and a field survey it was possible to achieve a complex understanding of ongoing processes due to land-use change.

The three main objectives of the study were:

**(i) Study of short term effects on SOM bioavailability due to aggregate disruption at a laboratory scale**

The main goal of the first part of the present work was to unravel effects of artificially enhanced release of dissolved organic matter due to aggregate disruption e.g. due to tillage or freezing-thawing cycles. Therefore, the influence on C mineralisation (within 18 days) of the release of SOM formerly stabilised by spatial inaccessibility was tested.

**(ii) Development of SOM composition and distribution after soil homogenisation due to land-use change at a medium scale**

At a lysimeter scale the development of SOM depth gradients within four years after tillage was studied. The study represented recovering soils after deep ploughing and land-use change towards new afforestation. The incorporation of OM into differently stabilised SOM fractions within four months was evaluated by the application of <sup>15</sup>N labelled litter.

**(iii) Long term effects of historic land-use changes on SOM dynamics**

The impact of historic land-use changes on C distribution and composition was studied on adjacent sites at field scale. Possible alterations of C stabilised within different SOM fractions (inter- vs. inner-aggregate SOM) were evaluated in the course of changing historic land-use at timescales over 50 years.

### 3. Materials and methods

#### 3.1 Simulating aggregate disruption at laboratory scale

##### 3.1.1 Soil material

For the study of enhanced bioavailability of dissolved organic matter (DOM) after soil disruption soil samples were taken from an arable soil classified as Leptic Cambisol (eutric) (WRB, 2006) which is regularly ploughed and fertilized. The site is located in eastern Germany in the Saxon Ore-Mountains 25 km south of the city of Dresden near Luchau (50°51' N; 13°44' E). The area is situated 480 m a.s.l. and has a mean annual precipitation of about 800 mm and a mean annual temperature of about 6.5 °C. Soil for preliminary experiments and experiment A was sampled in April (*soil A*) and additional soil material for experiment B in August (*soil B*) 2006, which differed in C and N content (Table 1). Soil material was taken from the upper 5 cm of the Ap horizon. Soil samples were air dried and gently sieved through a 2 mm sieve and homogenised for all later analyses and experiments.

**Table 1** Texture, pH (in water and in 10 mM CaCl<sub>2</sub>), C/N ratios and C and N contents of the soil material used for the study of enhanced bioavailability of dissolved organic matter after soil disruption. Soils were sampled in April 2006 (*experiment A*) and August 2006 (*experiment B*).

experiment / soil material	sand	silt	clay	C	N	C/N	pH	
							H <sub>2</sub> O	CaCl <sub>2</sub>
<i>soil A</i>	483	310	206	45.3	4.0	11.2	6.1	5.5
<i>soil B</i>				38.9	3.3	11.7	6.8	6.2

##### 3.1.2 Soil extraction and experimental design

Aliquots of the soil material were subjected to wet extraction in order to evaluate the amount and composition of additionally released soluble OM due to soil disruption. For the extraction of salt extractable OM (SEOM), 10 mM K<sub>2</sub>SO<sub>4</sub> solution was used at a soil to solution ratio of 1 to 2 (w/w). The highly hygroscopic freeze dried SEOM extracted by the widely used CaCl<sub>2</sub> were not measurable by solid state NMR. Due to the paste-like status of the hygroscopic CaCl<sub>2</sub>-SEOM the zirconium dioxide rotor could not be loaded equally and failed to rotate at 6.8 kHz. Therefore, K<sub>2</sub>SO<sub>4</sub> was used as an extraction solvent which is regularly used for extraction of microbial

biomass after chloroform fumigation (VANCE et al., 1987). Thereby a non-hygroscopic fine powdered sample was obtained after freeze drying which was easily measurable by solid state NMR. The air-dried soil was gently suspended with 10 mM K<sub>2</sub>SO<sub>4</sub> solution and horizontally shaken for 10 min. After subsequent centrifugation (5466 g, 10 min), the supernatant was filtered with polypropylene membrane filters (GH Polypro, Pall) of 0.45 µm mesh size.

For the sequential extraction of water extractable OM (WEOM), deionised water was used instead of K<sub>2</sub>SO<sub>4</sub> solution. After filtration, replicates of SEOM and WEOM aliquots were pooled in equal parts and instantly freeze dried for <sup>13</sup>C-CPMAS NMR spectroscopy and analyses of neutral sugars. Due to the low total amounts of extracted C composite samples had to be created in order to meet the detection limits of the two methods. The total mass of the freeze dried composite SEOM and WEOM samples ranged between 400 and 500 mg with C contents of approx. 30 mg g<sup>-1</sup>.

The study consisted of two incubation experiments (duration of 18 days each) with the following treatments in triplicate (Figure 1):

- experiment A (*soil A*): (i) intact bulk soil mixed with quartz sand (*soilA*) and (ii) soil after aggregate disruption mixed with quartz sand (*soilA+U*)
- experiment B (*soil B*): (i) intact bulk soil mixed with quartz sand (*soilB*), (ii) soil after aggregate disruption mixed with quartz sand (*soilB+U*) and (iii) bulk soil after aggregate disruption followed by sequential (5 steps) extraction of WEOM (see below) mixed with quartz sand (*soilB-WEOM*)

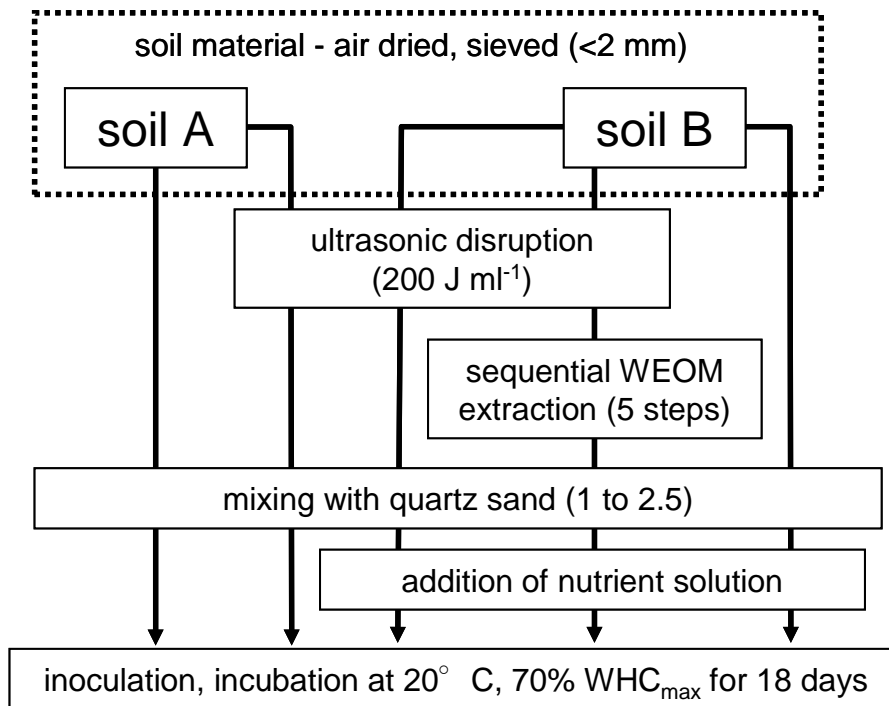


**Figure 1** Experimental design of the two incubation experiments. Black vertical arrows indicate the different treatments of the sample sub-sets. Prior and after incubation salt extractable OM was extracted by 10 mM  $K_2SO_4$  from all aliquots.

Prior to the incubation experiment, sub-sets (approx. 50 gram per aliquot) from soil material A and B were suspended with deionised water at a soil to water ratio of 1 to 5, followed by ultrasonication with a 13 mm probe tip and an un-pulsed energy input of  $200 J g^{-1}$  (Sonopuls 2200, Bandelin). Probe output power was calibrated according to NORTH (1976). It averaged 56 W at 70% of the maximum setting. The probe tip was placed 15 mm below the suspension surface. A water cooling jacket was used during the ultrasonic treatment to prevent any heating of the soil suspensions and therefore a possible denaturing of the SOM. After aggregate disruption, all soil suspensions were dried. According to STEMMER et al. (1998), who used  $170 J g^{-1}$  in a study about enzyme activity in soil fractions, the energy level is comparable to forces on soil aggregates under field conditions, e.g. raindrops or ploughing. In the studied soils the energy input led to a complete disruption of macroaggregates, but left the microaggregates rather undispersed. This was demonstrated by over 84% of undispersed clay ( $<2 \mu m$ ) and 19% undispersed fine silt ( $2 \mu m$  to  $6.3 \mu m$ ), which were not removed from the microaggregates ( $>6.3 \mu m$ ). To test the impact of the chosen ultrasonication energy level on the release of water extractable OC (WEOC), litter from a grassland Oi layer was used as a reference material for POM. A significant higher WEOC release (Figure 2) was found after freezing-thawing (4 days

freezing;  $79.6 \pm 0.2$  mg DOC ( $\text{g C}^{-1}$ ) than after ultrasonication ( $200 \text{ J g}^{-1}$ ;  $63.9 \pm 3.4$  mg DOC ( $\text{g C}^{-1}$ ) or shaking (10 min,  $42.8 \pm 4.7$  mg DOC ( $\text{g C}^{-1}$ )).

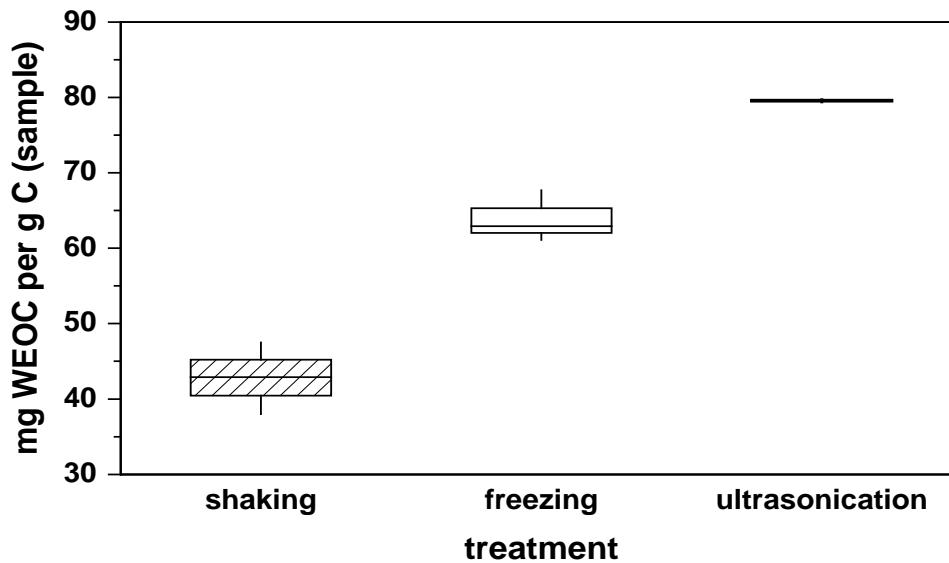


**Figure 2** Water extractable organic matter (WEOC) of litter material from an Oi layer of a grassland after shaking (10 min), freezing (4 days) and ultrasonication ( $200 \text{ J ml}^{-1}$ ).

To produce a disrupted soil material diluted in extractable OM prior to the experiment *B*, the WEOM (see above) of *soilB+U* was sequentially extracted (5 steps). The same WEOM extraction procedure was additionally applied to intact soil samples (*soilB*), in order to study the WEOM extractability and composition of intact soil aggregates. Deionised water was used for this sequential extraction in order to avoid a possible influence of high salt concentrations on microbial growth. After the sequential WEOM removal the samples were dried.

In preliminary experiments (data not shown) the influence of added nutrient solutions was studied on SOM mineralisation of *soilA* with and without quartz sand additions. Increasing respiration rates due to nutrient additions could only be found in soils without quartz sand additions. Therefore all incubated samples in this study were mixed with acid washed quartz sand at a ratio of 1 to 2.5 (w/w), in order to increase pore space and therefore the oxygen supply. The maximal water holding capacity ( $\text{WHC}_{\text{max}}$ ) was determined in triplicate from aliquots of each sample. Steel rings of  $100 \text{ cm}^3$  were filled with soil material and drained on a porous plate for two hours at 10 hPa. The  $\text{WHC}_{\text{max}}$  was calculated by difference. All soil treatments were wetted to 70%  $\text{WHC}_{\text{max}}$  and incubated at  $20^\circ\text{C}$  for 18 days. In order to provide a comparable microbial community in every sample at the beginning of the experiments, the

samples were inoculated with 100 µl of a soil solution. For the inoculum, a mixture of ten soils (7 Cambisols, 2 Luvisols and 1 Fluvisol) differing in land-use was incubated for two weeks. The pre-incubated soil mixture was capillary saturated with deionised water at a ratio of 1 to 2 (w/w), gently shaken for 60 minutes and filtered with a polycarbonate membrane filter (Isopore™, Millipore) of 2 µm mesh size. For experiment B a nutrient solution according to INGESTAD and LUND (1986) was added to the samples adjusting the C/N ratio to 10, to balance a possible leaching of nutrients due to the prior extraction of WEOM of the *soilB-WEOM* samples. The nutrient solution contained both macro- ( $\text{NH}_4\text{NO}_3$ ,  $\text{CaSO}_4$ ,  $\text{MgSO}_4$ ,  $\text{CaH}_2\text{PO}_4$ ,  $\text{K}_2\text{SO}_4$ ) and micronutrients ( $\text{Fe}_2(\text{SO}_4)_3$ ,  $\text{MnSO}_4$ ,  $\text{H}_3\text{BO}_3$ ,  $\text{CuCl}_2$ ,  $\text{ZnSO}_4$ ,  $\text{Na}_2\text{MoO}_4$ ). The nutrient solution was added in a way to obtain a water content of 70%  $\text{WHC}_{\text{max}}$  of the samples.

### 3.1.3 Incubation setup

An automated system was used for continuous soil respiration measurements with 24 sample lines modified according to HEINEMEYER et al. (1989) (Figure 3 and Figure 5). In contrast to the original setup the numerous membrane pumps were exchanged by a single oil-free air compressor less susceptible to errors, e. g. drastic air flow fluctuations. The whole equipment was placed in a room of constant temperature at 20°C. The ambient  $\text{CO}_2$  was absorbed via pumping the air through tubes filled with soda-lime (Merck, Germany) placed in front (acryl-tubes with approx. 1900 cm<sup>3</sup>) and behind (glass tubes with approx. 1200 cm<sup>3</sup>) the compressor. The air flow rates were adjusted for every single sample line by needle valves in contrast to the original potentiometric adjustment of the membrane pumps. The  $\text{CO}_2$  concentration was measured by an infrared  $\text{CO}_2$ -analyzer (Type 225 Mk3, ADC BioScientific Ltd.) and the air flow rate by a flow meter (Tylan FM 260, Mykrolis).



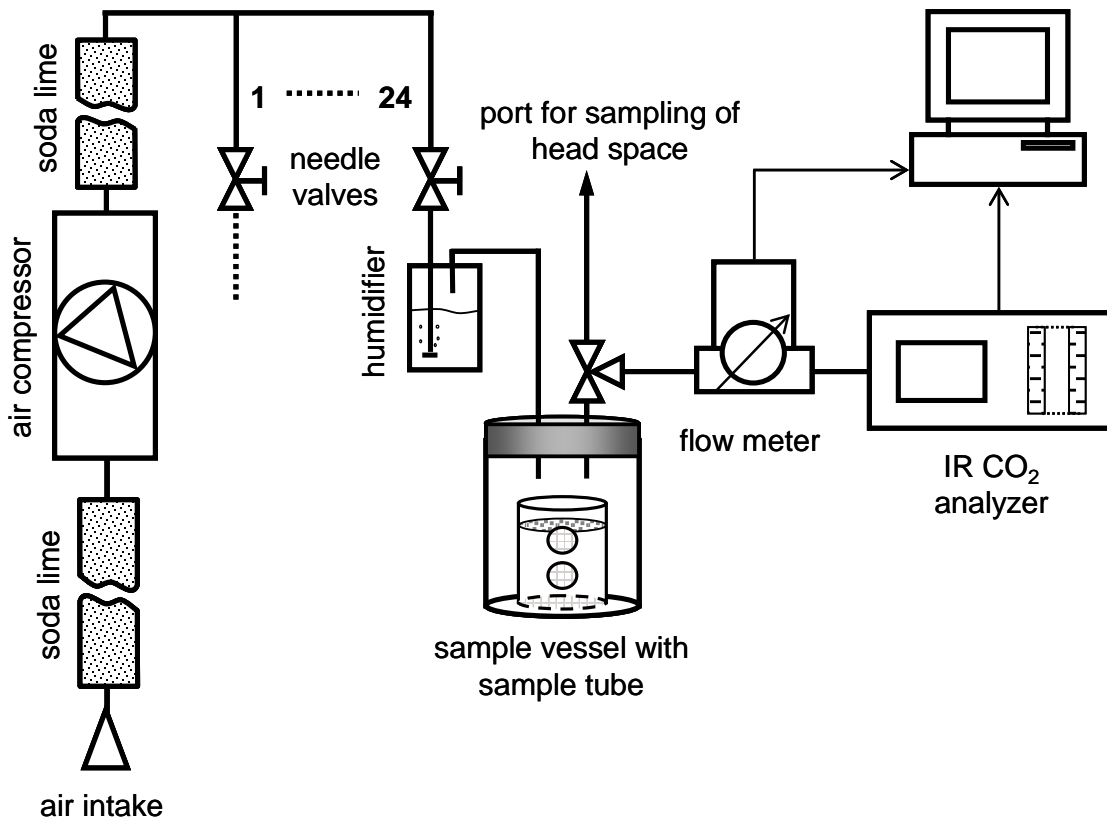


**Figure 3** Incubation system setup and gas flow scheme modified according to HEINEMEYER et al. (1989)

HEINEMEYER et al. (1989) used a forced aeration of the soil samples in acryl tubes, which in former experiments led to preferential air flow and uncontrolled desiccation of the incubated soil material (EUSTERHUES, personal communication).



**Figure 4** Sample tube capped with polyester fibre used for incubation experiments (see p. 29).

By contrast, in the present work it was tried to imitate quasi-natural gas diffusion conditions. The samples were filled into plastic sample tubes (Figure 4) which were

placed in airtight sealed 1 L glass bottles (Schott AG, Germany) (Figure 3 and Figure 5). To ensure oxic sample conditions, the bottom hole and four opposing holes at the side of the sample tubes (Figure 4) were capped with polyester fibre of 23  $\mu\text{m}$  mesh size (PET 1500, Sefar AG). Before the  $\text{CO}_2$ -free air reached the sample jars, the air was purged through 500 ml gas washing bottles (Schott AG, Germany) filled with deionised water. The water was acidified by  $\text{H}_2\text{SO}_4$  adjusting a pH of 2.5 in order to sustain a constant water content of the incubated soil material by wetting the air entering the 1 L glass bottles. The sample vessels and therefore the samples were continuously flushed with the preconditioned air.

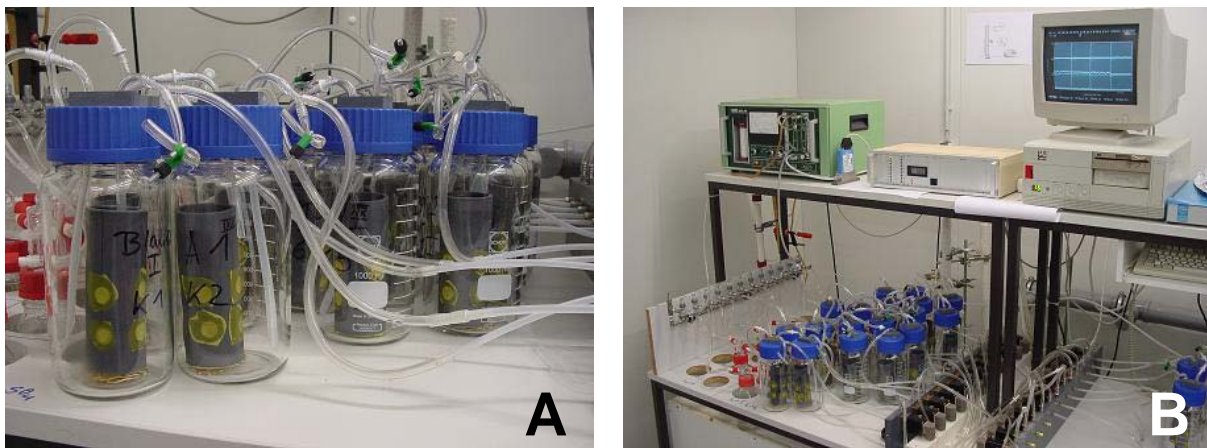


**Figure 5 (A) sealed 1L glass bottles containing sample tubes and (B) an overview of the automated system for soil respiration measurement according to HEINEMEYER et al. (1989).**

## 3.2 Simulating land-use change at lysimeter scale

### 3.2.1 Soil material and lysimeter setup

The experiment was conducted at the outdoor lysimeter station of the Helmholtz Centre Munich (48°13' N 11°36' E, 490 m), Germany (Figure 6). Mean annual precipitation at the lysimeter field ranged from 546 mm (dry year in 2003) to 876 mm (in 2005) (WINKLER et al., 2009). Mean annual temperatures ranged from 8.2°C (2005) to 8.9°C (2003, 2006). The experimental setup of the forest soil lysimeters is described in detail by WINKLER et al. (2009). The lysimeters were filled with soil material (Haplic Cambisol (dystric)) from the forest site “Höglwald” (48°18' N; 11°05' E, 540 m) near Augsburg (Bavaria, Germany). The soil comprised of 24% sand, 56% silt and 21% clay with pH values (in 10 mM  $\text{CaCl}_2$ ) of about 3.8 (Table 2).

The C and N contents and stocks of the eight lysimeters showed a good reproducibility between the single lysimeters (Table 3)

**Table 2 Texture, pH (in 10 mM CaCl<sub>2</sub>) and bulk density of the upper four soil layers (0–20 cm) of the analysed beech lysimeters at the Helmholtz Centre München given as mean values with standard deviation (n=8).**

depth cm	sand	silt mg g <sup>-1</sup>	clay	pH (CaCl <sub>2</sub> )	bulk density g cm <sup>-3</sup>
0 to 2				3.9±0.0	1.16±0.12
2 to 5				3.8±0.1	1.16±0.12
5 to 10	235±10	559±10	206±17	3.8±0.1	1.23±0.06
10 to 20				3.7±0.0	1.29±0.06

**Table 3 Carbon, nitrogen contents and stocks and C/n ratios of the upper four soil layers (0–20 cm) of the analysed beech lysimeters at the Helmholtz Centre München given as mean values with standard deviation (n=8).**

depth cm	C mg g <sup>-1</sup>	N mg g <sup>-1</sup>	C kg m <sup>-2</sup>	N g m <sup>-2</sup>	C / N
0 to 2	44.1±6.3	2.8±0.4	0.97±0.14	61.3±7.6	15.8±0.3
2 to 5	32.8±5.4	2.1±0.3	1.08±0.18	69.6±10.0	15.5±0.4
5 to 10	25.4±5.2	1.7±0.3	1.56±0.32	104.4±15.0	14.9±1.5
10 to 20	15.8±1.9	1.1±0.1	2.05±0.25	141.4±12.9	14.5±0.7

In brief, eight lysimeters, each with a surface area of 1 m<sup>2</sup> and a depth of 2 m, were filled in 1999 with soil material of a Haplic Cambisol (dystric) (WRB, 2006). The upper 30 cm of the lysimeters were filled in summer 2002 with freshly homogenised soil material. Therefore, a homogeneous soil material was assumed for the upper 30 cm at the start of the experiment similar to topsoil after ploughing.

Each lysimeter was planted with four 3-year-old saplings of *Fagus sylvatica* L. in autumn 2002. The space around the lysimeter cylinders was filled with the same soil and also planted with beech trees in the density as in the lysimeters to provide a homogeneous stand climate and to avoid edge effects.



**Figure 6** View on the lysimeter station at the Helmholtz Centre Munich with the 8 beech (*Fagus sylvatica* L.) lysimeters in the centre of the picture.

In spring 2006, the original leaf litter layer of each lysimeter was removed and weighed. Average leaf dry mass per lysimeter was 134 g. In May 2006, the control lysimeters #5-8 were again covered with 134 g of their original leaf litter. Lysimeters #1-4 were covered with 134 g of  $^{15}\text{N}$ -labelled beech (*Fagus sylvatica* L.) leaves (approx. 1 atom%  $^{15}\text{N}$  enrichment), corresponding to a total N mass of 18.6 mg and a  $^{15}\text{N}$  content of  $0.176 \text{ mg g}^{-1}$ . After distributing the leaves on the surface of the lysimeters, they were covered with a fine mesh (Figure 7) to avoid a relocation of litter to the neighbouring lysimeters and a contamination with unlabelled litter.



**Figure 7** View on the top of a single lysimeter after cutting of beech (*Fagus sylvatica* L.) trees while the final harvest in September 2006 with visible mesh and instrumentation for matrix potential measurements.

In September 2006 all eight lysimeters were finally harvested. The topmost 100 cm of each lysimeter were cut into slices (Figure 8) of 20 cm thickness (RETH et al., 2007). Bulk soil samples were taken at different depths, i.e. 0–2 cm, 2–5 cm, 5–10 cm, 10–



20 cm. In order to maintain the natural aggregation, soil material was gently sieved under field moist condition with a sieve of 6.3 mm mesh size. The sieved bulk soil material was air-dried for all further analyses.



**Figure 8** Single soil slice (20 cm thickness) before sampling after cutting of the soil monolith, with steel rings for bulk density determination on top.

### 3.3 Historic land-use change at field scale

#### 3.3.1 Study area, soil material and sampling scheme

The area of the historic land-use study is located in eastern Germany in the Saxon Ore-Mountains 25 km south of the city of Dresden near Luchau (48°17' N; 11°04' E). The area is situated 480 m a.s.l. and has a mean annual rainfall of about 800 mm and a mean annual temperature of about 6.5 °C. Beginning with the German settlement and deforestation in the early 13<sup>th</sup> century, the former old growth temperate forests were altered into a characteristic mosaic (Figure 9) of different land-use systems (BLASCHKE, 1966). Burning of tree residues after felling and charcoal production for the local mining industry was widespread, but not historically documented for the studied sites. Before the first settlement, the vegetation was dominated by beech forests (*Fagus sylvatica* L.). Starting in the 19<sup>th</sup> century, a conversion to Norway spruce (*Picea abies* L. Karst) monocultures took place on a large scale.



**Figure 9** View from the North over the Eastern Saxon Ore Mountains showing the historic mosaic of different land-use systems. In the background the tertiary volcano “Geisingberg” is visible. White arrow is indicating the study site.

Two adjacent forested and one grassland site on a 200 m transect were investigated on a plateau. The two forested sites were (i) an even aged Norway spruce (*Picea abies* L. Karst) forest established in 1927 on a continuously forested site (F-F) and (ii) a former agricultural cropland (C-F) afforested in 1930 with even aged Norway spruce. The (iii) grassland site (F-G) was cleared of Norway spruce forest in 1953 and ploughed once. Remaining roots and branches were burnt at the site after the clear cut. During its existence, the grassland was mainly used for hay production and therefore fertilized and limed regularly.



**Figure 10** The historic land-use site in Saxony. On the left hand site the former cropland (C-F) and from the centre to the background the grassland site (F-G) is visible.

The soils were characterized as Leptic Cambisols (dystric) at the forested sites and Leptic Cambisol (eutric) under grassland (WRB, 2006). The soils are rich in coarse

material and evolved from gneiss, the dominant parent material in the Saxon Ore-Mountains. An abrupt boundary between A and B horizons at the former cropland and the grassland indicated former tillage. At the forested sites, the organic horizons Oe and Oa were composed of acidic needle litter with abrupt boundaries between the horizons. The organic horizons (sum of Oe and Oa) had a thickness of  $6.3\pm 1.0$  cm at the continuous forest and  $5.2\pm 1.5$  cm at the former cropland. Soil mineralogy was very similar among all three sites; the clay separates were composed of: 70% chlorite, 20% illite and 10% kaolinite. The clay content changed slightly from continuous forest (F-F) to former cropland (C-F) and grassland (F-G) (Table 4). Soil pH in all soils ranged from 3.5 in the forest soils to 5.7 in the grassland soils, indicating the absence of carbonates. pH, cation exchange capacity (CEC) and base saturation (BS) were significantly different between the sites, with high pH and BS under grassland concomitant with low CEC values (Table 5).

**Table 4 Thickness of horizon, bulk density and texture (n=3) of continuous forest (F-F), former cropland (C-F) and grassland (F-G). Data are given as mean value with standard deviation.**

site	horizon	thickness cm	bulk density g cm <sup>-3</sup>	sand g kg <sup>-1</sup>	silt g kg <sup>-1</sup>	clay g kg <sup>-1</sup>
F-F	Ah	5±1	0.86±0.08	397±10	357±9	246±15
	Bw	28±2	1.27±0.13	402±18	391±38	207±20
C-F	Ap	12±2	1.05±0.15	441±9	349±9	209±5
	Bw	27±3	1.32±0.14	461±40	347±26	192±13
F-G	Ap	15±1	0.91±0.07	449±3	350±10	202±13
	Bw	20±3	1.51±0.11	556±42	283±10	161±31

**Table 5 pH values in H<sub>2</sub>O and 10 mM CaCl<sub>2</sub>, effective cation exchange capacity (ECEC), potential cation exchange capacity (PCEC) and base saturation (BS) of continuous forest (F-F), former cropland (C-F) and grassland (F-G). Data are given as mean value with standard deviation.**

site	pH / H <sub>2</sub> O	pH / CaCl <sub>2</sub>	ECEC μmol <sub>c</sub> g <sup>-1</sup>	PCEC μmol <sub>c</sub> g <sup>-1</sup>	BS %
F-F	3.6±0.1	2.9±0.1	156.3±5.8	344.3±23.1	9.4±2.9
	3.9±0.1	3.4±0.3	110.2±9.4	238.7±34.2	9.7±5.0
C-F	3.8±0.1	3.2±0.1	127.4±5.4	276.8±31.6	9.8±2.1
	4.2±0.1	3.7±0.1	68.6±9.8	199.5±17.2	13.3±2.5
F-G	5.2±0.2	4.6±0.2	124.3±19.1	244.3±18.4	94.2±3.8
	5.4±0.3	4.6±0.3	56.2±5.4	161.8±14.6	63.3±16.8

Soil samples were taken in July 2006 from the A and B horizons at the three sites, additionally the litter (Oi) at all sites and the organic horizons (Oe, Oa) at the two forested sites were sampled. I also sampled eight pits on a circle ( $r = 5$  m) around the main soil pit in the centre (Figure 11), in order to obtain bulk density, pH values, cation exchange capacity (CEC) as well as C and N contents. Due to the chosen circular sampling scheme, I obtained highly significant data sets describing a single pedon for every site.

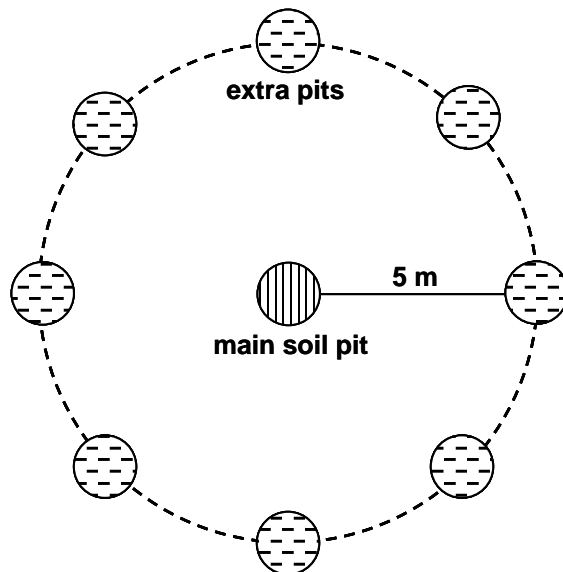


**Figure 11** Sampling design for the determination of historic land-use effects, main soil pit in the centre and eight additional pits on a circle of 5 m radius.

### 3.4 Fractionation of bulk soils

#### 3.4.1 Density fractionation

Air dried soil material (20 to 30 g,  $<2$  mm), were capillary-saturated with sodium polytungstate solution ( $\text{Na}_6[\text{H}_2\text{W}_{12}\text{O}_{40}]$ ;  $1.8 \text{ g cm}^{-3}$ ) and allowed to settle over night. The floating free particulate organic matter (fPOM) was extracted by sucking via a water jet pump. The remaining slurry was dispersed ultrasonically (Bandelin, Sonopuls HD 2200) with an energy input of  $440 \text{ J ml}^{-1}$  in order to break down soil aggregates. The energy input was tested in advance, to avoid disruption of coarse POM along with aggregate disruption. Centrifugation (30 minutes at 3074 g) was used to separate the occluded POM (oPOM) from the mineral residue. To remove the Na-polytungstate from the POM fractions, the samples were washed several times with deionised water over a sieve of  $20 \mu\text{m}$  mesh size. The obtained fraction



(oPOM<sub>small</sub>) from the washing of the oPOM was washed via pressure filtration until the electric conductivity dropped below 5  $\mu\text{S cm}^{-1}$ . All fractions were lyophilized, weighed and subjected to C N elemental analysis.

#### *3.4.2 Particle size fractionation*

Sand (>63  $\mu\text{m}$ ) and coarse silt (>20  $\mu\text{m}$  to 63  $\mu\text{m}$ ) from the mineral residue of the density separation were separated by wet sieving. Medium silt (6.3  $\mu\text{m}$  to 20  $\mu\text{m}$ ), fine silt (2  $\mu\text{m}$  to 6.3  $\mu\text{m}$ ) and clay (<2  $\mu\text{m}$ ) were obtained by sedimentation in Atterberg cylinders. All fractions were lyophilized, weighed and subjected to C N elemental analysis.

### 3.5 Determination of physical parameters

#### *3.5.1 Bulk density*

The bulk density of the mineral soil horizons was determined on undisturbed soil cores (100  $\text{cm}^3$ ) by the core method (BLAKE and HARTGE, 1986), with 3 replicates per horizon. The samples were dried at 105°C for 24 hours and the amount of coarse material was subtracted. Organic horizons were sampled in triplicate with a wooden frame (10 cm x 10 cm). From the dry weight the bulk density was calculated.

#### *3.5.2 Particle size distribution and mineralogy*

For soil texture analysis, organic matter was oxidized ( $\text{H}_2\text{O}_2$  30%), and 2.5 mM  $\text{Na}_4\text{P}_2\text{O}_7$  solution was subsequently used for particle dispersion. The fractions >63  $\mu\text{m}$  were determined via wet sieving and weighing. The fractions <63  $\mu\text{m}$  were determined using the X-ray attenuation method (Micromeritics, Sedigraph 5100).

The mineralogy of the soils from the Saxon historic land-use site was determined on clay separates from Bw horizons (after OC removal by  $\text{H}_2\text{O}_2$ ) by X-ray diffractometry using K- $\alpha$ -radiation (Philips, PW 1830).

## 3.6 Determination of chemical parameters

### 3.6.1 Determination of total carbon and nitrogen content

The C and N contents were measured in duplicate by dry combustion (Elementar, vario MAX CNS Analyzer for bulk soils; vario EL CN Analyzer for SOM fractions). Since all samples were free of carbonates, the measured C concentrations equal the organic C concentrations.

DOC in the SEOM / WEOM extracts was measured by high temperature combustion with a Total Carbon Analyzer (TOC-5050A, Shimadzu) including 2 min purging with C-free synthetic air to remove purgeable C.

### 3.6.2 pH measurements

The pH values of the bulk soils were measured after 30 min equilibration in the supernatant of a 2.5 to 1 (w/w) deionised H<sub>2</sub>O and 10 mM CaCl<sub>2</sub> solution/soil suspension with a glass electrode (WTW, pH Meter 340).

### 3.6.3 Determination of cation exchange capacity and base saturation

For the analysis of exchangeable base cations, 1 M ammonium acetate and for the re-exchange 1 M KCl was used (VAN REEUWIJK, 2002). The percolates were measured for K, Mg, Ca and Na with an ICP-OES (Varian, Vista Pro). The NH<sub>4</sub><sup>+</sup> concentrations from the re-exchange were measured with a Segmented Flow Analyzer (at the Fachgebiet für Waldernährung und Wasserhaushalt, TUM) and accounted for the potential cation exchange capacity (PCEC). For the determination of exchangeable Al, Fe, Mn and acidity, 1 M KCl was used. The percolates were also measured with ICP-OES (Varian, Vista Pro). The exchangeable acidity was calculated from the difference of the pH values from the 1 M KCl stock solution and the percolates. From the obtained data, the effective CEC (ECEC) and the base saturation (BS) were calculated.

### 3.6.4 Determination of <sup>15</sup>N and <sup>13</sup>C abundance

For isotopic measurements SOM fractions were analyzed in tin capsules (Elementar Analysensysteme GmbH, Hanau, Germany) for  $\delta^{13}\text{C}$  against Vienna – Pee Dee Belemnite (V-PDB) and  $\delta^{15}\text{N}$  against air-N<sub>2</sub> with an isotope ratio mass spectrometer (Delta V Plus, ThermoFisher, Bremen, Germany) coupled to an elemental analyzer

(Vario EL, Elementar Analysensysteme GmbH, Hanau, Germany) at the Centre of Stable Isotopes of Forschungszentrum Karlsruhe, Institute for Meteorology and Climate Research (IMK-IFU, Garmisch-Partenkirchen, Germany). Working standard (mineral soil), calibrated against the primary standards USGS 40 (glutamic acid,  $\delta^{13}\text{C}_{\text{CV-PDB}} = -26.389$ ) and USGS 41 (glutamic acid,  $\delta^{13}\text{C}_{\text{CV-PDB}} = +37.626$ ) for  $\delta^{13}\text{C}$  and USGS 25 (ammonium sulphate,  $\delta^{15}\text{N}_{\text{Air}} = -30.4$ ) and USGS 41 ( $\delta^{15}\text{N}_{\text{Air}} = +47.6$ ) for  $\delta^{15}\text{N}$ , was analyzed after every twelfth sample to detect a potential instrument drift over time and to determine the analytical precision of the instrument which was smaller than  $\pm 0.15$  for  $\delta^{13}\text{C}$  and  $\pm 0.25$  for  $\delta^{15}\text{N}$  (SD for  $n = 6-8$ ). For  $\delta^{13}\text{C}$  analyses a blank correction was performed to account for the background signal of the tin capsules. For  $\delta^{15}\text{N}$  analyses no blank correction was necessary, as the background signal of the tin capsules was negligible. Due to the large range of  $\delta^{15}\text{N}$  values a correction of  $\delta^{15}\text{N}$  of the samples was performed, using a two-point calibration with USGS 25 and USGS 41 as anchor points.

### 3.6.5 Radiocarbon analyses

The  $^{14}\text{C}$  values were obtained at the KECK Carbon Cycle AMS Facility at the Earth System Science Department of the University of California Irvine. For the  $^{14}\text{C}$  measurements,  $^{14}\text{C}$ -free acetanilide was used as sample background. All  $^{14}\text{C}$  results have been corrected for isotopic fractionation according to the convention of STUIVER and POLACH (1977). Organic material with  $\Delta^{14}\text{C}$  values  $>0\%$  indicate the presence of bomb C, reflecting higher  $^{14}\text{C}$  activities than the 1950 atmosphere. Negative  $\Delta^{14}\text{C}$  values indicate that the main part of the C has resided long enough in the soil for a significant radioactive decay (TRUMBORE, 2000).

### 3.6.6 Determination of specific UV absorbance

Spectroscopic properties of the SEOM and WEOM extracts were identified by UV/Vis spectroscopy (Cary 50 conc, Varian Inc.). From the DOC concentrations and the UV-absorbance at 254 nm the specific UV-absorbance ( $\text{SUVA}_{254}$ ) was calculated (WEISHAAR et al., 2003).

### 3.6.7 HF-treatment

Prior to  $^{13}\text{C}$ -CPMAS NMR spectroscopy, bulk soils and clay fractions from the study site in Saxony (see page 60) were treated with 10% hydrofluoric acid (HF) to remove

mineral material, including paramagnetic compounds such as iron, and to concentrate the SOM (SCHMIDT et al., 1997; SCHÖNING et al., 2005b). Approximately 2.5 g of ground soil sample or particle size separate were shaken with 20 ml 10% (v/v) HF for 2 hours. After centrifugation (10 min, 2470 g) at 4°C, the supernatant was removed. The procedure was repeated five times. The remaining sediment was washed 6 times with 20 ml deionised water and freeze-dried. Carbon recovery after HF treatment is shown in Table 6.

**Table 6 Carbon recovery after treatment with 10% hydrofluoric acid (HF) of bulk soils and clay fractions from continuous forest (F-F), former cropland (C-F) and grassland (F-G).**

site	horizon	C recovery after HF treatment (%)	
		bulk soil	clay
F-F	Ah	80.5	79.3
	Bw	41.7	53.2
C-F	Ap	81.3	72.8
	Bw	45.9	49.0
F-G	Ap	49.7	75.1
	Bw	68.9	55.0

### 3.6.8 Solid state $^{13}\text{C}$ CPMAS NMR spectroscopy

$^{13}\text{C}$ -CPMAS NMR spectroscopy was accomplished with a Bruker DSX 200 spectrometer (Bruker BioSpin). The samples were filled into zirconium dioxide rotors and spun in a magic angle spinning probe at a rotation speed of 6.8 kHz to minimize chemical anisotropy. A ramped  $^1\text{H}$  pulse was used during a contact time of 1 ms to prevent Hartmann–Hahn mismatches. The delay times were set from 300 ms (freeze dried SEOM / WEOM extracts and bulk soils) to 1000 ms (litter and POM fractions). For samples with low total C content (freeze dried SEOM / WEOM) up to 300.000 scans had to be collected in order to obtain sufficient signal to noise ratios, which accounts for total measurement times of up to 24 hours per single sample. Chemical shifts are referenced to tetramethylsilane (TMS = 0 ppm). For integration, chemical shift regions (Figure 12) were used as given: alkyl C ((-10) to 45 ppm), O/N-alkyl C (45 to 110 ppm), aryl/olefine C (110 to 160 ppm) and carbonyl/carboxyl/amide C (160 to 220 ppm).

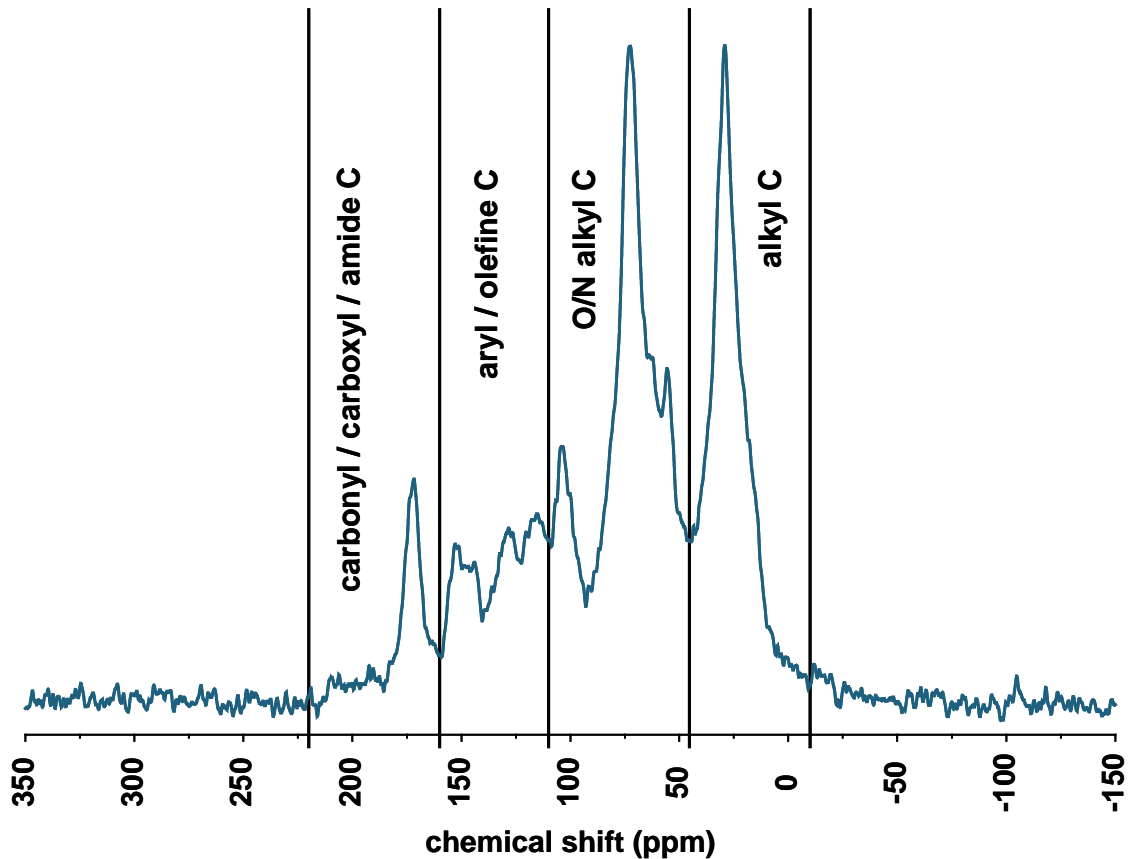


Figure 12  $^{13}\text{C}$ -CPMAS NMR spectra with indicated chemical shift regions (fPOM from 0–2 cm layer of the lysimeter study, see page 46).

### 3.6.9 Determination of neutral sugars

Freeze-dried SEOM and WEOM extracts were analysed for seven neutral sugars (rhamnose, fucose, arabinose, xylose, mannose, galactose and glucose) from non-cellulosic carbohydrates according to SPIELVOGEL et al. (2007). This was done to evaluate the proportion of microbial and plant derived sugars as indicators for the source of the extracted soluble C. Microbial populations synthesize dominantly galactose, glucose and mannose. Therefore, the ratio of galactose+mannose / arabinose+xylose (GM / AX) is low (<0.5) for plant derived carbohydrates and high (>2.0) for microbial derived carbohydrates (OADES, 1984). Briefly, the analysis was carried out in three steps: (1) Hydrolysis of samples with 4 M trifluoroacetic acid (AMELUNG et al., 1996), (2) acetate alditol derivatisation according to BLACK and FOX (1996) modified by RUMPEL and DIGNAC (2006), followed by (3) GC-FID (Agilent, 6890) analysis of the extracted monomers. The extract of one sample was injected twice and standard errors are given in Table 9. According to the C contents between 150 and 250 mg of the freeze dried composite SEOM and WEOM samples were

weighed in for the extractions. The mean recovery of the sum of neutral sugars was  $69\pm 6\%$ . The sugar yields were normalized on mg DOC ( $\text{g C soil}^{-1}$ ) to obtain more mechanistic information about the dissolvable neutral sugars per unit C of the soil material as shown in Table 10.

### 3.7 Data analyses

#### 3.7.1 Calculation of atom% $^{15}\text{N}$ excess and normalized carbon stocks

The atom%  $^{15}\text{N}$  excess of the SOM fractions (Table 14) was calculated as difference between the atom%  $^{15}\text{N}$  of the labelled SOM fractions and the atom%  $^{15}\text{N}$  of the unlabelled SOM fractions.

To exclude the influence of the differing thickness of horizon on total C and N stocks, the values were normalized on 1 cm thickness of horizon (Eq. (1)):

$$\text{normalized C; N stocks (g m}^{-2}\text{ cm}^{-1}\text{)} = \text{C; N stock (g m}^{-2}\text{)} / \text{thickness of horizon (cm)} \quad (1).$$

#### 3.7.2 Test statistics

For statistical analysis of the datasets, SPSS 16.0 for Windows (SPSS Inc., Chicago) was used. Significant differences of soil parameters from the land-use and lysimeter study were tested by the nonparametric Mann-Whitney U test. Significant differences of the extract data (WEOM, SEOM yields and  $\text{SUVA}_{254}$ ) were tested by the nonparametric Wilcoxon test for related samples.

Treatment effects on SOC mineralisation (see page 38) were statistically tested by comparing respiration rates (RR) of soils without physical disruption to those with physical disruption. An one-way repeated measures analysis of variance (ANOVA) was used to test differences between the RR by treatment ( $\text{RR} = f(\text{treatment})$ ). The analysis of variance was executed with R 2.4.1. (R Development Core Team, Vienna, Austria).

## 4. Enhanced bioavailability of dissolved organic matter after artificial soil aggregate disruption

The main objective of this study at laboratory scale was to unravel effects of artificially enhanced DOM release on SOM mineralisation (see page 10). By artificial aggregate disruption via ultrasonication forces occurring under field conditions were imitated (e. g. due to frost or tillage) and a homogenised soil material was obtained. The influence of the release of SOM formerly stabilised by spatial inaccessibility was tested on C mineralisation. By the extraction and spectroscopic analyses of salt extractable OM (SEOM), imitating a natural occurring ionic strength, it was possible to predict how CO<sub>2</sub> release may be affected by amount and composition of extractable DOM of the incubated soil materials. The net effects of SOM release on mineralisation were studied by prior sequential leaching of water extractable OM (WEOM). The different extraction procedures enabled a comparison of amounts and composition of dissolved OM in relation to the extracting solvent.

### 4.1 Sequential extraction of water extractable OM – amount and composition

Prior to experiment B, WEOM of *soilB+U* was sequentially (5 steps) extracted in order to obtain a disrupted soil material depleted in bioavailable WEOM.

By the first extraction step more ( $p < 0.01$ ) WEOC (per unit C in the soil) was extracted by deionised water than by 10 mM K<sub>2</sub>SO<sub>4</sub> solution (Figure 13 and Table 7) accounting for +72% (*soilB+U*) and +58% (*soilB*) more WEOC. During the first three extraction steps significant larger amounts ( $p < 0.05$ ) of WEOC (+111%) were extracted from the soil material subjected to prior ultrasonication (Figure 13). A large standard deviation for the WEOC was detected for extraction steps 1 and 2 from the disrupted samples, whereas the standard deviation of *soilB* extracts was very low over the whole extraction procedure. In total +96% (+4.94±1.09 mg (gC)<sup>-1</sup>) WEOC were extracted during the 5 steps from disrupted *soilB+U* compared to the intact *soilB*.

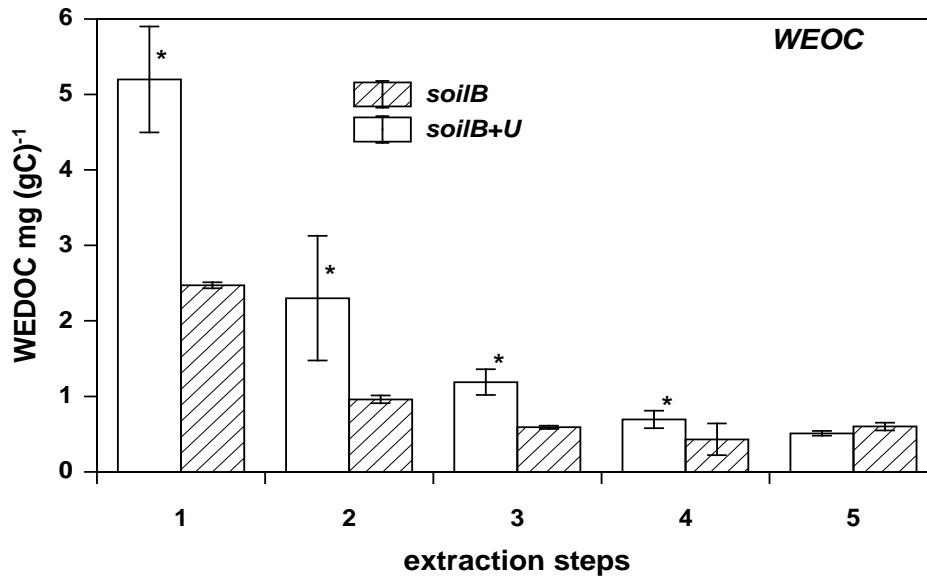


**Figure 13 Experiment B: Sequentially water extractable organic carbon (WEOC) of untreated bulk soil (*soilB*) and the bulk soil after soil disruption (*soilB+U*) (n = 5). Statistical significant differences between the treatments are indicated by \* ( $p < 0.05$ ).**

The  $SUVA_{254}$  values of the WEOM extracts showed maxima at the third (*soilB*) and fourth (*soilB+U*) extraction step (Figure 14). Higher  $SUVA_{254}$  values were shown for the extraction steps 1 ( $p < 0.05$ ) and 2 for *soilB* compared to *soilB+U*, whereas the WEOM extracts of *soilB+U* showed higher values at the final three extraction steps compared to *soilB* (step 5:  $p < 0.05$ ). No close correlation was found for the percent aromatic C obtained by  $^{13}C$ -CPMAS NMR and the  $SUVA_{254}$  values.

The decrease of O/N-alkyl C from the first to the third step was much more pronounced in the WEOM extracts of the intact *soilB* than of the disrupted *soilB+U* (Figure 15 and Table 8). A strong increase of carbonyl C and aromatic C was found for the WEOM extracts of *soilB*, whereas no clear change was detectable in the extracts of *soilB+U*. The increasing relative dominance of aromatic structures was also visible by the increasing aromatic / alkyl C ratio of the *soilB* extracts (Table 8). A distinctive lower release of O/N-alkyl C was shown for SEOM extracts in contrast to WEOM extracts, which is corroborated by larger sugar yields in 10 mM  $K_2SO_4$  extracts (Table 9). Higher neutral sugar contents were observed in the WEOM extracts of *soilB* compared to *soilB+U*, mainly due to higher glucose contents (Table 9). The normalized amounts of neutral sugars of WEOM extracts of *soilB+U* (Table 10) were twofold larger in relation to that of *soilB*, with a dominance of glucose. The GM/AX ratio was higher in the WEOM extracts of *soilB* (7.54) than in the extracts of *soilB+U* (6.68).



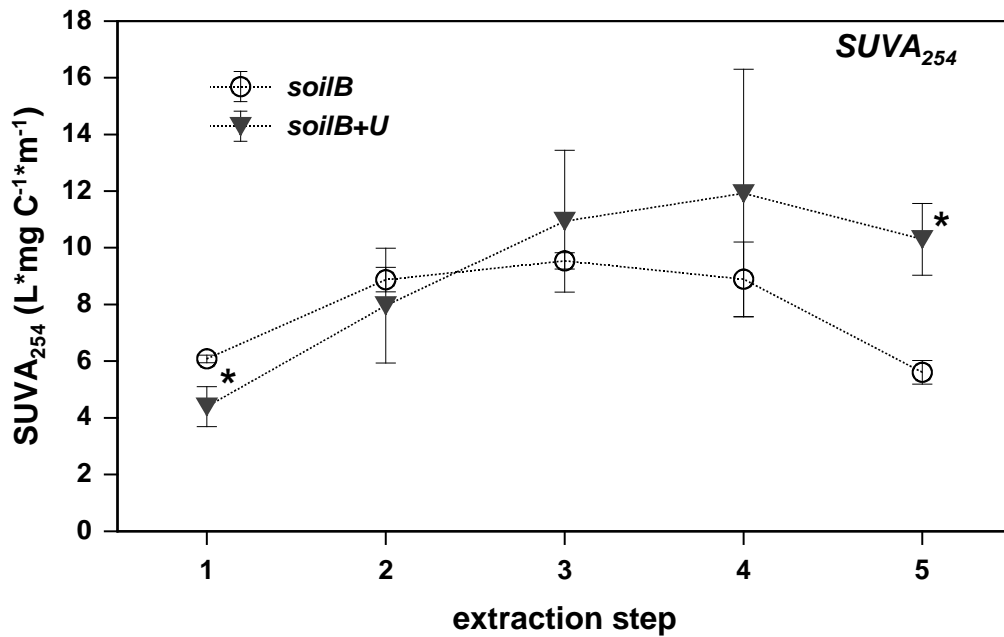


Figure 14 Experiment *B*: Specific UV absorbance at 254 nm (SUVA<sub>254</sub>) of water extractable organic matter from untreated bulk soil (*soilB*) and the bulk soil after soil disruption (*soilB+U*) ( $n = 5$ ). The *soilB+U* after sequential WEOM extraction was used as *soilB-WEOM* for experiment *B* after this extraction procedure. Statistical significant differences between the treatments are indicated by \* ( $p < 0.05$ ).

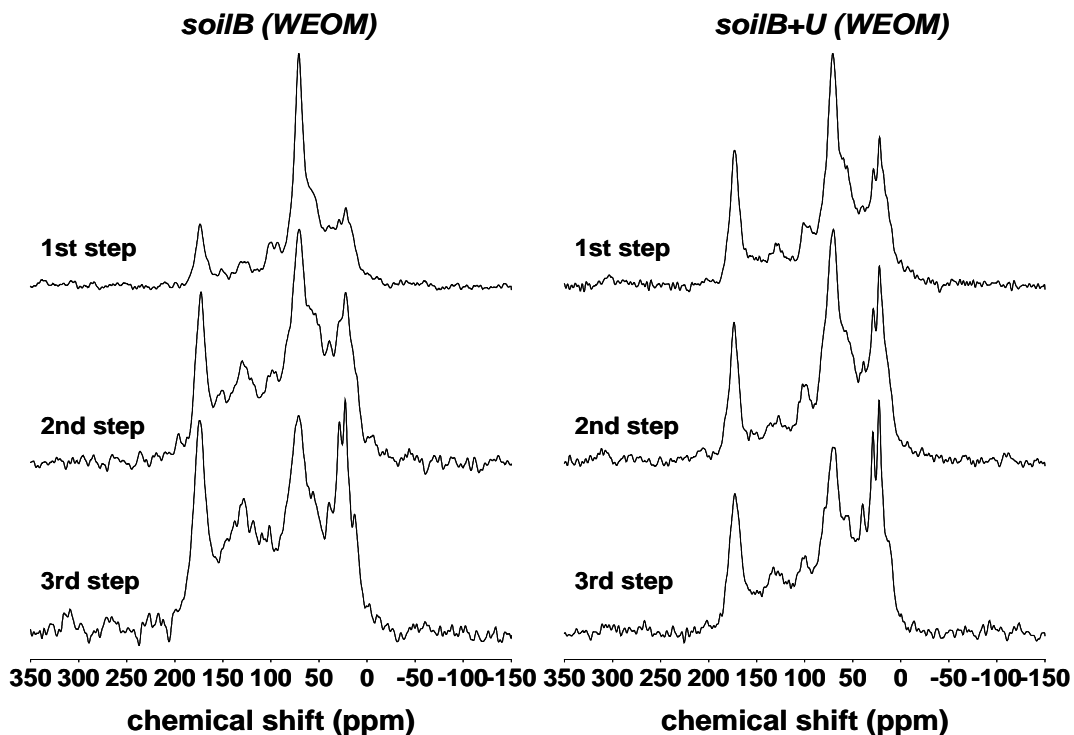


Figure 15 Experiment *B*: <sup>13</sup>C CPMAS NMR spectra of the sequentially extracted WEOM (first 3 steps) of untreated bulk soil (*soilB*) and the bulk soil after soil disruption (*soilB+U*). Due to the declining yields of extractable OM only the WEOM of the first 3 steps (out of 5) were measurable.

## 4.2 Salt extractable OM – amounts and composition

From the aliquots of the *soilA+U* material, statistically significant larger amounts of SEOC (Table 7) were extractable compared to the *soilA* material, +81% before and +67% after the incubation experiment. Standard deviation of extractable SEOC was larger for disrupted samples and after the experiment. Larger amounts of SEOC were also detected for *soilB* (+34%) and *soilB+U* (+158%) in relation to *soilB-WEOM* before incubation. These differences decreased but were still detectable after the incubation experiment; therefore, the amounts of  $K_2SO_4$  extractable DOC were larger in aliquots of *soilB* (+13%) and *soilB+U* (+49%) compared to *soilB-WEOM*. The difference in SEOC was only significant between the treatments after experiment A ( $p < 0.05$ ). The SEOC values between intact and disrupted soil before experiment A and B were only different at a level of  $p = 0.109$  due to the low number of replicates ( $n = 3$ ). The amounts of extractable SEOC (Table 7) of *soilA* / *soilA+U* were remarkable larger (+194% / +176%) than that of *soilB* / *soilB+U* ( $p < 0.01$ ).

**Table 7** Salt extractable organic carbon (SEOC) contents, specific UV-absorbance at 254 nm (SUVA<sub>254</sub>) of the 10 mM  $K_2SO_4$  solution extracts before ( $t_0$ ) and after ( $t_x$ ) the incubation experiment of soil aliquots and cumulative released  $CO_2$ -C from bulk soil (*soilA*, *soilB*), bulk soil after soil disruption (*soilA+U*, *soilB+U*) and bulk soil after soil disruption and subsequent sequential WEOM extraction (*soilB-WEOM*). Statistical significant differences between different treatments are indicated by \* ( $p < 0.05$ ).

		experiment A		experiment B		
		<i>soilA</i>	<i>soilA+U</i>	<i>soilB</i>	<i>soilB+U</i>	<i>soilB-WEOM</i>
SEOC mg (gC) <sup>-1</sup>	$t_0$	4.60±1.00	8.33±1.14	1.57±0.29	3.02±0.52	1.17±0.08
	$t_x$	3.72±0.67	6.20±2.06	0.68±0.16	0.90±0.06	0.60±0.09
SUVA <sub>254</sub> L*mg C <sup>-1</sup> *m <sup>-1</sup>	$t_0$	2.98±0.26	2.37±0.02	3.86±0.16	3.69±0.28	2.41±0.19
	$t_x$	5.07±0.10	2.78±0.05	5.84±0.41	6.43±0.38	6.20±1.00
CO <sub>2</sub> -C mg (gC) <sup>-1</sup>		12.46±0.41	17.14±0.77	7.52±0.56	9.55±0.18	7.67±0.15

The SUVA<sub>254</sub> values of the SEOM extracts were similar for both sets of samples before experiment A, but increased by the factor 2 in the SEOM extracts of *soilA* after the incubation (Table 7). The SUVA<sub>254</sub> of the extracts from *soilB-WEOM* before experiment B were lower ( $p = 0.109$ ) than the SUVA<sub>254</sub> of the other two sets of samples (Table 7). The SUVA<sub>254</sub> was clearly higher in the extracts of the soil material

from experiment *B* compared to experiment *A*; thus, was consistent with the aromaticity obtained by  $^{13}\text{C}$ -CPMAS NMR. No distinctive differences of the chemical composition were detectable by  $^{13}\text{C}$ -CPMAS NMR spectroscopy for the SEOM extracts of experiment *A* between both sets of samples and between  $t_0$  and  $t_x$  (Table 8). In contrast to experiment *A*, clear differences between the  $\text{K}_2\text{SO}_4$  extracts of the different sample sets were detectable by  $^{13}\text{C}$ -CPMAS NMR spectroscopy (Table 8). A clear trend of decreasing contents of O/N-alkyl C was shown in the order of *soilB* to *soilB+U* and *soilB-WEOM*. For the O/N-alkyl C and aromatic C compounds, clear differences could also be shown between the extracts obtained before and after the incubation. In all SEOM extracts, the relative O/N-alkyl C intensities decreased after the incubation, whereas the aromatic C increased.

Table 8 Integrated chemical shift regions obtained by  $^{13}\text{C}$  CPMAS NMR for the sequentially extracted WEOM of untreated bulk soil (*soilA*, *soilB*), the bulk soil after soil disruption (*soilA+U*, *soilB+U*), and the SEOM before ( $t_0$ ) and after ( $t_x$ ) the incubation experiment of aliquots from the incubated soil materials of experiment A and B.

sample	alkyl-C		O/N-alkyl-C		aromatic-C		carbonyl-C		alkyl/O/N- aromatic/alkyl-C		aromatic/alkyl-C	
	(%)	(%)	(%)	(%)	(%)	(%)	(%)	(%)	alkyl-C	alkyl-C	alkyl-C	/N-alkyl-C
<b>WEOM extraction</b>	<b>soilB</b>	1st step	23	56	11	10	0.42	0.47	0.20			
		2nd step	23	41	21	15	0.56	0.89	0.50			
		3rd step	22	35	23	20	0.64	1.05	0.66			
	<b>soilB+U</b>	1st step	25	46	15	15	0.55	0.58	0.32			
		2nd step	27	45	13	16	0.59	0.50	0.30			
		3rd step	28	39	17	15	0.72	0.61	0.44			
	<b>soilA</b>	$t_0$	21	64	5	10	0.33	0.25	0.08			
		$t_x$	22	60	7	10	0.37	0.30	0.11			
	<b>soilA+U</b>	$t_0$	21	63	6	10	0.33	0.30	0.10			
$t_x$		18	60	9	13	0.30	0.47	0.14				
<b>soilB</b>	$t_0$	15	61	10	13	0.25	0.67	0.17				
	$t_x$	20	50	16	14	0.41	0.77	0.31				
<b>soilB+U</b>	$t_0$	21	58	8	14	0.36	0.37	0.13				
	$t_x$	23	50	13	13	0.47	0.57	0.27				
<b>soilB- WEDOM</b>	$t_0$	20	54	12	13	0.37	0.60	0.22				
	$t_x$	21	46	17	15	0.46	0.83	0.38				

The contents of neutral sugars were higher in the SEOM extracts of *soilA* than in the SEOM extracts of *soilA+U* (Table 9). The total sugar yields for SEOM of *soilA* changed only slightly between  $t_0$  and  $t_x$ , whereas the sugar yields of *soilA+U* clearly decreased due to the decreasing SEOC. The arabinose and xylose contents in the SEOM extracts of both sample sets showed a distinctive increase from  $t_0$  to  $t_x$ . The normalized yields of neutral sugars extracted by 10 mM  $K_2SO_4$  before the incubation were clearly larger from the *soilA+U* material (Table 10) than from the *soilA* material, mainly caused by a nearly twofold higher yield of galactose, mannose, xylose, arabinose and rhamnose. The glucose yields were similar for both sets of samples before the incubation. The galactose+mannose / arabinose+xylose (GM/AX) ratios were higher in the extracts from the intact soil material of *soilA* compared to *soilA+U*. Total sugar yields per unit C of the soil material decreased for both sets of samples. This decrease in neutral sugars was mainly due to lower amounts of glucose for the *soilA* material and lower amounts of glucose, galactose and mannose for the *soilA+U* material after the incubation. After incubation, extracted amounts of fucose, xylose and arabinose increased in both sets of samples. The highest contents of neutral sugars in experiment *B* were detected for the SEOM extracts of *soilB*, mainly derived from glucose, followed by the extracts of *soilB-WEOM* (Table 9). For all extracts, lower sugar contents of the SEOM extracts were shown after the incubation. All extracts had distinctive higher galactose contents after the incubation. Also for the amounts of neutral sugars normalized on extractable SEOC (Table 10), a clear decrease was observed for all extracts after the incubation. The largest normalized amounts of  $K_2SO_4$  extractable sugars were found in aliquots of *soilB+U* dominated by glucose with 42% of the total sugar yield. The lowest sugar yields were found in extracts of *soilB-WEOM*. In contrast to the SEOM extracts of *soilA* / *soilA+U*, the extracts of *soilB* / *soilB+U* showed a drastic decline of arabinose and xylose after incubation (Table 9 and Table 10). Therefore, no meaningful GM / AX ratios were obtained for the extracts with arabinose contents below the detection limit. Before the incubation, the extracts from the intact *soilB* material showed a distinctive higher GM / AX ratio (15.8) than the extract of the disrupted *soilB+U* material (4.7).

Table 9 Contents of neutral sugars derived from SEOM extracted by 10mM K<sub>2</sub>SO<sub>4</sub> of experiment A and B (before (t<sub>0</sub>) and after (t<sub>x</sub>) the incubation), and in water extractable DOM from the first extraction step. The abbreviation n.d. indicates values below the detection limit. Standard error is given in parentheses.

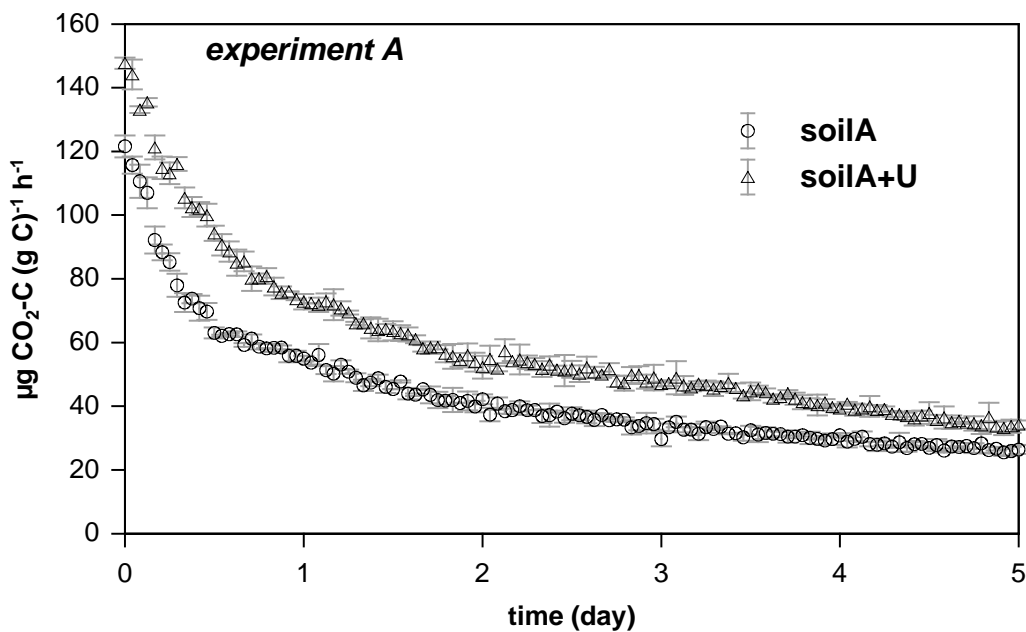
sugar mg g <sup>-1</sup> DOC	experiment A						experiment B						WEOM extraction, 1st step	
	soi/A		soi/A+U		soi/B		soi/B+U		soi/B-WEOM		soi/B	soi/B+U		
	t <sub>0</sub>	t <sub>x</sub>	t <sub>0</sub>	t <sub>x</sub>	t <sub>0</sub>	t <sub>x</sub>	t <sub>0</sub>	t <sub>x</sub>	t <sub>0</sub>	t <sub>x</sub>	t <sub>0</sub>	t <sub>x</sub>		
rhamnose	18.0 (0.3)	25.4 (0.3)	25.6 (0.3)	27.0 (0.1)	14.3 (0.3)	12.3 (1.1)	28.3 (0.5)	17.1 (0.4)	25.4 (0.3)	15.6 (0.4)	14.1 (1.4)	19.5 (0.9)		
fructose	n.d.	5.2 (0.2)	0.6 (0.1)	7.3 (0.2)	n.d.	n.d.	8.8 (0.3)	n.d.	n.d.	n.d.	0.7 (0.1)	4.3 (0.2)		
arabinose	6.7 (0.0)	13.5 (0.3)	7.4 (0.1)	13.5 (0.1)	3.5 (0.1)	n.d.	12.6 (0.3)	n.d.	n.d.	n.d.	4.5 (0.1)	9.3 (0.3)		
xylose	6.3 (0.1)	14.0 (0.2)	8.1 (0.2)	14.2 (0.3)	6.7 (0.2)	2.6 (0.0)	13.7 (0.3)	6.1 (0.1)	6.1 (0.2)	2.1 (0.0)	6.3 (0.2)	8.5 (0.3)		
mannose	73.5 (2.1)	79.6 (1.9)	79.4 (0.1)	55.9 (1.0)	31.4 (0.7)	23.1 (0.3)	44.7 (0.7)	21.6 (0.3)	37.0 (0.3)	30.0 (0.3)	18.2 (0.9)	17.4 (0.4)		
galactose	98.3 (2.4)	118 (2.1)	112.1 (3.0)	102.6 (1.7)	131.4 (2.8)	170.5 (1.3)	78.3 (0.9)	134.9 (1.8)	186.0 (2.3)	210.6 (1.8)	63.3 (1.9)	101.2 (2.1)		
glucose	183.3 (4.2)	190.1 (3.3)	99.2 (0.7)	50.6 (0.9)	406.2 (5.9)	161.9 (3.7)	136.5 (1.1)	59.0 (0.9)	240.1 (3.4)	74.5 (1.6)	233.8 (6.8)	157.0 (3.2)		
GM / AX ratio	13.1	7.2	12.3	5.7	15.8	4.7	7.5	6.7	7.5	6.7	7.5	6.7		
<b>total</b>	<b>386.1 (8.1)</b>	<b>445.8 (1.5)</b>	<b>332.3 (4.6)</b>	<b>271.1 (2.3)</b>	<b>593.5 (5.9)</b>	<b>370.4 (4.3)</b>	<b>322.8 (2.6)</b>	<b>238.7 (1.6)</b>	<b>494.6 (4.3)</b>	<b>332.8 (3.2)</b>	<b>340.9 (11.6)</b>	<b>317.2 (6.0)</b>		

Table 10 Normalized yields of neutral sugars in relation to units C in the soil material extracted by 10mM K<sub>2</sub>SO<sub>4</sub> of experiment A and B (before (t<sub>0</sub>) and after (t<sub>x</sub>) the incubation), and in water extractable DOM from the first extraction step. n.d. – values below detection limit.

sugar µg / g C	experiment A		soil+U		soil		soil+U		soil-WEDOM		WEDOM extraction 1st step	
	t <sub>0</sub>	t <sub>x</sub>	t <sub>0</sub>	t <sub>x</sub>	t <sub>0</sub>	t <sub>x</sub>	t <sub>0</sub>	t <sub>x</sub>	t <sub>0</sub>	t <sub>x</sub>	soil	soil-WEDOM
rhamnose	82.7	94.3	213.1	167.5	22.3	8.4	85.4	15.3	29.7	9.4	34.7	101.4
fucose	0.0	19.3	5.1	45.2	0.0	0.0	26.5	0.0	0.0	0.0	1.8	22.4
arabinose	31.0	50.2	61.7	83.6	5.5	0.0	38.2	0.0	0.0	0.0	11.2	48.1
xylose	29.2	52.1	67.8	88.0	10.6	1.8	41.4	5.5	7.1	1.3	15.5	44.2
mannose	337.8	296.1	661.4	346.5	49.2	15.8	135.1	19.3	43.3	18.1	44.9	90.4
galactose	452.3	438.9	933.7	635.8	205.9	116.5	236.8	121.0	217.6	127.0	156.1	526.1
glucose	843.2	707.3	826.3	314.1	636.3	110.6	412.7	52.9	280.9	45.0	577.0	816.3
<b>total</b>	<b>1776.2</b>	<b>1658.2</b>	<b>2768.9</b>	<b>1680.7</b>	<b>929.9</b>	<b>253.1</b>	<b>976.1</b>	<b>214.0</b>	<b>578.7</b>	<b>200.8</b>	<b>841.2</b>	<b>1649.0</b>

### 4.3 Influence of soil disruption and OM removal on C mineralisation

In Figure 16, the respiration rate of the first 5 days of experiment *A* are shown starting with the first peak after an equilibration time of 12 hours after wetting. From the beginning a significant higher CO<sub>2</sub> release was detected for the disrupted soil material *soilA+U* compared to the untreated soil *A* (Figure 16). Within the first 5 days of incubation, disrupted soil material (*soilA+U*) had released +56.8% ( $\mu\text{g CO}_2\text{-C (g C)}^{-1}$ ) than the intact *soilA* material. The trend of higher SOC mineralisation continued throughout the experiment. As illustrated in Figure 18, at the end of experiment *A* (after 18 days), the difference between the two sample sets decreased to +38% ( $\mu\text{g CO}_2\text{-C (g C)}^{-1}$ ). In experiment *A* respiration rates were found to be significantly different between disrupted and undisrupted soil aggregates ( $F[1,4] = 74.98, p < 0.001$ ) throughout the experiment.



**Figure 16 Experiment A: Respiration rates as mean values with standard deviation ( $n = 3$ ) of the first 5 days of bulk soil (soil A), bulk soil after soil disruption (soilA+U).**

At the beginning of incubation experiment *B*, the respiration rates increased from *soilB-WEOM* to *soilB* and *soilB+U*, whereas every set of samples showed a distinctive peak at the start of the experiment (Figure 17). The disrupted soil samples, *soilB+U* and *soilB-WEOM*, showed subsequent peaks between day 0.5 and 3 after the first peak at the beginning of the experiment. The maximum of a second single peak was visible after 1.5 days for *soilB-WEOM*. The respiration rates of the *soilB+U* samples showed two additional peaks after day 1 and around day 2. For the



respiration rates of the intact soil material of *soilB* an exponential decrease and no additional peaks were detected (Figure 17).

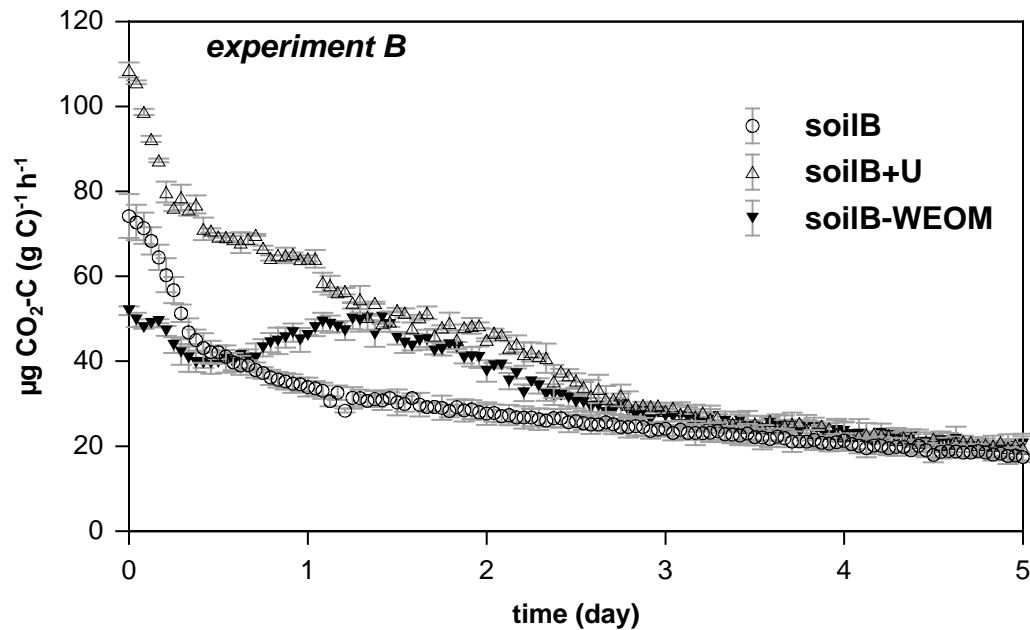


**Figure 17 Experiment B: Respiration rates as mean values with standard deviation ( $n = 3$ ) of the first 5 days of bulk soil (*soilB*), bulk soil after soil disruption (*soilB+U*) and bulk soil after soil disruption and subsequent sequential WEOM extraction (*soilB-WEOM*).**

After 1/3 of experiment *B* (day 6), *soilB+U* (+42% CO<sub>2</sub>-C per unit C) and *soilB-WEOM* (+14% CO<sub>2</sub>-C per unit C) released more CO<sub>2</sub> than the *soilB* samples (Figure 19). At the end of experiment *B*, the cumulative CO<sub>2</sub>-C release (per unit C of the soil material) of the *soilB-WEOM* equalled that of *soilB*, whereas the *soilB+U* samples released +27% in relation to *soilB*. In experiment *B* the differences were not statistical significant on the  $p < 0.05$  level ( $F[2,6] = 5.09$ ,  $p = 0.051$ ) for the whole duration of the experiment. Nevertheless, splitting of the respiration rate of experiment *B* (Figure 17) into the first 2.5 days ( $F[2,6] = 9.26$ ,  $p = 0.015$ ) and days 2.5 to 18 ( $F[2,6] = 5.42$ ,  $p = 0.045$ ) led to significant differences. Therefore the first flush effects until day 2.5 and also the later basal respiration were significantly different.

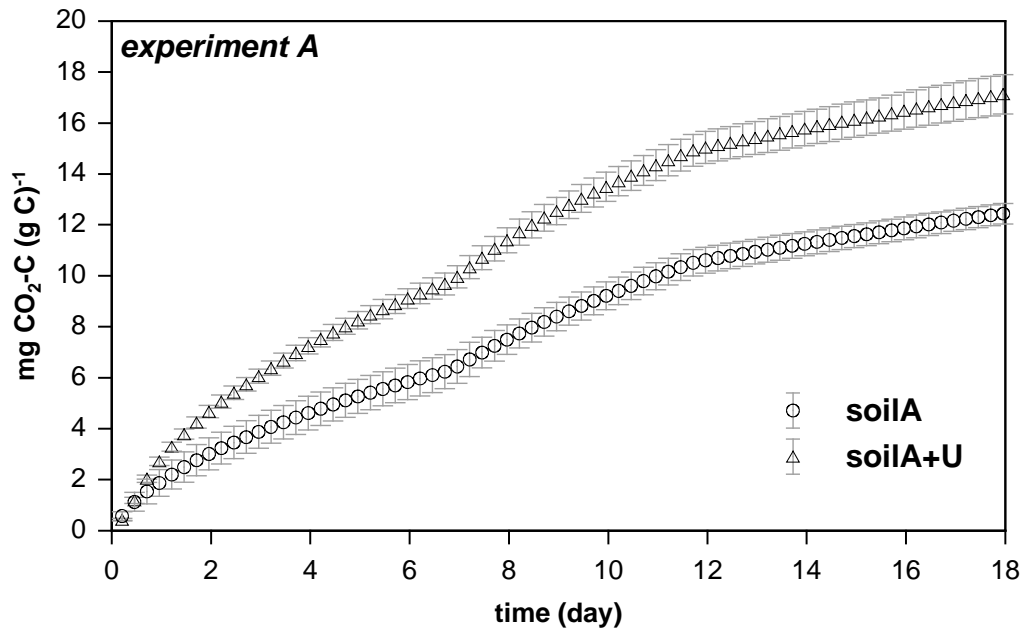


Figure 18 Cumulative  $\text{CO}_2\text{-C}$  release per g C within the sample, shown for experiment A as mean values with standard deviation ( $n = 3$ ).

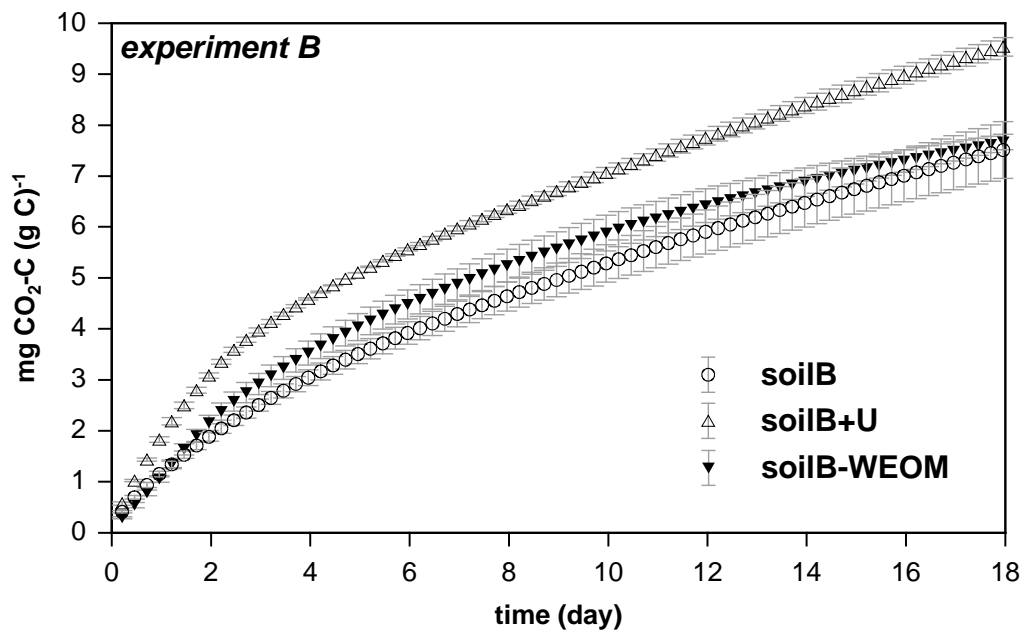


Figure 19 Cumulative  $\text{CO}_2\text{-C}$  release per g C within the sample, shown for experiment B as mean values with standard deviation ( $n = 3$ ).

The effect of interaction between the factors “treatment” and “time” on soil respiration ( $RR=f(\text{treatment} * \text{time})$ ) was also tested for both experiments, which differ significantly between the two treatment groups in both experiments (experiment A:  $F[540,2169] = 11.109$ ,  $p < 0.001$ ; experiment B:  $F[912,2736] = 11.68$ ,  $p < 0.001$ ).

Due to the low number of replicates ( $n = 3$ ) the cumulative released  $\text{CO}_2\text{-C}$  per unit C of the sample (Table 7) differed between the intact and disrupted soil material only at a level of  $p=0.109$ .

#### 4.4 Influence of aggregate disruption on amount and composition of extractable OM

Increased releases of SEOM and WEOM after ultrasonication of soil material indicated the dissolution of formerly protected SOM. Although the amounts of extractable OM differed clearly between the two soil materials (*soilA* and *soilB*), the mechanism which enhanced the solubility of formerly protected SOM are assumed to be the same. The exposure of plant residues formerly occluded within soil aggregates may be seen as major source for the elevated SEOC (+81% for *soilA+U* and +92% for *soilB+U*) concentrations of the disrupted soil material. In an experiment about aggregate stability FULLER and GOH (1992) obtained increasing amounts of dissolved carbohydrates with increasing aggregate disruption, and explained it mainly by the increase in exposed mineral bound SOM on clay minerals. Contrary to this finding, less neutral sugars were obtained in SEOM extracts of disrupted soil compared to intact soil. Taking the decreasing O/N-alkyl signals (from step 1 to 3) for the sequentially extracted WEOM of *soilB* into account, the dissolution of carbohydrates may be sustained in disrupted soils (*soilB+U*, Figure 15), maybe also due to the disruption of POM tissue. Larger contents of plant derived carbohydrates (arabinose + xylose) were shown for the extracts of the disrupted soil material (+19% for *soilA+U* and +158% for *soilB+U*). A higher dissolution of plant derived instead of microbial derived carbohydrates was indicated by the lower GM / AX ratios of the SEOM extracts from the disrupted soil. This also may indicate a stronger release of plant derived compounds from POM due to ultrasonication. SCHMITT et al. (2008) found lower sugar amounts in bulk soils after freezing-thawing. The authors suggested the decreased sugar contents to be affected by increased DOM release and a possible change in soil structure. In the present study a possible microbial cell lysis by ultrasonication was not demonstrated by the composition of the analysed neutral sugars, although other cell compounds could have been affected. A possible enhanced release of microbial C after cell lysis due to an osmotic shock following rewetting of the dry soil materials would have affected both intact and disrupted

samples in the same way. This is supported by APPEL (1998) who demonstrated that additional water extractable organic nitrogen after drying of soil material was not preferentially derived from newly killed microbes. FIERER and SCHIMEL (2003) also showed an increased extractability of non-microbial OM after drying-rewetting of two semi-arid soils assuming an enhanced release of formerly inaccessible SOM from aggregate interiors.

Clear differences were obtained for the SEOM properties of the two soil materials. The SEOM extracted from the *soilA* was less aromatic and showed higher O/N-alkyl C intensities than the extracts of *soilB*. KALBITZ et al. (2003) showed that DOM rich in aromatic compounds was relatively stable against biodegradation. From this point, it seemed that in soil material *B*, the more labile and less aromatic DOM components may already have been utilized, whereas in soil material *A*, by the composition of the extractable DOM a larger proportion of labile components was reflected for the soil matrix.

#### 4.5 Alterations in composition of WEOM during sequential extraction

Increased ionic strength showed a clear influence on SOM mobilisation by the lower SOC extractability of 10 mM K<sub>2</sub>SO<sub>4</sub> compared to the extraction with deionised water (Figure 13 and Table 7). The increase of extractable WEOC compared to SEOC ( $p < 0.01$ ) extractable from the samples was at the same magnitude as shown by ZSOLNAY (1996), who obtained +50 to +100% by the extraction with deionised water in contrast to the extraction with 4 mM CaSO<sub>4</sub>.

The lower amounts and the faster decline of extractable WEOM of the intact *soilB* compared to the *soilB+U* material reflected the influence of spatial inaccessibility on the mobilisation of WEOM. Although the repeated WEOM extraction procedure may have also disrupted additional aggregates of the intact soil, a sustained preservation of dissolvable SOM components could be shown for the intact soil after several extraction steps. It seemed that repeated shaking of soil suspensions had no distinctive effect on the integrity of the soil aggregates and therefore the leaching of WEOM. No clear evidence could be found for additional biomass release due to cell lysis and destruction of pore space as proposed by ZSOLNAY (1996) for repeated DOM extractions. Nevertheless, the extracts from both sets of samples showed a similar alteration of chemical composition with cumulative extractions steps. Although

such a highly significant correlation between  $SUVA_{254}$  and aromaticity obtained by  $^{13}C$  NMR as shown by WEISHAAR et al. (2003) could not be found, increasing  $SUVA_{254}$  values were obtained with increasing aromatic C intensities for the WEOM extracts. In the present study the  $SUVA_{254}$  of WEOM from the disrupted *soilB+U* tended to be higher after the third extraction step. In a study on frost impacts on soils in southern Norway AUSTNES and VESTGARDEN (2008) also showed a significant increase in  $SUVA_{254}$  in the course of fast cycling freezing-thawing events.

Prolonged dissolution of WEOM during sequential extraction from disrupted soil material was reflected by the low changes in carbonyl C and aromatic C. By the drastic decline of O/N-alkyl C concomitant to the pronounced increase of carbonyl and aromatic C compounds in extracts of intact *soilB*, it could be shown that labile DOM fractions were rapidly leached out from intact soil samples. A prolonged dissolution and mobilisation process of DOM is assumed after drastic physical disruption also for soil systems under field conditions e.g. after tillage or aggregate cracking due to rain drops or freezing-thawing cycles.

The GM / AX ratios were in the same order of magnitude as shown by KAISER et al. (2001) for DOM of seepage water under a beech (*Fagus sylvatica* L.) forest. No considerable leaching of microbial biomass is assumed due to the sequential extraction with deionised water prior to experiment *B* (*soilB-WEOM* samples). Nevertheless, the usage of 10 mM  $K_2SO_4$  instead of deionised water led to a drastic increase of microbial derived sugars in the extracts, enabling a more sensitive distinction between the dominating sources of the extractable carbohydrates. The distinctive higher amounts of plant derived sugars (arabinose and xylose) in the WEOM extracts after ultrasonication indicated the enhanced bioavailability of formerly occluded plant derived OM and probably enhanced C release from POM tissue, which was also demonstrated for SEOM extracts and soil material *A*.

#### 4.6 Enhanced mineralisation of former inaccessible OM after aggregate disruption

Both respiration experiments (*A* and *B*) revealed a distinctively enhanced  $CO_2$  release and therefore an enhanced microbial activity after the artificial soil disruption. A direct influence on the SOC mineralisation is assumed due to the absence / lowering of the spatial inaccessibility of SOM. Furthermore, a clear coherency could

be demonstrated between the previous OM removal by sequential WEOM extraction and the decrease in respired CO<sub>2</sub> for the *soilB-WEOM* samples. The distinctive higher respiration rates of the disrupted *soilA+U* and *soilB+U* at the start of the experiments were induced by an enhanced bioavailability of former protected DOM. FIERER and SCHIMEL (2003) explained the increased CO<sub>2</sub> release after drying and rewetting mainly by additional available cytoplasmic C resulting from microbial cell lysis due to the osmotic shock. By labelling with <sup>14</sup>C enriched glucose HERRMANN and WITTER (2002) showed a predominance of microbial derived CO<sub>2</sub> after freeze-thaw cycles. In the present experiments these findings might explain the first CO<sub>2</sub> flush which were found in every sample, but could not explain the additional amount of released CO<sub>2</sub> due to artificial physical disruption. Similar initial conditions can be concluded as all samples were rewetted to the same extent. Furthermore, the larger amounts of extractable plant derived sugars (along with lower GM / AX ratios) after ultrasonic disruption may disprove a dominant role of microbial components as source of the additionally respired CO<sub>2</sub>.

After the first CO<sub>2</sub> flush mainly related to the additional available DOM, a second peak of the respiration rates was detected after 1 to 2 days for the disrupted samples. This effect was much more pronounced in soil material *B* with less SEOM (*soilB+U* and *soilB-WEOM*). An increase in the utilisation of artificially exposed surfaces (particulate and mineral-bound SOM) may have taken place after the mineralisation of the readily available DOM fractions at the start of the experiments. The differences in the sugar yields between experiment *A* and *B* before and after the incubation supported this finding. As microbial activity is mainly restricted to the liquid phase, the increase of plant derived sugars (arabinose and xylose) in the SEOM after experiment *A* could evidence an increased microbial utilisation of plant residues. In a study on the seasonal changes of the quality of soil solutions KAWAHIGASHI et al. (2003) also proposed a stronger release of plant derived sugars due to enhanced microbial activities. On the contrary, the plant derived sugars were nearly absent in the extracts of the soil material *B*. It seemed that more DOM was mobilised than could be mineralised during experiment *A*, whereas the increased galactose contents of the SEOM extracts after experiment *B* may indicate a complete mineralisation of dissolved plant derived sugars and enhanced re-synthesis of microbial residues. This is supported by the differences of total CO<sub>2</sub>-C yields and SEOC for *soilB+U* and *soilB-WEOM* in relation to *soilB*. The additional released amount of CO<sub>2</sub>-C

(*soilB+U* =  $2.8 \pm 0.4$  mg; *soilB-WEOM* =  $2.7 \pm 0.0$  mg) equals nearly the additional total SEOC (*soilB+U* =  $2.0 \pm 0.4$  mg; *soilB-WEOM* =  $3.1 \pm 0.0$  mg) in relation to *soilB*. The yields of neutral sugars within SEOM and therefore fractional DOM bioavailability seemed to be unaffected by the bulk SOM, but highly affected by a small labile pool of plant residues.

## 5. Differentiation of vertical soil organic matter distribution and composition four years after soil homogenisation

Especially in the course of land-use change from cropland to forest the new establishment of SOM depth gradients is of major concern for C and N cycles, but also for the nutrient supply of the growing trees. Therefore, studying lysimeters stocked with trees offers a unique chance to analyse these SOM processes at an early stage after the disturbance of the soil system (see page 16). In the given work I studied how depth gradients of SOM content and composition developed within 4 years after soil homogenisation. By using eight lysimeters filled with the same soil material a unique data set was gained to demonstrate SOM changes on a statistically significant level. The soil material which was taken at a beech forest site and homogenised afterwards, was assumed to have no depth gradient at the beginning of the experiment. To track the differentiation of certain SOM fractions with depth a set of different techniques was combined. By a coupled density and particle-size fractionation protocol together with the application of  $^{15}\text{N}$  labelled beech litter it was aimed to study the incorporation of litter derived N in different SOM fractions. The spectroscopic analyses ( $^{13}\text{C}$ -CPMAS NMR) of the SOM fractions helped to unravel the development of depth gradients of SOM composition after soil homogenisation.

### 5.1 Depth distribution of mass and C and N contents of SOM fractions

The mass of the particle size fractions (sand, silt and clay) was evenly distributed within the top 20 cm of the lysimeters (Figure 20), with a clear dominance of the silt fraction. A clear trend of decreasing mass was observed for all fPOM ( $-79\pm 8\%$ ), oPOM ( $-74.6\pm 13.3\%$ ) and oPOM<sub>small</sub> ( $-57.9\pm 27.7\%$ ) fractions from the 0–2 cm to the 10–20 cm layer. Although the observed mass range of POM fractions was large, the decrease in mass with depth was in most cases significant at  $p < 0.05$ .

The highest C and N contents were found for the oPOM, followed by the fPOM and oPOM<sub>small</sub> fractions (Table 11). A significant decrease of C contents was only observed with depth for oPOM<sub>small</sub>, whereas the N contents decreased significantly with depth in all three POM fractions.



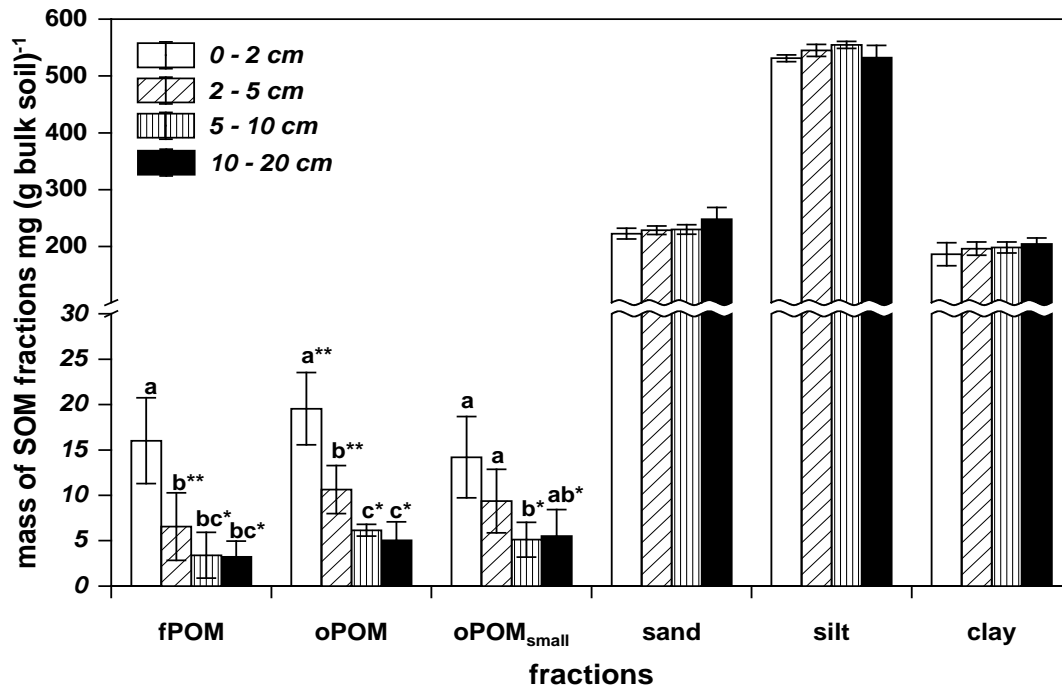


Figure 20 Mass distribution of the SOM and particle size fractions from the studied lysimeters. Data points are the mean values of 8 replicates with error bars representing standard deviations. Significant differences of the masses between different soil layers of a single SOM fraction are indicated by letters and \* ( $p < 0.05$ ), \*\* ( $p < 0.01$ ).

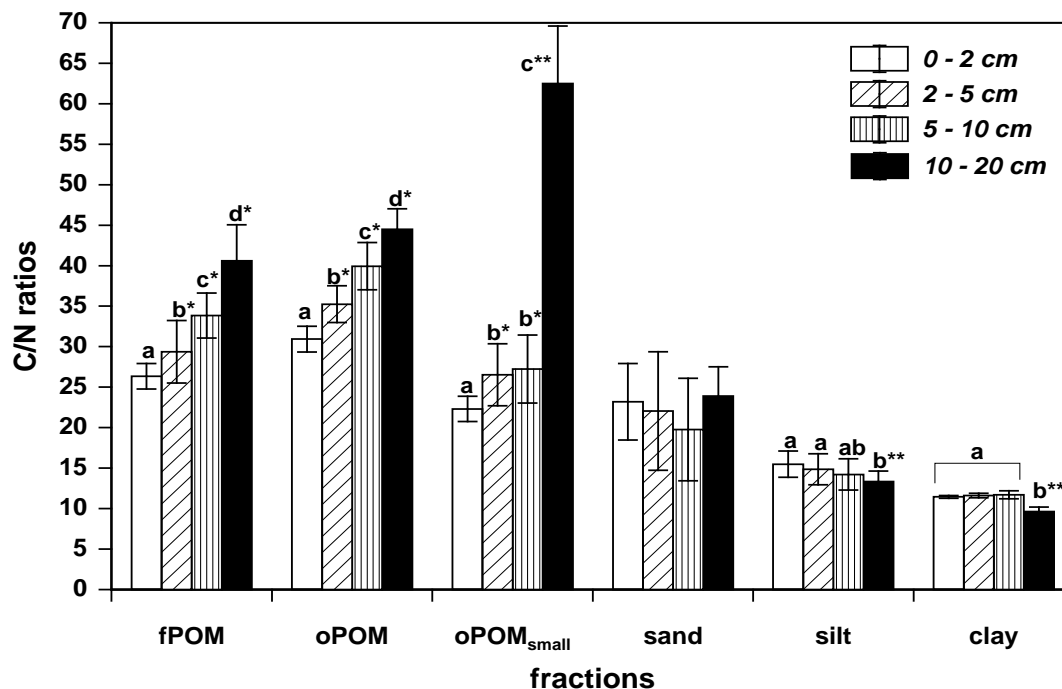


Figure 21 Carbon to nitrogen ratios of the SOM and particle size fractions from the studied lysimeters. Data points are the mean values of 8 replicates with error bars representing standard deviations. Significant differences of the C/N ratios between different soil layers of a single SOM fraction are indicated by letters and \* ( $p < 0.05$ ), \*\* ( $p < 0.01$ ).

The C/N ratio of the fPOM at 0–2 cm ( $26.3 \pm 1.6$ ) was not significantly lower than the initial C/N ratio of the litter of the Oi layer ( $28.7 \pm 2.4$ ). A clear increase ( $p < 0.05$ ) of C/N ratios with depth was detected for all POM fractions with a maximum of the POM<sub>small</sub> ( $62.5 \pm 7.1$ ) in the 10–20 cm layer (Figure 21). For all replicates within a single soil layer a clear decrease could be demonstrated in C/N ratios from the POM to the mineral-bound SOM fractions.

Large proportions of C (Figure 22) were stored within the fraction  $< 63 \mu\text{m}$  (silt and clay), from  $47 \pm 3.7\%$  (10–20 cm) to  $60.3 \pm 5.9\%$  (5–10 cm). Within the  $< 63 \mu\text{m}$  fraction the C storage was clearly dominated by the clay separates in all soil layers, culminating at  $46.4 \pm 5.2\%$  clay-bound C in the 5–10 cm layer. From the 0–2 cm layer to the 5–10 cm layer the C content of the POM fractions clearly decreased ( $p < 0.05$ ). For every POM fraction a slight increase in C content in relation to the bulk soil was observed in the 10–20 cm layer. Thus, the C content of the oPOM<sub>small</sub> had its maximum within the 10–20 cm layer. The N storage also was clearly dominated by the mineral fractions accounting for about  $82.1 \pm 7.7\%$  on average over all soil layers (Figure 22). A clear trend of decreasing N storage with depth was found for both fPOM and oPOM fractions ( $p < 0.05$ ). Nitrogen amounts related to the clay size separates increased significantly ( $p < 0.01$ ) with depth.

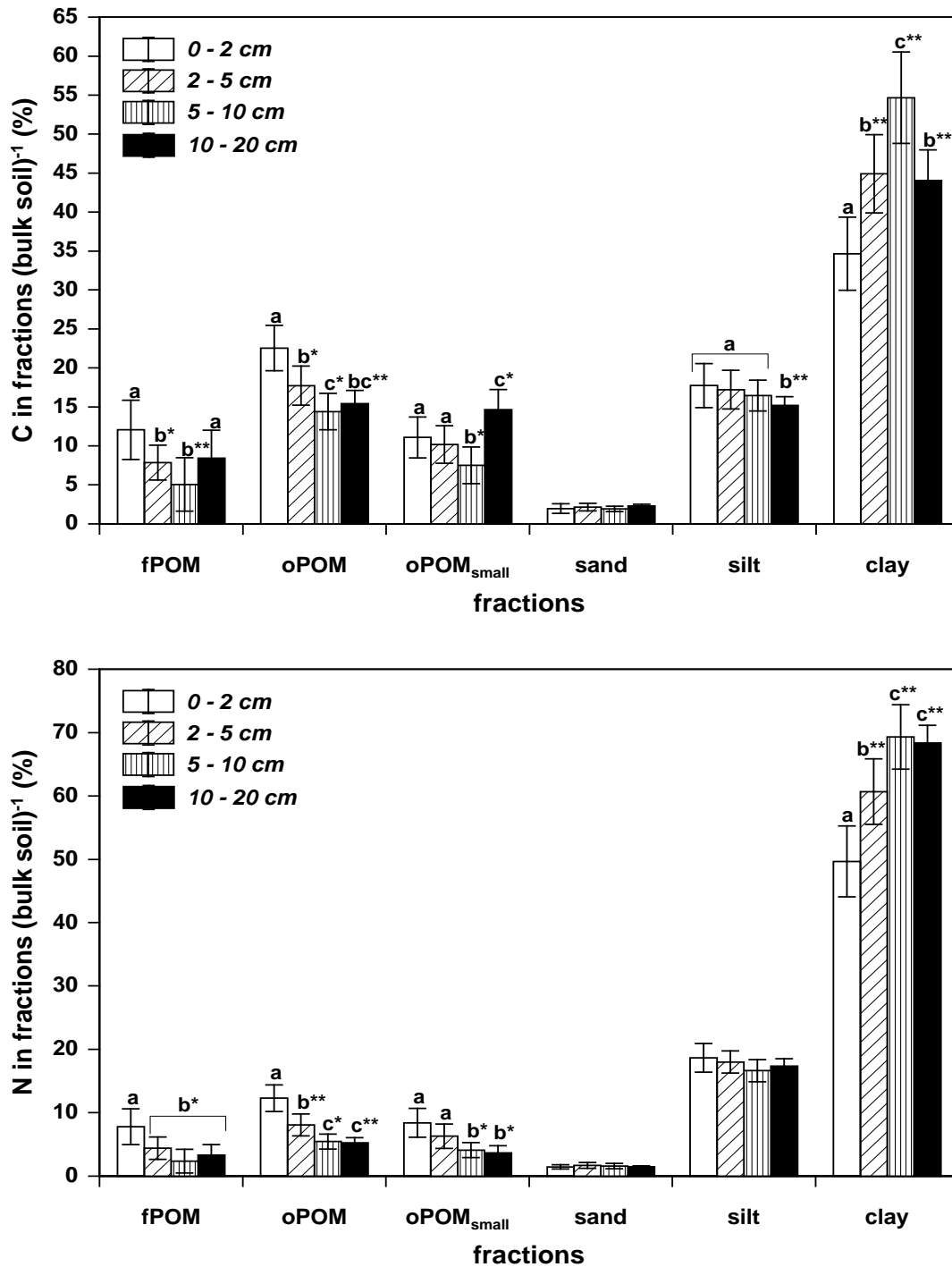


Figure 22 Carbon and nitrogen distribution within SOM and particle size fractions related to bulk soil (<math><6.3\text{ mm}</math>) for the four soil layers studied. Data points are the mean of 8 replicates with error bars representing standard deviations. Significant differences of the C- and N-amounts between different soil layers of a single SOM or particle size fraction are indicated by letters and \* ( $p < 0.05$ ), \*\* ( $p < 0.01$ ).

Table 11 Carbon and nitrogen contents of the density (POM) and particle size fractions (sand, silt and clay). Data is given as mean values with standard deviation (n = 8). Significant differences related to the soil layer of C and N contents of a single SOM fraction is indicated by letters and \* ( $p < 0.05$ ) and \*\* ( $p < 0.01$ ).

	depth	fraction					
		fPOM	oPOM	oPOM <sub>small</sub>	sand	silt	clay
OC mg (g bulk soil) <sup>-1</sup>	0 to 2 cm	312.4±16.8 a	447.3±28.8	305.0±29.5 a	3.6±1.0 a	19.4±2.7 a	73.1±8.5 a
	2 to 5 cm	324.3±33.5 a	452.2±27.6	297.0±45.7 ab	2.6±0.6 a	12.7±2.0 b**	61.4±8.3 b**
	5 to 10 cm	332.4±30.1 a	449.3±54.7	267.7±30.6 b*	1.6±0.3 b**	8.6±1.7 c**	51.8±7.0 c*
	10 to 20 cm	337.8±22.5 b*	408.7±92.9	353.6±83.1 ac*	1.2±0.2 c*	4.7±1.0 d**	28.1±4.3 d**
N mg (g bulk soil) <sup>-1</sup>	0 to 2 cm	11.9±0.9 a	14.5±1.4 a	13.7±1.5 a	0.2±0.0	1.3±0.2 a	6.4±0.7 a
	2 to 5 cm	11.1±1.2 ab	12.9±1.4 b*	11.2±1.0 b*	0.1±0.0	0.9±0.1 b**	5.3±0.6 b**
	5 to 10 cm	9.9±1.4 b*	11.2±2.1 b*	9.9±1.6 b*	0.1±0.0	0.6±0.1 c**	4.4±0.4 c**
	10 to 20 cm	8.5±1.0 b*	9.5±2.2 b**	5.8±0.9 c**	0.1±0.0	0.4±0.1 d**	2.8±0.4 d**

## 5.2 Changing composition of SOM fractions with depth

In Figure 23 the  $^{13}\text{C}$ -CPMAS NMR spectra of the SOM fractions of lysimeter #1 are given exemplarily for the set of the spectra obtained, relative intensities of the integrated shift regions are given in Table 12. From the initial litter to the fPOM of the 0–2 cm layer the O/N-alkyl C intensities decreased significantly ( $p < 0.01$ ), while the content of alkyl C increased ( $p < 0.01$ , Table 12). The trend of increasing alkyl / O/N-alkyl C ratios of the fPOM fraction continued throughout the topmost 10 cm with significant higher ( $p < 0.01$ ) ratios in the 5–10 cm layer. Increasing alkyl / O/N-alkyl C ratios with depth were also detected for the oPOM for the upper 10 cm. A remarkable increase was observed for the alkyl C from the fPOM to the oPOM and oPOM<sub>small</sub>. With a relative intensity of alkyl C of  $52.7 \pm 1.6\%$  the oPOM<sub>small</sub> showed a very high content of aliphatic structures in the 5–10 cm layer. For the aromatic and carbonyl C contents no clear trend was observed in the soil layers and fractions. Also no depth-dependent trend was observed for the relative intensities of the chemical shift regions of the mineral-bound SOM of the clay fractions. By contrast, the aromatic C intensities of the clay bound SOM showed a slight increase with depth.

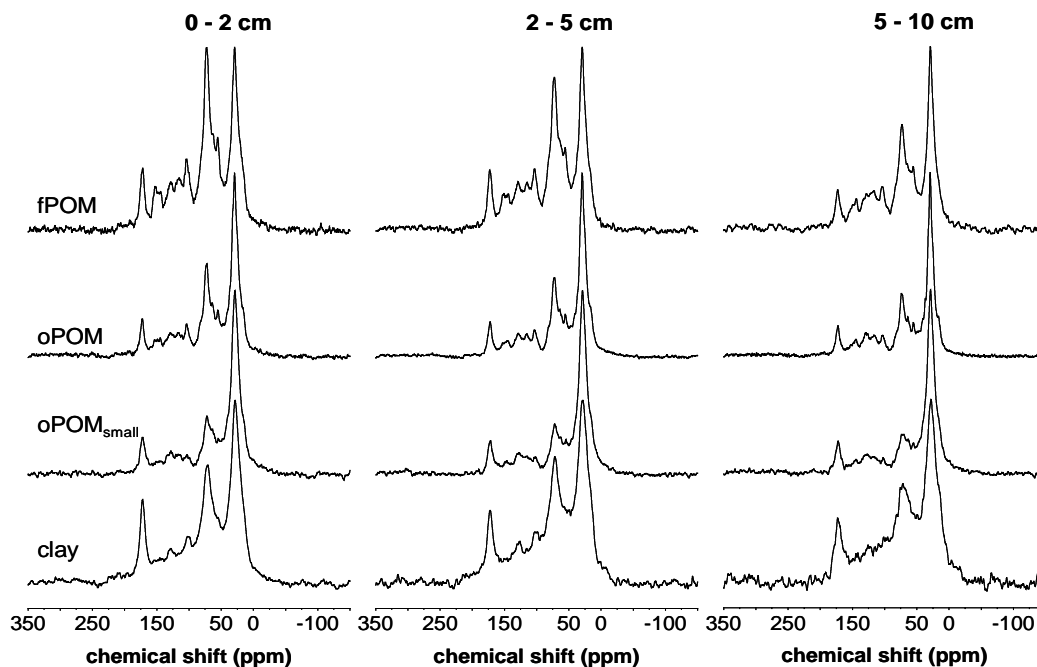


Figure 23  $^{13}\text{C}$ -CPMAS NMR spectra of SOM fractions of the soil layers 0–2 cm, 2–5 cm and 5–10 cm from lysimeter 1.

**Table 12** Relative contents of alkyl C, O/N-alkyl C, aryl C, carbonyl C and alkyl / O/N-alkyl C ratios obtained by <sup>13</sup>C-CPMAS NMR spectroscopy of the litter and the fPOM, oPOM, oPOM<sub>small</sub> and clay fractions of the three uppermost soil layers from the studied lysimeters. Data is given as mean value with standard deviation. Significant differences between single fractions according to depth are indicated by letters and <sup>\*</sup>(*p*<0.05), <sup>\*\*</sup>(*p*<0.01), the litter was tested versus the fPOM of the 0-2 cm layer.

layer	fraction	alkyl C	O/N-alkyl C	aromatic C	carbonyl C	alkyl / O/N-alkyl C
		%	%	%	%	alkyl C
	litter (n = 8)	17.9 ± 1.9 <sup>**</sup>	56.7 ± 4.0 <sup>**</sup>	18.4 ± 2.1	7.0 ± 1.8 <sup>*</sup>	0.32 ± 0.05 <sup>**</sup>
0-2 cm	fPOM (n = 7)	25.7 ± 1.8 a	45.7 ± 2.3 a	19.7 ± 1.2	8.9 ± 1.4	0.56 ± 0.05 a
	oPOM (n = 6)	39.9 ± 3.2 a	34.7 ± 1.0 a	16.8 ± 1.4	8.6 ± 1.8	1.15 ± 0.11 a
	oPOM <sub>small</sub> (n = 4)	47.9 ± 4.5 a	26.7 ± 1.6 a	15.7 ± 1.7	9.7 ± 1.4	1.80 ± 0.29 a
	clay (n = 3)	37.9 ± 3.3	37.4 ± 1.2	13.0 ± 2.5	11.7 ± 1.6	1.01 ± 0.08
2-5 cm	fPOM (n = 6)	28.7 ± 2.8 a	43.5 ± 3.5 a	19.7 ± 1.7	8.1 ± 0.8	0.67 ± 0.11 a
	oPOM (n = 3)	45.8 ± 2.0 b <sup>*</sup>	30.6 ± 1.8 b <sup>*</sup>	15.9 ± 0.2	7.6 ± 0.5	1.50 ± 0.15 b <sup>*</sup>
	oPOM <sub>small</sub> (n = 3)	48.4 ± 2.6 b <sup>*</sup>	25.4 ± 0.3 b <sup>*</sup>	15.8 ± 0.7	10.4 ± 1.8	1.90 ± 0.12 b <sup>*</sup>
	clay (n = 3)	38.1 ± 6.3	37.0 ± 3.4	14.6 ± 3.2	10.3 ± 2.3	1.05 ± 0.28
5-10 cm	fPOM (n = 6)	33.5 ± 2.2 b <sup>**</sup>	35.8 ± 5.1 b <sup>**</sup>	22.0 ± 3.2	8.8 ± 1.3	0.96 ± 0.21 b <sup>**</sup>
	oPOM (n = 4)	46.6 ± 2.9 b <sup>*</sup>	29.3 ± 2.4 b <sup>*</sup>	16.8 ± 2.5	7.3 ± 1.5	1.60 ± 0.17 b <sup>*</sup>
	oPOM <sub>small</sub> (n = 3)	52.7 ± 1.6 b <sup>**</sup>	22.9 ± 0.8 b <sup>**</sup>	15.5 ± 0.8	8.9 ± 1.2	2.08 ± 0.15 b <sup>**</sup>
	clay (n = 3)	33.1 ± 3.5	35.7 ± 0.1	18.9 ± 2.8	12.3 ± 0.5	0.93 ± 0.10

### 5.3 Depth distribution of $^{13}\text{C}$ and $^{15}\text{N}$ signatures of SOM fractions

The  $\delta^{13}\text{C}$  values for the three POM, fine silt and clay fractions are displayed in Table 13. The  $\delta^{13}\text{C}$  values of the oPOM<sub>small</sub> were only significantly different ( $p < 0.01$ ) from the other two POM fractions within the 0–2 cm soil layer. Although it was not significant, a trend of decreasing  $\delta^{13}\text{C}$  values in the order of oPOM<sub>small</sub> to oPOM and fPOM was observed in all soil layers. The  $\delta^{13}\text{C}$  values of the fine silt were significantly lower ( $p < 0.01$ ) than the  $\delta^{13}\text{C}$  values of the clay fractions in all studied soil layers. Only a subtle depth gradient was observed for the  $\delta^{13}\text{C}$  values for particulate and mineral-bound SOM, leading to lower values for the POM and higher values for the mineral bound SOM.

**Table 13**  $\delta^{13}\text{C}$  values (vs. V-PDB) of the three POM fractions (fPOM, oPOM and oPOM<sub>small</sub>) and the fine silt and clay fractions from the studied lysimeters. Data is given as mean values with standard deviations ( $n = 8$ ), significant differences between different soil layers of a single SOM or particle size fraction are indicated by letters and \* ( $p < 0.05$ ) and \*\* ( $p < 0.01$ ).

depth cm	fraction; $\delta^{13}\text{C}$ vs. V-PDB (‰)				
	fPOM	oPOM	oPOM <sub>small</sub>	fine silt	clay
0 to 2	-28.7±0.1 a	-28.9±0.2	-27.9±0.3 a	-27.7±0.2 a	-26.7±0.2 a
2 to 5	-28.6±0.3 a	-29.0±0.1	-28.1±0.3 a	-27.5±0.1 a	-26.4±0.1 b*
5 to 10	-29.0±0.2 b*	-29.0±0.1	-28.1±0.7 a	-27.4±0.2 a	-26.4±0.1 b*
10 to 20	-29.0±0.3 b*	-28.8±0.9	-29.0±0.2 b**	-26.3±0.4 b**	-25.6±0.2 c**

The  $\delta^{15}\text{N}$  values of the SOM fractions of the studied soil layers are displayed in Figure 24. The natural abundance  $\delta^{15}\text{N}$  values of the control lysimeters increased with depth and from POM to mineral bound fractions. A high variability of the  $\delta^{15}\text{N}$  values was found for the SOM fractions of the labelled lysimeters compared to the control. Four months after label application, significantly higher  $^{15}\text{N}$  concentrations ( $p < 0.05$ ) of the POM fractions could be found in the topmost layer of 0–2 cm of the labelled lysimeters compared to the control. A significant enrichment ( $p < 0.05$ ) was detected for the fPOM and oPOM<sub>small</sub> fractions of the soil layer of 2–5 cm. Within the 5–10 cm layer a clear trend of enrichment was found for fPOM and oPOM. A variable enrichment in  $^{15}\text{N}$  (0.1‰ to 4.4‰  $\delta^{15}\text{N}$  vs. air) was observed for the oPOM<sub>small</sub> within the 10–20 cm layer. Besides the oPOM, no SOM fraction showed a significant enrichment in the 10–20 cm layer. Besides the small increase in  $^{15}\text{N}$  values in the

fine silt and clay of the 0–2 cm layer, no enrichment was found in the mineral fractions. A similar pattern as for the  $^{15}\text{N}$  concentrations was observed for the atom%  $^{15}\text{N}$  excess of the labelled SOM fractions (Table 14). A clear trend of increased  $^{15}\text{N}$  excess due to the labelling could be shown for fPOM and oPOM fractions. The largest  $^{15}\text{N}$  excess was shown for the oPOM fractions. The oPOM<sub>small</sub> and the mineral fractions only showed a pronounced atom%  $^{15}\text{N}$  excess in the 0-2 cm layer. For the mineral bound N of the fine silt and clay, the atom%  $^{15}\text{N}$  excess was at reasonable detection limit between 5 to 20 cm depth.

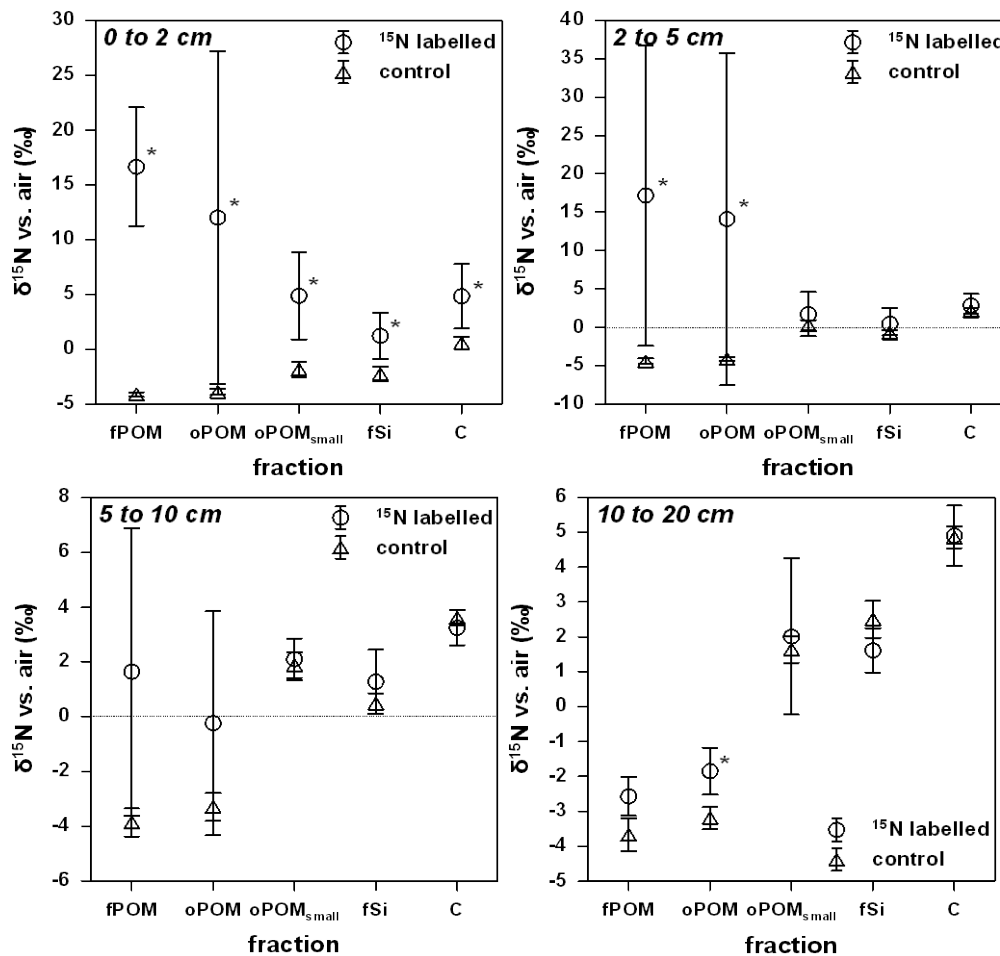


**Figure 24**  $^{15}\text{N}$  abundances expressed as  $\delta$  values vs. air of SOM fractions in control lysimeters and lysimeters treated with  $^{15}\text{N}$ -labelled beech litter. Data points are the mean of 4 replicates with error bars representing standard deviations. Significant differences between  $^{15}\text{N}$  labelled and control lysimeters are shown by  $*(p < 0.05)$ . fSi, fine silt; C, clay.



**Table 14 Atom%  $^{15}\text{N}$  excess of the SOM fractions, calculated as difference between atom%  $^{15}\text{N}$  of SOM fractions from labelled and control lysimeters. Standard error is given in parentheses.**

depth cm	fraction; atom% $^{15}\text{N}$ excess				
	fPOM	oPOM	oPOM <sub>small</sub>	fine silt	clay
0 to 2	0.0065 (0.0013)	0.0058 (0.0025)	0.0023 (0.0007)	0.0013 (0.0004)	0.0016 (0.0008)
2 to 5	0.0026 (0.0057)	0.0067 (0.0035)	0.0005 (0.0005)	0.0007 (0.0003)	0.0002 (0.0024)
5 to 10	-0.0027 (0.0044)	0.0029 (0.0021)	0.0008 (0.0005)	0.0000 (0.0003)	-0.0001 (0.0023)
10 to 20	0.0004 (0.0001)	0.0005 (0.0004)	-0.0037 (0.0013)	-0.0002 (0.0003)	0.0001 (0.0002)

#### 5.4 Vertical differentiation of SOM 4 years after soil homogenisation

Due to the equal mass distribution of the particle size fractions (sand, silt and clay) among the lysimeters (Table 2) it can be assumed that the eight studied pedons were still homogeneous 4 years after the start of the experiment. The assumed homogeneity of the eight lysimeters is supported by GAYLER et al. (2009), who could show a high conformity of soil properties among the studied eight soil systems. The pH values within the topmost 20 cm also showed no development of a depth gradient (Table 2). Nevertheless, the depth gradient of the amount of the POM fractions clearly implied an ongoing soil evolution over the experiment duration. The clear decrease in the mass of fPOM indicated the beginning development of a depth gradient of free SOM particles. From the initial litter to the fPOM within the 0–2 cm layer no significant decrease in C/N ratios was observed.

The amount and the composition of occluded SOM depend on the extent and the turnover of soil aggregates (SIX et al., 2002). From the significant decrease of the mass of the two oPOM fractions (oPOM, oPOM<sub>small</sub>) with depth, a fast aggregate turnover can be assumed. This is supported by the high decomposition degrees revealed by  $^{13}\text{C}$ -NMR (alkyl / O/N-alkyl C in Table 12) of the occluded SOM particles. The clear dominance of highly aliphatic C structures within the oPOM fractions is assumed to result from favourable decomposition conditions accompanied by a rapid aggregate turnover. This process led to a pronounced decomposition of compounds rich in O/N-alkyl C. Due to the spatial inaccessibility of the oPOM for microbial decay, soils with slower aggregate turnover show lower alkyl C contents (GOLCHIN et al., 1994). The given assumption is also supported by the significant decrease in C which is attributed to the oPOM fractions in relation to bulk soil (Figure 22). The increase of

the decomposition degree with depth for the three POM fractions shown by the increasing alkyl / O/N-alkyl C ratios (Table 12) is corroborated by the increasing C/N ratios. From the initial litter to both oPOM fractions a distinctive increase in the C/N ratios took place. The relative increase in long-chain aliphatic structures (alkyl C) and the decomposition of O/N-alkyl-dominated SOM is accompanied by a relative decrease in N (Table 11). The increase of the C/N ratios of the single POM fractions with depth was explained by the increased contents of aliphatic C with concomitant decreasing N contents. The assessment of the decomposition degree for the studied SOM fractions exclusively by C/N ratios would have led to wrong assumptions.

Although the decrease in aromatic C represents only a trend (Table 12), an obvious decrease of the peaks at 115, 128 and 152 ppm (Figure 23 and Table 12) was detected. The decrease in aromatic C was in the range reported for the decomposition of pine needles by PARFITT and NEWMAN (2000). The mineral-bound SOM dominated both the C and N storage. The increasing dominance in C storage of the clay-bound SOM (Figure 22) also demonstrated the starting development of the natural shift from particulate C to mineral-bound C with depth. For undisturbed soils this shift towards a dominance of mineral-bound SOM with depth was already documented (EUSTERHUES et al., 2003). For the studied soils an accelerated SOM decomposition can be assumed due to the drastic disturbance by homogenisation at the start of the experiment. Also in field studies it could be shown that ploughing and therefore soil disruption and homogenisation led to similar effects on labile C pools (GRANDY and ROBERTSON, 2007; OORTS et al., 2007). The new C input of the young beech trees and the accelerated decomposition of old SOM may have counteracted in the studied soils. The high standard deviation of the POM-related properties demonstrated the wide range of differentiation of SOM after topsoil homogenisation, e.g. after ploughing. This led to the assumption that the beginning development of heterogeneous soil profiles was observed, comparable to the heterogeneity of natural soil systems.

### 5.5 Forming of depth gradients of $^{13}\text{C}$ and $^{15}\text{N}$ after soil homogenisation

The  $\delta^{13}\text{C}$  values of the POM fractions indicated only subtle but significant depth gradients for the lysimeter soils. An increase of  $\delta^{13}\text{C}$  values was observed for the mineral-bound SOM in the 10–20 cm layer in relation to the upper 10 cm. This

increase is in accordance with other reported depth profiles of  $^{13}\text{C}$  (WYNN et al., 2006). By isotopic studies on permanent grasslands, ACCOE et al. (2003) could show a reasonable correlation between C decomposition rates and  $\delta^{13}\text{C}$  values for the upper 20 cm. On the contrary KRAMER et al. (2003) found no clear trend for  $\delta^{13}\text{C}$  values in relation to the decomposition degree measured as aliphaticity of the SOM. In the studied soil the POM fractions mainly influenced by litter input and aggregate turnover showed no clear vertical isotopic fractionation. The mineral-bound SOM of deeper soil layers is assumed to be more influenced by an accelerated decomposition due to the initial soil disruption. A lower influence of fresh SOM inputs on mineral bound SOM can be stated for deeper soil layers, as indicated by vertical  $^{13}\text{C}$  enrichment.

For all studied soil layers, an enrichment in  $^{15}\text{N}$  was observed from fPOM to oPOM to mineral bound SOM. A natural enrichment in  $^{15}\text{N}$  takes place by the accumulation of N as mineral bound and recalcitrant N within aggregates (HÖGBERG, 1997). In addition to the found differences between fractions a subtle depth gradient of the  $\delta^{15}\text{N}$  values was also found for every studied SOM fraction of the control (natural abundance  $^{15}\text{N}$ ) and labelled lysimeters. More positive  $^{15}\text{N}$  values for the whole soil in relation to plant and decaying litter was reported before (POERTL et al., 2007). Koba et al. (1998) also found increasing  $\delta^{15}\text{N}$  values for total and inorganic N with depth. Due to the dilution of the upper soil layers with fresh litter having low  $^{15}\text{N}$  contents a depth gradient developed as the residual N became enriched in  $^{15}\text{N}$  with ongoing decomposition (HÖGBERG, 1997). KRAMER et al. (2003) demonstrated a positive relationship between natural abundance  $\delta^{15}\text{N}$  and the degree of aliphaticity and therefore the degree of decomposition. Furthermore the preservation and illuviation of  $^{15}\text{N}$ -enriched material may also have contributed to the enrichment of  $^{15}\text{N}$  with depth (Koba et al., 1998).

The POM fractions of the topmost soil layer of 0–2 cm from the labelled lysimeters showed a predicted decrease in excess  $^{15}\text{N}$  concentrations from free to occluded particles. SWANSTON and MYROLD (1997) also observed the highest  $^{15}\text{N}$  recovery in the topmost soil layers <5 cm and the light fraction, while below 5 cm depth the  $^{15}\text{N}$  recoveries were low and variable. In a decomposition study with  $^{15}\text{N}$  labelled beech litter, after 3 years ZELLER et al. (2000) found 62% of the released N in the surface soil but only 12% below 2 cm. From the given  $^{15}\text{N}$  concentrations a natural incorporation cascade is assumed for this first layer (0–2 cm). The pathway of OM

into the soil matrix of the lysimeters may have been initialised by faunal fragmentation (SETÄLÄ et al., 1996) of partly decomposed litter which were separated as fPOM, and a subsequent occlusion of POM in the form of oPOM and oPOM<sub>small</sub>. This assumption is also supported by the atom% <sup>15</sup>N excess shown in Table 14. For soil from 2–20 cm depth no such clear pattern was observed. An enhanced <sup>15</sup>N enrichment was detected for occluded particles, whereas in the 10–20 cm layer no enhanced <sup>15</sup>N enrichment of the fPOM was found. KÖLBL et al. (2006) explained the high recovery of <sup>15</sup>N labelled material in the oPOM after 161 days by a relatively fast aggregate formation due to the fresh partly decomposed litter additions which promote aggregation. Nevertheless, the <sup>15</sup>N enrichment especially of the POM fractions at the lysimeters showed a very large variability. As C contents and the amounts of SOM fractions were very similar between the lysimeters (Figure 20 and Figure 22) differing aggregate dynamics could not explain this variability. BUCHMANN et al. (1996) could demonstrate the high ability of fungal hyphae for N transport by highly <sup>15</sup>N-enriched fruit bodies of fungi growing on plots with no <sup>15</sup>N addition of a labelling study in *Picea abies* plantations. In the labelled lysimeters of the present study highly enriched ectomycorrhizae with  $\delta^{15}\text{N}$  values of up to 24‰ vs. air for *Tomentella* sp. were found at 0–20 cm depth. Since even more interestingly rhizomorphs of *Tomentella* sp. showed  $\delta^{15}\text{N}$  values of up to 32‰ vs. air (PRITSCH, personal communication), it is assumed that the high <sup>15</sup>N concentrations of the occluded POM fractions are influenced by fungal hyphae which may contribute to POM during fractionation. But also an active contribution of fungal hyphae to the aggregate build-up seems to be reasonable for the studied soil, as fungal hyphae play an important role as binding agents in the development of macroaggregates >250  $\mu\text{m}$  (Six et al., 2004). From these findings an active transport is hypothesised for litter-derived N, but presumably also C by fungal hyphae into inner-aggregate spheres during aggregate build-up. Some indication comes from a sample of *Xerocomus* sp. representing a long-distance exploration type (AGERER, 2001) with extensive rhizomorphs. The fact that  $\delta^{15}\text{N}$  values of 4.01‰ vs. air were found in mycorrhizae of *Xerocomus* even at a depth of 60 cm may indicate mobilisation by hyphae and transport from the litter through rhizomorphs. The extensive mycelium of such species as *Xerocomus* and of course also saprotrophic fungi may provide the structure to distribute C and N in soil. The reciprocal transfer of litter C into soil and soil N into the litter layer was found by FREY et al. (2003), whereas the authors

assumed a preferential fungal transfer of litter derived C into macroaggregates (>250  $\mu\text{m}$ ).

A very high variability of  $\delta^{15}\text{N}$  values was found especially in the enriched POM fractions. The application of whole leaves on top of the soil without artificial incorporation into the soil material, i.e. ploughing, resulted in spatially heterogeneous incorporation degrees of the material. But also fungal mycelia with their locally heterogeneous distribution may influence the transfer of N compounds into the given SOM fractions.

Clear excessive  $\delta^{15}\text{N}$  values of the mineral bound SOM fractions were only found in the 0–2 cm layer. A rapid translocation was not found for  $^{15}\text{N}$  labelled material from fPOM to fine mineral fractions as it was shown by KÖLBL et al. (2006), who found up to 25% of the applied  $^{15}\text{N}$  in clay-sized fractions after 161 days on a cropland. SWANSTON and MYROLD (1997) showed that after 21 months of incubation only one third of the  $^{15}\text{N}$  recovered from labelled red alder leaves were situated in the heavy fraction. Microbial immobilisation as one of the key factors leading to stabilisation of N (HERRMANN and WITTER, 2008) but also C in the mineral associated fractions did therefore only lead to significant  $^{15}\text{N}$  enrichments in the uppermost soil layer. On the short timescale of  $^{15}\text{N}$ -litter exposure within the present study, faunal and fungal mechanisms may have dominated the incorporation mechanisms for the labelled compartments.

## 6. Historic land-use effects on soil organic carbon distribution and composition

Changing management systems affect soils and C sequestration on a long term. Historic alterations in land-use from forest to grassland and cropland to forest were used to determine impacts on C stocks and distribution and SOM characteristics on adjacent Cambisols in Eastern Germany (see page 19). Due to the additional sampling of organic horizons and subsoils, a better prediction of alterations in C stocks and distributions induced by differing land-use was possible in the present work. I aimed to elucidate whether and how historic land-use alterations are reflected by C stocks, C distribution, C allocated to soil fractions (inter- vs. inner-aggregate SOM) and the chemical composition of the SOM on sites differing only in management.

### 6.1 Differences of C and N stocks between land-use systems

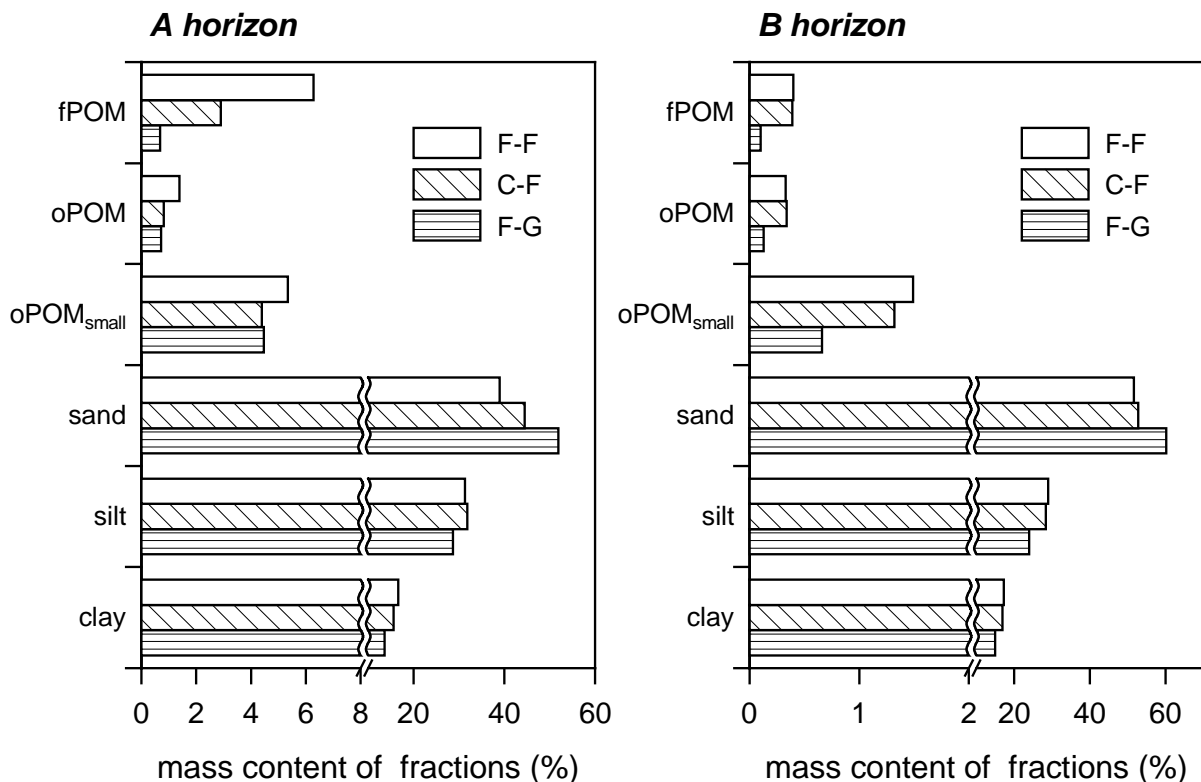
A large amount of C was present in the organic horizons under forest (Table 15). No significant differences were found for the total C stocks of the mineral soils between continuous forest ( $8.3 \text{ kg m}^{-2}$ ) and grassland ( $8.2 \text{ kg m}^{-2}$ ). The C stocks normalized on 1 cm (Table 15) were significantly different ( $p < 0.01$ ) between all three sites and between A and Bw horizons. The lowest normalized C stocks for the A horizons were detected at the former cropland (Table 15). The normalized C stocks of the B horizons showed a clear trend towards lower values under former cropland and grassland (F-F > C-F > F-G). Under grassland the decrease of the normalized C stocks was less pronounced in the Ap horizon (-28%) than in the Bw horizon (-48%) compared with continuous forest. The organic horizons at the former cropland contained less N ( $112.0 \pm 15 \text{ g N m}^{-2}$ ) than under continuous forest ( $127.4 \pm 16 \text{ g N m}^{-2}$ ). The highest N-stocks of the A horizons could be detected under grassland and the lowest at the former cropland (Table 15). A clear trend towards lower N-stocks was shown for the Bw horizons in the order of continuous forest to former cropland and grassland. In contrast to the C stocks, the largest total N-stocks of the mineral horizons were found under grassland (F-F =  $448.2 \text{ g N m}^{-2}$ , C-F =  $437.9 \text{ g N m}^{-2}$ , F-G =  $701.2 \text{ g N m}^{-2}$ ).

Table 15 Carbon, N contents and stocks as mean values (n = 9) with standard deviations from continuous forest (F-F), former cropland (C-F) and grassland (F-G).

site	horizon	C mg g <sup>-1</sup>	N mg g <sup>-1</sup>	C/N	C-stock kg m <sup>-2</sup> normalized on 1 cm thickness	C-stock kg m <sup>-2</sup> normalized on 1 cm thickness	N-stock g m <sup>-2</sup> normalized on 1 cm thickness
F-F	Oe	440.9 ± 38.5	17.8 ± 0.8	24.8 ± 1.2	0.83 ± 0.29	0.45 ± 0.08	33.5 ± 11.5
	Oa	357.5 ± 42.1	17.2 ± 1.0	20.7 ± 1.0	1.95 ± 0.54	0.43 ± 0.08	93.9 ± 26.1
	Ah	90.6 ± 6.9	4.7 ± 0.5	20.0 ± 0.6	2.9 ± 0.4	0.58 ± 0.09	144.2 ± 21.8
	Bw	22.6 ± 3.3	2.4 ± 0.5	17.8 ± 0.8	5.4 ± 0.5	0.19 ± 0.02	304.0 ± 21.7
	Σ				11.1 ± 0.7		575.6 ± 20.8
C-F	Oe	465.8 ± 40.1	21.5 ± 1.6	21.7 ± 1.2	0.80 ± 0.15	0.46 ± 0.14	37.0 ± 6.9
	Oa	443.3 ± 39.5	22.7 ± 1.1	19.5 ± 1.1	1.46 ± 0.47	0.48 ± 0.13	75.0 ± 23.9
	Ap	43.5 ± 9.4	4.5 ± 0.7	18.1 ± 1.1	3.7 ± 0.7	0.31 ± 0.06	205.6 ± 30.8
	Bw	15.2 ± 1.9	1.3 ± 0.2	15.3 ± 0.9	3.6 ± 0.9	0.13 ± 0.03	232.3 ± 53.4
	Σ				9.6 ± 1.7		549.9 ± 75.4
F-G	Ap	52.5 ± 8.5	1.1 ± 0.2	11.6 ± 0.2	6.3 ± 1.2	0.42 ± 0.08	544.0 ± 100.2
	Bw	9.2 ± 1.0	0.8 ± 0.1	12.3 ± 0.6	1.9 ± 0.3	0.10 ± 0.01	157.2 ± 23.5
	Σ				8.2 ± 1.2		701.2 ± 21.7

## 6.2 Distribution and quality of SOM fractions

Clear differences in the mass content of the three POM fractions could be found between the sites (Figure 25), with most distinctive differences in the fPOM fractions. The highest fPOM contents were obtained for soils of the forested sites. For the A horizons, the oPOM and oPOM<sub>small</sub> contents were similar under grassland and former cropland ( $\Sigma[\text{oPOM}, \text{oPOM}_{\text{small}}] = 52.0 \text{ mg g}^{-1}$ ).



**Figure 25** Mass contents of fractions and distribution of organic carbon within soil fractions of bulk soil <2 mm originated from continuous forest (F-F), former cropland (C-F) and grassland (F-G).

Contents of both oPOM fractions decreased in the order of continuous forest to former cropland and grassland in the Bw horizons. The content of clay-sized fractions decreased in the same order in both horizons.

To obtain more detailed and mechanistic information about the C distribution, the C concentrations of the SOM fractions are given in relation to their total mass content (Figure 26). At the continuously forested site, the largest portion of POM related C was found in the fPOM fraction, whereas for the grassland the oPOM<sub>small</sub> showed the largest C content in relation to the bulk soil of the A horizons. The values of the POM fractions from the former cropland were on an intermediate level between the two



other sites. For C situated in the clay fraction, slightly larger values were observed for the former cropland and the grassland. Most of the C within the Bw horizons was present in the clay fractions. The total C present in sand and silt ranged between 12% (C-F, Ap horizon) and 26% (F-G, Bw horizon) in relation to the bulk soils (Figure 26).

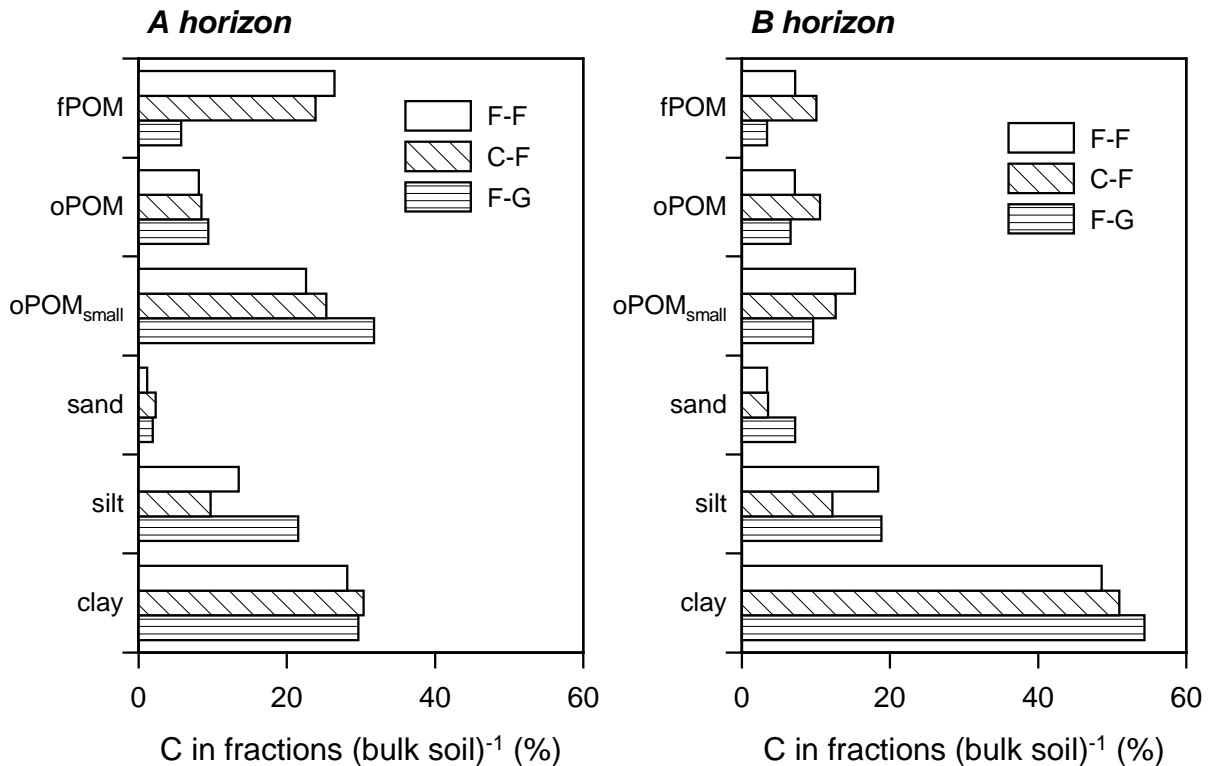


**Figure 26** Distribution of organic carbon within soil fractions of bulk soil <2 mm originated from continuous forest (F-F), former cropland (C-F) and grassland (F-G).

The total C stocks of the single SOM fractions normalized on 1 cm thickness of horizon are given in Figure 27. The lowest C stocks of the occluded SOM, silt and sand in the A horizons were found at the former cropland. The largest C stocks of the POM fractions within the Bw horizons were found under forest, whereas a clear decrease of mineral-bound C stocks was observed in the order of continuous forest to former cropland and grassland.

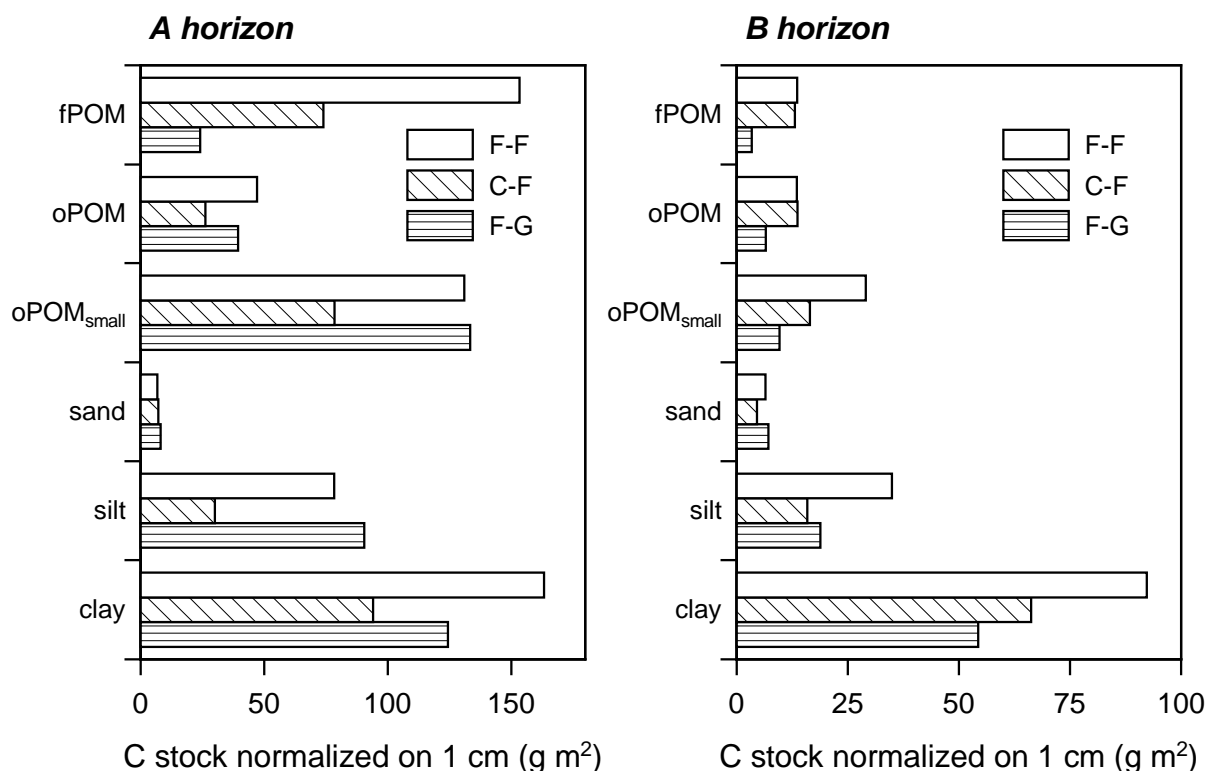


**Figure 27** Total C stocks within soil fractions normalized on 1 cm thickness of horizon for the continuous forest (F-F), former cropland (C-F) and grassland (F-G).

### 6.3 Chemical composition of SOM fractions under different land-use

Major resonances of the measured bulk soils and fractions showed differing intensities in the NMR spectra, with peaks centred around 27 to 30, 55 to 57, 70 to 73, 100 to 105, 115, 125 to 129, 148 to 151, 170 to 175 and 201 to 205 ppm (Figure 28). The signal between 27 and 30 ppm is typical for methylene C from lipids and aliphatic biopolymers such as suberin and cutin (KÖGEL-KNABNER, 2002). Signals around 72 and 103 ppm and the shoulders around 65 and 80 to 90 ppm arise mainly from cellulose and hemicellulose (KÖGEL-KNABNER, 1997; PRESTON et al., 1998). The resonances around 56, 130 and 150 ppm are attributed to methoxyl, H-/C-substituted and phenolic C in lignin and tannins. The high relative intensity around 130 ppm for C-substituted aromatic C can mark highly altered lignin structures, but also material which is derived from black C or soot (KÖGEL-KNABNER, 1997). Figure 28 shows the <sup>13</sup>C-CPMAS NMR spectra obtained from the bulk A and B horizons and soil fractions, and Table 16 lists the integrated areas; in Figure 29 the spectra of material from the organic horizons and roots are shown.

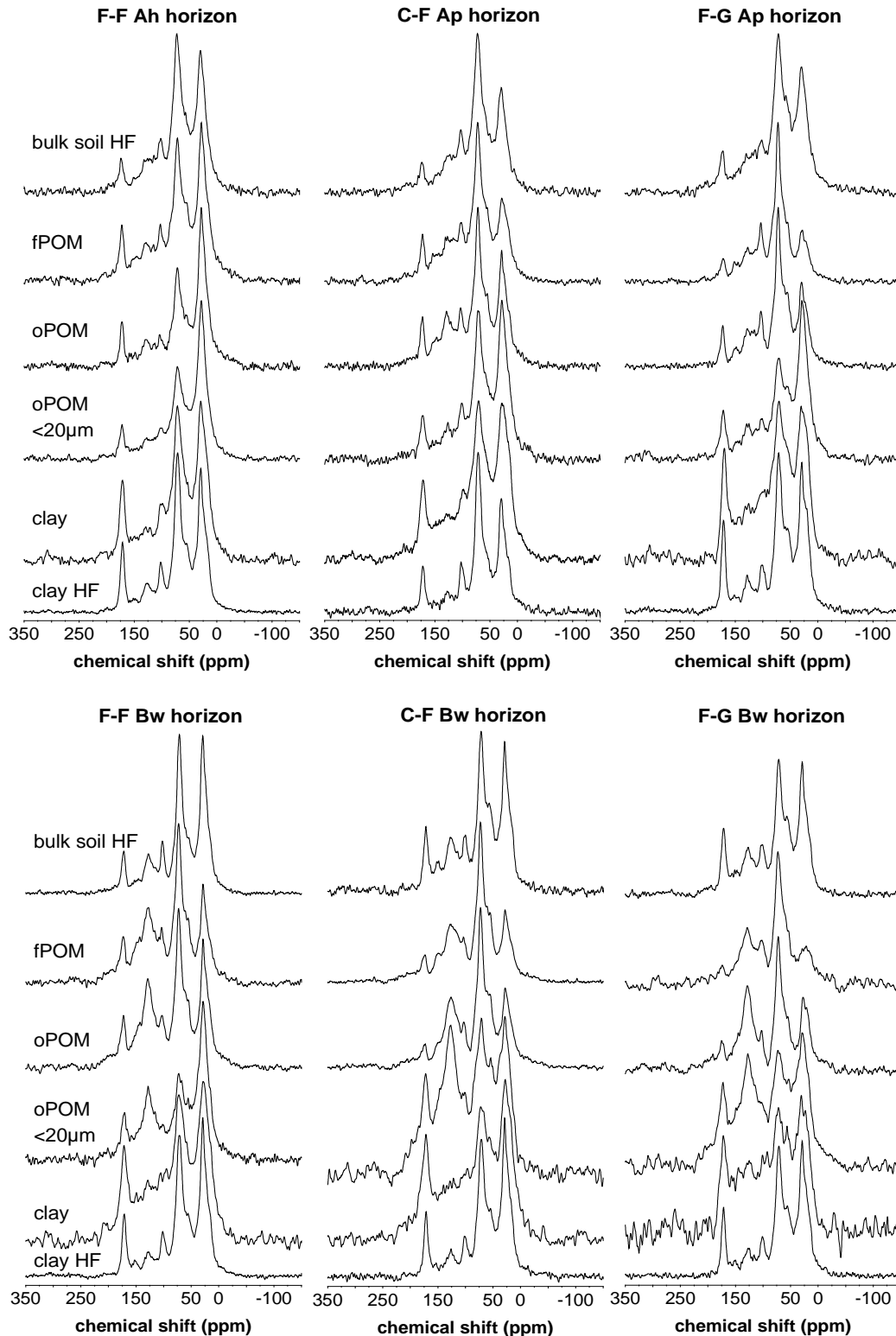


**Figure 28**  $^{13}\text{C}$ -CPMAS-NMR spectra of the bulk soils and SOM fractions from the A and Bw horizons of continuous forest (F-F), former cropland (C-F) and grassland (F-G).

The spectra of the litter samples (Oi) from all three sites showed a major peak in the O/N-alkyl C region (Figure 29). Spruce litter (forested sites) showed higher values in the alkyl C and aromatic C region in contrast to the grass litter (grassland).

Very similar NMR spectra were obtained for the more decomposed Oe and Oa horizons of both forested sites. A distinctive increase in the alkyl C and carbonyl C signals was detected for the Oe and Oa horizons compared with the Oi layer.

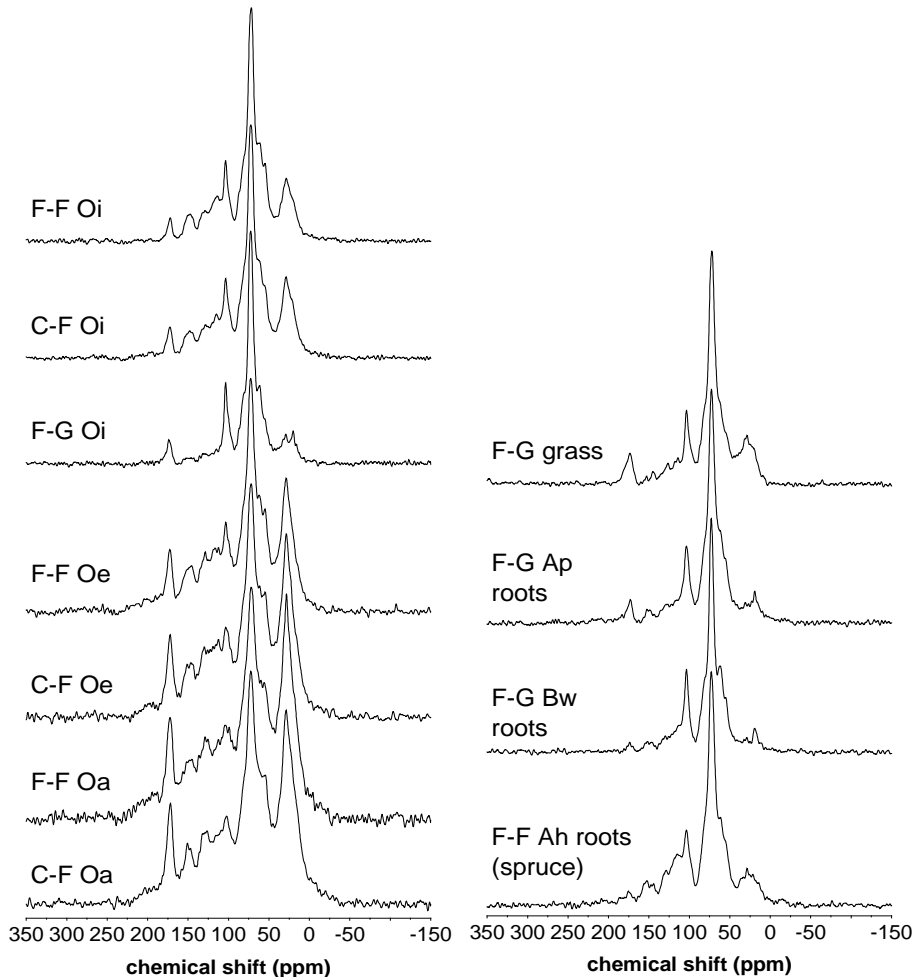


**Figure 29**  $^{13}\text{C}$ -CPMAS-NMR spectra of the organic layers / horizons as well as grass and root samples from the grassland (F-G) and Norway spruce roots from the Ah horizon under continuous forest (F-F).

The spectra of the bulk soil material from the A and B horizons were similar for all sites, except slightly higher signal intensities in the alkyl C region of the samples from the continuous forest (Table 16). A clear trend of decreasing intensities in the alkyl C region and increasing resonances in the O/N-alkyl C region was found for the fPOM in the sequence from continuous forest to former cropland and grassland (Figure 28 and Table 16). Therefore, the spectra of the fPOM from the A horizons were similar to the Oi material under grassland and former cropland. Clear differences between the sites could be detected for the alkyl C and O/N-alkyl C of the fPOM and oPOM from the A horizons. This is well reflected in the decrease of the alkyl / O/N-alkyl C

ratios in the order of continuous forest to former cropland and grassland (Table 16). The lowest O/N-alkyl C contents were found for both horizons in the oPOM<sub>small</sub>. In comparison to the A horizons, very high aromatic C signals (21-29%) were detected in the POM fractions of the B horizons. The highest signal intensities of aromatic C were found in the oPOM of the former cropland and the oPOM<sub>small</sub> of the grassland.

The spectra of the clay fractions after HF treatment were very similar for all sites in both horizons (Figure 28 and Table 16), dominated by alkyl C (44-52%) and O/N-alkyl C (34-38%). Aromatic C (8-10%) and carbonyl C (7-11%) signals were considerably lower. The alkyl / O/N-alkyl C ratios (0.7 to 0.8) were the same before and after HF treatment, whereas the aromatic C / alkyl C ratios decreased from values of around 0.5 to values of around 0.3, due to HF treatment (Table 16). The signals of the O/N-alkyl C region were larger for all samples after HF treatment.

#### 6.4 <sup>14</sup>C abundance of SOM fractions from forest and grassland

Samples from the unaltered continuous forest and the most altered grassland were analysed for <sup>14</sup>C abundance in order to obtain distinctive differences of the radiocarbon data related to different land-use, as given in Table 17. The radiocarbon data showed clear differences between the continuous forest and grassland. The values for bulk soil material of the A horizons at both sites ( $\Delta^{14}\text{C}$  F-F = -15.4‰, F-G = 92.0‰) were higher than in the B horizons ( $\Delta^{14}\text{C}$  F-F = -31.1‰, F-G = -0.4‰), whereas the grassland soils showed a higher content of bomb C. A high incorporation of bomb C was especially observed for the samples of the A horizon from the grassland. In contrast to the continuous forest, the lowest <sup>14</sup>C activity under grassland could be observed for the oPOM fraction in both horizons ( $\Delta^{14}\text{C}$  F-G, Ap = 55.6‰, Bw = -92.9‰), whereas the lowest  $\Delta^{14}\text{C}$  values of the material from continuous forest were observed in the oPOM<sub>small</sub> fraction ( $\Delta^{14}\text{C}$  F-F, Ah = -30.7‰, Bw = -68.6‰). In all cases, the clay fractions showed higher radiocarbon activities than the oldest POM fractions. A trend towards increasing  $\Delta^{14}\text{C}$  values was observed in the order of oPOM < oPOM<sub>small</sub> < clay for both horizons under grassland.

**Table 16 C/N ratios and relative contents of alkyl C, O/N-alkyl C, aryl C, carbonyl C, alkyl / O/N-alkyl C and aromatic / alkyl C ratios of the bulk soils and the SOM fractions as revealed by <sup>13</sup>C-CPMAS NMR spectroscopy for continuous forest (F-F), former cropland (C-F) and grassland (F-G).**

site	sample	C/N	alkyl C	O/N-alkyl C	aromaticC	carbonylC	alkyl C /O/N-alkyl C	aromatic C /alkyl C
<b>A horizon</b>			(%)	(%)	(%)	(%)		
F-F	bulk soil		34	48	12	6	0.71	0.35
	fPOM	20.8	35	43	13	8	0.83	0.37
	oPOM	22.5	44	38	11	7	1.16	0.25
	oPOM <sub>small</sub>	14.6	44	39	9	7	1.13	0.21
	clay	14.3	35	43	11	11	0.81	0.31
	clay HF	15.4	34	47	10	9	0.71	0.3
C-F	bulk soil		27	52	14	7	0.52	0.5
	fPOM	23.9	24	50	17	8	0.48	0.72
	oPOM	24.9	28	47	18	8	0.6	0.64
	oPOM <sub>small</sub>	18.6	37	45	11	7	0.84	0.28
	clay	14.8	31	41	17	12	0.75	0.55
	clay HF	15.4	33	52	8	7	0.63	0.24
F-G	bulk soil		31	48	13	8	0.65	0.42
	fPOM	24	19	58	17	6	0.33	0.87
	oPOM	17.3	25	53	16	6	0.49	0.61
	oPOM <sub>small</sub>	12.5	41	39	12	8	1.04	0.29
	clay	10.8	30	44	16	10	0.69	0.52
	clay HF	11	34	45	10	11	0.75	0.3
<b>Bw horizon</b>								
F-F	bulk soil		37	42	12	9	0.89	0.33
	fPOM	33.5	21	43	25	10	0.49	1.18
	oPOM	30.6	26	40	25	10	0.64	0.96
	oPOM <sub>small</sub>	21.5	37	32	21	10	1.15	0.58
	clay	12.4	32	39	16	13	0.81	0.51
	clay HF	12.3	37	45	9	9	0.83	0.25
C-F	bulk soil		30	44	16	9	0.68	0.54
	fPOM	32.9	20	49	23	8	0.42	1.14
	oPOM	31.6	23	47	24	7	0.48	1.07
	oPOM <sub>small</sub>	15.1	23	35	27	14	0.66	1.18
	clay	11.4	31	37	16	16	0.82	0.53
	clay HF	10.4	38	44	9	9	0.86	0.24
F-G	bulk soil		30	44	16	10	0.69	0.52
	fPOM	43.8	18	50	24	8	0.37	1.29
	oPOM	35	22	40	29	10	0.55	1.31
	oPOM <sub>small</sub>	16.3	26	34	25	14	0.77	0.96
	clay	9.7	28	40	21	12	0.7	0.75
	clay HF	10.2	36	45	10	9	0.81	0.28

**Table 17 Radiocarbon data of bulk soils and SOM fractions from continuous forest (F-F) and grassland (F-G). For the samples with  $\Delta^{14}\text{C}$  values below 0‰ the conventional radiocarbon ages in years before present (1950) are given.**

site	horizon		bulk soil	oPOM	oPOM <sub>small</sub>	clay
F-F	Ah	$\Delta^{14}\text{C}$ (‰)	-15.4±1.3	-9.7±1.5	-30.7±1.3	-27.2±1.3
		age (year BP)	70±15	25±15	195±15	165±15
F-F	Bw	$\Delta^{14}\text{C}$ (‰)	-31.1±1.7	3.5±1.4	-68.6±1.3	-37.7±1.3
		age (year BP)	200±15	modern	515±15	255±15
F-G	Ap	$\Delta^{14}\text{C}$ (‰)	92.0±1.5	55.6±2.1	67.4±1.4	88.9±1.6
		age (year BP)	modern	modern	modern	modern
F-G	Bw	$\Delta^{14}\text{C}$ (‰)	-0.4±1.4	-92.9±1.2	-46.4±1.3	7.9±1.4
		age (year BP)	modern	730±15	325±15	modern

## 6.5 Altered C stocks and distribution due to land-use changes

No clear difference of total C stocks was found between continuous forest and grassland in the mineral soil (Table 15). This contradicts the findings of JOHN et al. (2005) who observed distinctively lower total C stocks in the mineral soil in an 80-year-old Norway spruce forest compared with a grassland established in 1961. GUO and GIFFORD (2002) also showed an increase in soil C by 8% in a global meta analysis, due to conversion from forest to pasture, but primarily in tropical and subtropical ecosystems. The observed difference of the total C stocks (Table 15) between continuous forest and grassland accounted for 2.9 kg m<sup>-2</sup>, representing approximately the amount of C situated in the organic horizons at the forested sites. This finding highlights the important contribution of organic horizons to the amount of C sequestered in acidic forest soils. Although the study was conducted in central Europe, a similar influence of the removal or rebuilding of organic horizons on the C balance is assumed on a global scale. It is assumed that the effects found are applicable to a wide range of forest ecosystems with naturally occurring organic horizons, e.g. a wide range of evergreen forests.

The main reason for the high N stocks under grassland was their periodic fertilisation. The concomitant decrease of the C/N ratios (Table 15) together with higher pH and BS values led to more favourable conditions for decomposition under grassland.

The low normalized C stocks (Table 15) at the former cropland, 77 years after afforestation, did not achieve the specific C stocks of the continuous forest. Defining

the continuous forest as the climax stage of the C accumulation under the given conditions, it is assumed that the former cropland has still not reached a new equilibrium of OM input and output. The lower normalized C stocks of the Ap horizon at the former cropland can also be explained by the delayed OM input resulting from the still ongoing C accumulation in the organic horizons after afforestation of the arable land. This is supported by the lower thickness of the organic horizons on the former cropland compared to the continuous forest. Other studies also found higher C stocks on permanent woodlands 60 to 120 years after afforestation of cultivated land, mainly due to lower C stocks of the organic horizons (COMPTON and BOONE, 2000; WALL and HYTONEN, 2005). Via the specific normalized C stocks (Table 15) it was possible to unravel land-use impacts on C sequestration not only in the topsoil but also in the Bw horizons. In addition to the C stocks, the amount and distribution of SOM fractions entering the mineral soil was also affected by the organic horizons under forest. Using  $^{14}\text{C}$  measurements, BAISDEN et al. (2002) showed that greater than or equal to 90% of fPOM turns over in less than 10 years. In the present study the C located in the fPOM could be ranked as continuous forest to former cropland and the regularly limed grassland for the A horizons. The favourable conditions for decomposition (low C/N, higher pH and BS) under grassland (Table 5) due to liming and faster decomposing plant species, led to higher proportions of occluded C, whereas an accumulation of fPOM was found under forest. A clear relationship was observed between soil properties, such as pH, ECEC and BS, and the distribution and amount of C sequestered in distinctive SOM fractions. FOEREID et al. (2006) also showed that a large part of fPOM was decomposed over a short period after liming on acidic grasslands in Scotland. Large amounts of particulate C were situated within the oPOM<sub>small</sub> fraction of the Ap horizon under grassland. GERZABEK et al. (2006) also showed large C amounts under grassland and arable land within particle size fractions to be situated in the silt sized fraction, mainly present as POM or adsorbed to mineral surfaces as revealed by thermogravimetric analysis. The large C amounts stored in the POM fractions found in the A horizons at my sites disagreed with findings of DEGRYZE et al. (2004), who observed a clear dominance of mineral bound C also in 0-7 cm soil depth under forests and arable lands. Nevertheless, in the Bw horizons, the total C situated in mineral fractions (clay, sand and silt in Figure 2) superimposed that in POM at all three sites. Concomitantly with the vertical decrease in POM related C, the amount of mineral associated SOM increased with soil depth



at all sites. GUGGENBERGER et al. (1995) also showed that conversion from primary forest to arable land and pasture considerably reduced SOM related to POM, but barely affected the mineral bound SOM in silt and clay separates. The normalized C stocks per square meter within soil fractions showed clear differences between the pedons induced by land-use alterations. The mathematical combination of normalized C stocks with the masses of SOM fractions led to even more pronounced differences between the pedons. In the top- and subsoil, the largest amounts of clay bound C per square meter were found under continuous forest. These differences found in mineral bound C exceeded the textural differences between the sites. This reflects the high potential of longer lasting C sequestration within fractions of slower turnover under forest in contrast to that under grassland, e.g. SOM bound on clay surfaces.

## 6.6 SOM composition affected by historic land-use changes

Low decomposition degrees and therefore good bioavailability of fresh SOM particles was shown by a low alkyl / O/N-alkyl C ratio of the fPOM from the Ap horizon under grassland (Table 16). The composition of the fPOM was slightly altered and similar to the composition of the Oi layer and grass material. At the forested sites, decomposition processes in the overlying organic horizons altered the SOM entering the mineral soils, whereas a direct litter input took place at the grassland. For this reason, the radiocarbon activities were higher under grassland than under continuous forest. The radiocarbon activity of the bulk soil and SOM fractions of the Ap horizon pointed to a higher incorporation of bomb C under grassland, indicating also a direct litter input together with more favourable decomposition conditions. SCHÖNING and KÖGEL-KNABNER (2006) suggested a direct influence of the type of forest floor on the radiocarbon age of the A horizons, leading to higher ages under spruce, due to a delayed litter incorporation in comparison with beech forests without organic horizons. Both Oi and fPOM material of the forested sites showed the relative increase in the alkyl C region accompanied by decreasing intensities of the O/N-alkyl C. The increase of alkyl / O/N-alkyl C ratios from 0.3 (F-F - Oi) to 0.6 (F-F - Oa) suggested an increased extent of decomposition in deeper organic horizons (BALDOCK et al., 1997). The fPOM of the A horizons, especially under continuous forest, did not show the signature of the initial litter of the Oi layer (Figure 28 and

Figure 29). Forest clearing and subsequent tillage led to the mentioned direct litter input at the grassland, whereas the influence of historic tillage was concealed at the former cropland, due to the build-up of new organic horizons. The differences in the chemical composition of the fPOM between the study sites contradict the findings of GOLCHIN et al. (1994), who found no distinctive differences in the fPOM between forested and grassland sites. MACDONALD et al. (2007) also found no clear differences, using  $^{13}\text{C}$ -CPMAS NMR between the light fractions of an adjacent pasture and bush land. The oPOM<sub>small</sub> represented the most decomposed SOM fraction as revealed by the highest alkyl / O/N-alkyl C ratios over all sites and horizons. These SOM particles were subject to decomposition over a long time and represented a fraction mainly preserved by chemical recalcitrance and spatial inaccessibility. GOLCHIN et al. (1994) considered the oPOM as an SOM pool that has been accreted within aggregates over decades of root growth. Therefore, the oPOM, especially in the Bw horizons, can be seen as a good indicator for historic land-use before afforestation (former cropland) and deforestation (grassland) at the studied sites.

A large increase in aromatic structures was found in the POM fractions of the Bw horizons in relation to the A horizons at all sites. POM fractions of the Bw horizons showed aromatic C contents of over 20%, whereas the oPOM from grassland (28.8%) and the oPOM<sub>small</sub> from the former cropland (27.5%) showed the highest values, with large peaks around 125 to 129 ppm. Probably the high intensities at the aromatic C shift region are mainly due to the presence of charred plant material, as supported by the similarity to  $^{13}\text{C}$ -CPMAS NMR spectra of mineral soil fractions which were found to be enriched in char obtained by PRESTON et al. (2002). In accordance with the present findings, several authors also showed an enrichment of charred material in oPOM fractions in relation to fPOM fractions (BRODOWSKI et al., 2006; GOLCHIN et al., 1997). BRODOWSKI et al. (2006) also showed higher char contents under grassland than under forest, and suggested charred material to be an active contributor to the formation and stabilisation of microaggregates.

The ratio between aromatic C and alkyl C provided additional information on the components responsible for the chemical recalcitrance of stabilised SOM (Table 16). Indeed the lower decomposability of the aliphatic structures dominated the preserved SOM, as shown by the low aromatic C / alkyl C ratios (oPOM = 0.96, oPOM<sub>small</sub> = 0.58) of the Bw horizon under continuous forest, while the higher content

of aromatic C in relation to aliphatic C ( $\text{oPOM} = 1.31$ ,  $\text{oPOM}_{\text{small}} = 0.96$ ) played a dominant role in the preserved SOM of the Bw horizon under grassland. This was supported by the concomitant increase in the  $\Delta^{14}\text{C}$  values in the order of  $\text{oPOM} < \text{oPOM}_{\text{small}} < \text{clay}$  with increasing aromaticity under grassland. Therefore, the material from the forested site was dominated by younger but more decomposed SOM rich in aliphatic C in contrast to the dominance of older occluded char particles under grassland. The formation and turnover of soil aggregates seemed to be greatly influenced by the amount of charred material under grassland as already suggested by BRODOWSKI et al. (2006), although the  $\Delta^{14}\text{C}$  values were within the range reported for SOM studied on other Cambisols (EUSTERHUES et al., 2007; SCHÖNING and KÖGEL-KNABNER, 2006). A strong influence of historic burning of tree residues since the first settlement (13<sup>th</sup> century) was still visible by the high age of occluded SOM. The prediction of aggregate turnover solely based on  $^{14}\text{C}$  measurements may be biased by accumulated charred material, especially at sites with a high SOM turnover due to favourable decomposition conditions (low C/N, high pH and BS), as were present at my grassland. Nevertheless the charred SOM particles must have been subject to vertical transport as could be shown by the increased aromaticity of SOM fractions in the Bw horizons.

$^{13}\text{C}$ -CPMAS NMR spectra of the clay fractions (Figure 28 and Table 16) pointed to carbohydrates, aliphatics and organic acids as the major HF resistant components associated with clay minerals at my sites. No distinctive differences were obtained for the clay fractions after HF treatment between the sites, probably because management alterations did not influence the composition of presumably older mineral bound SOM at the studied sites. The similar clay mineralogy of the adjacent sites led to the preservation of similar HF resistant SOM compounds. Larger contents of O/N-alkyl C could be shown for the HF resistant SOM in my soils evolved from gneiss, in contrast to the Cambisol studied by EUSTERHUES et al. (2007) evolved from Triassic sandstone. No clear evidence was found for a preferential dissolution of aromatic compounds by HF as stated by EUSTERHUES et al. (2007), who found a stronger dissolution of aromatic compounds due to HF. SCHÖNING et al. (2005a) suggested lower alkyl C and O/N-alkyl C intensities, due to signal suppression by high Fe contents, which might explain the increased intensities in both regions after Fe removal by the HF treatment of my samples (Table 16). This finding is also supported by the relative similarities of alkyl C / O/N alkyl C ratios of the clay fractions

before and after HF treatment (Table 16). No distinctive translocation of old aromatic C into the clay separates was assumed, due to the similar chemical composition and higher radiocarbon activities of the clay fractions at my sites rich in old highly aromatic POM fractions (cp. Figure 28 and Table 17). The positive  $\Delta^{14}\text{C}$  values of the clay fractions from Ap and Bw horizon under grassland indicated a high incorporation of bomb C. Probably at the grassland site the turnover of mineral bound SOM, mainly driven by adsorption and desorption of DOM and microbial residues, occurred on a shorter timescale than that of charred POM compartments with a very low bioavailability.

## 7. Conclusions

The present study provided detailed information about effects of land-use change on the composition and distribution of soil organic matter (SOM) on completely different scales. It helped to better differentiate between short- and long-term processes which lead to stabilisation and destabilisation of SOM pools due to changing management practices, emphasising the importance of soil aggregation for SOM dynamics.

The physical disruption of soil aggregates led to an enhanced release of salt extractable (SEOM) and water extractable OM (WEOM) and to an increased microbial activity. The additionally released CO<sub>2</sub> due to aggregate disruption of the two incubation experiments (+27% and +38%) was mainly due to the increased accessibility of SOM. For soils under field conditions this implicates prolonged larger leaching and mineralisation of dissolved organic matter (DOM) directly after aggregate or plant tissue breakdown, e.g. after soil tillage or freezing-thawing.

A higher release of plant derived sugars was observed after complete disruption of macroaggregates, which may have led to a restart of microbial utilisation of formerly spatial inaccessible SOM particles. During repeated extraction of WEOM, the drastic increase of carbonyl C and aromatic C indicated the restricted SOM bioavailability of intact soils. By this, it was shown that aggregation not only lowers the quantity of soluble SOM but also its quality in terms of decomposability. In the short-term, it was demonstrated that enhanced mineralisation rates after aggregate disruption are closely correlated to the amounts and composition of additionally released DOM.

In a lysimeter study, four years after homogenisation of soil material were sufficient for the development of depth gradients of SOM properties. Although the SOM pools were far from equilibrium, a fast development of depth profiles was shown after severe soil disturbance. Differences between the soil layers could only be detected due to the close soil sampling scheme. Besides the mass distribution of SOM fractions also the chemical composition of the OM showed a clear depth-dependent differentiation. A drastic increase of aliphatic C compounds was observed from initial litter (17.9±1.9%) to occluded particulate organic matter (POM) in deeper soil layers (46.6±2.9% (oPOM) and 52.7±1.6% (oPOM<sub>small</sub>)). The relative accumulation of aliphatic C was also reflected by the increase of C/N ratios from litter to free POM and occluded POM. The evaluation of decomposition degrees solely by C/N ratios

can be biased by the accumulation of N-poor aliphatic compounds. Fungal hyphae are assumed to play an important role in the transport of N compounds into soil aggregates. This was proven by a high recovery of the  $^{15}\text{N}$  tracer in fungal hyphae down to 60 cm depth originating from the applied  $^{15}\text{N}$  labelled beech litter on top of the soils.

In the present study it could clearly be demonstrated that selective sampling of soil horizons can severely deteriorate predictions of the development of vertical differentiation of SOM properties. Especially after land-use changes and soil disturbances the knowledge about the reforming processes and dynamics of SOM fractions is crucial for the prediction of future C and N sequestration in managed soils.

The removal of organic horizons after conversion of forest to grassland, led to markedly lower total C stocks. Due to the transformation processes of the litter derived OM within the organic horizons under forest, these layers clearly contributed to the chemical quality and the amounts of SOM reaching the mineral soil as free POM. The ongoing C accumulation within re-growing organic horizons at the former cropland indicate the long lasting influence of land-use alterations, which might also be valid for other secondary forest ecosystems on other soil types.

The relative enrichment of highly altered OM compounds (mainly aliphatic C) within the fPOM fraction contributed significantly to the C stocks under forest. Larger specific C stocks of the clay fraction indicated a longer ranging ability for C sequestration of the continuously forested soils.

Residual char particles were predominantly situated within soil aggregates, suggesting an important contribution to the formation of aggregates. In contrast to the aromatic C structures under grassland, aliphatic C structures dominated the SOM under forest. The high aromaticity of the oPOM fractions was not reflected in the mineral associated SOM of the clay fractions.

Combined studies of SOM stocks and composition including a wide range of time and spatial scales should be extended to a wide range of land-use systems and soil types in order to enable global predictions of C cycling. The study of stabilising mechanisms and fluxes of C and N cycles simultaneously is crucial for further modelling.

---

## 8. References

- Accoe, F., Boeckx, P., Van Cleemput, O., and Hofman, G., 2003. Relationship between soil organic C degradability and the evolution of the delta C-13 signature in profiles under permanent grassland. *Rapid Commun. Mass Spectrom.* **17**, 2591-2596.
- Agerer, R., 2001. Exploration types of ectomycorrhizae - A proposal to classify ectomycorrhizal mycelial systems according to their patterns of differentiation and putative ecological importance. *Mycorrhiza* **11**, 107-114.
- Aita, C., Recous, S., and Angers, D. A., 1997. Short-term kinetics of residual wheat straw C and N under field conditions: Characterization by (CN)-C-13-N-15 tracing and soil particle size fractionation. *European Journal of Soil Science* **48**, 283-294.
- Amelung, W., Cheshire, M. V., and Guggenberger, G., 1996. Determination of neutral and acidic sugars in soil by capillary gas-liquid chromatography after trifluoroacetic acid hydrolysis. *Soil Biol. Biochem.* **28**, 1631-1639.
- Angers, D. A., Recous, S., and Aita, C., 1997. Fate of C and nitrogen in water-stable aggregates during decomposition of <sup>13</sup>C<sup>15</sup>N labelled wheat straw in situ. *European Journal of Soil Science* **48**, 295-300.
- Appel, T., 1998. Non-biomass soil organic N - the substrate for N mineralization flushes following soil drying-rewetting and for organic N rendered CaCl<sub>2</sub>-extractable upon soil drying. *Soil Biol. Biochem.* **30**, 1445-1456.
- Austnes, K. and Vestgarden, L. S., 2008. Prolonged frost increases release of C and N from a montane heathland soil in southern Norway. *Soil Biol. Biochem.* **40**, 2540-2546.
- Baisden, W. T., Amundson, R., Cook, A. C., and Brenner, D. L., 2002. Turnover and storage of C and N in five density fractions from California annual grassland surface soils. *Glob. Biogeochem. Cycle* **16**.

- 
- Baldock, J. A., Oades, J. M., Nelson, P. N., Skene, T. M., Golchin, A., and Clarke, P., 1997. Assessing the extent of decomposition of natural organic materials using solid-state  $^{13}\text{C}$  NMR spectroscopy. *Aust. J. Soil Res.* **35**, 1061-1083.
- Balesdent, J., Besnard, E., Arrouays, D., and Chenu, C., 1998. The dynamics of carbon in particle-size fractions of soil in a forest-cultivation sequence. *Plant and Soil* **201**, 49-57.
- Balesdent, J., Chenu, C., and Balabane, M., 2000. Relationship of soil organic matter dynamics to physical protection and tillage. *Soil Tillage Res.* **53**, 215-230.
- Batjes, N. H., 1998. Mitigation of atmospheric  $\text{CO}_2$  concentrations by increased carbon sequestration in the soil. *Biology and Fertility of Soils* **27**, 230-235.
- Black, G. E. and Fox, A., 1996. Recent progress in the analysis of sugar monomers from complex matrices using chromatography in conjunction with mass spectrometry or stand-alone tandem mass spectrometry. *J. Chromatogr. A* **720**, 51-60.
- Blake, G. R. and Hartge, K. H., 1986. Bulk density. In: Klute, A. (Ed.), *Methods of Soil Analysis Part I. Physical and Mineralogical Methods: Agronomy Monograph no. 9*.
- Blaschke, K., 1966. Die geschichtliche Entwicklung im Osterzgebirge. *Werte der deutschen Heimat* **10**, 187-193.
- Bossuyt, H., Denef, K., Six, J., Frey, S. D., Merckx, R., and Paustian, K., 2001. Influence of microbial populations and residue quality on aggregate stability. *Appl. Soil Ecol.* **16**, 195-208.
- Bradford, M. A., Fierer, N., and Reynolds, J. F., 2008. Soil carbon stocks in experimental mesocosms are dependent on the rate of labile carbon, nitrogen and phosphorus inputs to soils. *Functional Ecology* **22**, 964-974.
- Brodowski, S., John, B., Flessa, H., and Amelung, W., 2006. Aggregate-occluded black carbon in soil. *European Journal of Soil Science* **57**, 539-546.



- 
- Buchmann, N., Gebauer, G., and Schulze, E. D., 1996. Partitioning of N-15-labeled ammonium and nitrate among soil, litter, below- and above-ground biomass of trees and understory in a 15-year-old *Picea abies* plantation. *Biogeochemistry* **33**, 1-23.
- Chantigny, M. H., 2003. Dissolved and water-extractable organic matter in soils: a review on the influence of land use and management practices. *Geoderma* **113**, 357-380.
- Christensen, B. T., 2001. Physical fractionation of soil and structural and functional complexity in organic matter turnover. *European Journal of Soil Science* **52**, 345-353.
- Cole, C. V., Flach, K., Lee, J., Sauerbeck, D., and Stewart, B., 1993. Agricultural sources and sinks of carbon. *Water Air Soil Pollut.* **70**, 111-122.
- Compton, J. E. and Boone, R. D., 2000. Long-term impacts of agriculture on soil carbon and nitrogen in New England forests. *Ecology* **81**, 2314-2330.
- de Neergaard, A. and Gorissen, A., 2004. Carbon allocation to roots, rhizodeposits and soil after pulse labelling: a comparison of white clover (*Trifolium repens* L.) and perennial ryegrass (*Lolium perenne* L.). *Biology and Fertility of Soils* **39**, 228-234.
- DeGryze, S., Six, J., Paustian, K., Morris, S. J., Paul, E. A., and Merckx, R., 2004. Soil organic carbon pool changes following land-use conversions. *Global Change Biology* **10**, 1120-1132.
- Denef, K., Six, J., Bossuyt, H., Frey, S. D., Elliott, E. T., Merckx, R., and Paustian, K., 2001. Influence of dry-wet cycles on the interrelationship between aggregate, particulate organic matter, and microbial community dynamics. *Soil Biol. Biochem.* **33**, 1599-1611.
- Dou, F. G. and Hons, F. M., 2006. Tillage and nitrogen effects on soil organic matter fractions in wheat-based systems. *Soil Science Society of America Journal* **70**, 1896-1905.

- 
- Edwards, A. P. and Bremner, J. M., 1967. Microaggregates in soils. *Journal of Soil Science* **18**, 64-8.
- Ellerbrock, R., Höhn, A., and Gerke, H. H., 2001. FT-IR Studies on soil organic matter from long-term field experiments. In: M., R. R., Ball, B. C., Campbell, C. D., and Watson, C. A. Eds.), *Sustainable management of soil organic matter*. CABI Publishing.
- Eusterhues, K., Rumpel, C., Kleber, M., and Kögel-Knabner, I., 2003. Stabilisation of soil organic matter by interactions with minerals as revealed by mineral dissolution and oxidative degradation. *Org. Geochem.* **34**, 1591 - 1600.
- Eusterhues, K., Rumpel, C., and Kögel-Knabner, I., 2007. Composition and radiocarbon age of HF-resistant soil organic matter in a Podzol and a Cambisol. *Organic Geochemistry* **38**, 1356-1372.
- Fierer, N. and Schimel, J. P., 2003. A proposed mechanism for the pulse in carbon dioxide production commonly observed following the rapid rewetting of a dry soil. *Soil Science Society of America Journal* **67**, 798-805.
- Flessa, H., Amelung, W., Helfrich, M., Wiesenberg, G. L. B., Gleixner, G., Brodowski, S., Rethemeyer, J., Kramer, C., and Grootes, P. M., 2008. Storage and stability of organic matter and fossil carbon in a Luvisol and Phaeozem with continuous maize cropping: A synthesis. *Journal of Plant Nutrition and Soil Science* **171**, 36-51.
- Foereid, B., Dawson, L. A., Johnson, D., and Rangel-Castro, J. I., 2006. Fate of carbon in upland grassland subjected to liming using in situ (CO<sub>2</sub>)-C-13 pulse-labelling. *Plant and Soil* **287**, 301-311.
- Fontaine, S. and Barot, S., 2005. Size and functional diversity of microbe populations control plant persistence and long-term soil carbon accumulation. *Ecology Letters* **8**, 1075-1087.
- Fontaine, S., Barot, S., Barre, P., Bdioui, N., Mary, B., and Rumpel, C., 2007. Stability of organic carbon in deep soil layers controlled by fresh carbon supply. *Nature* **450**, 277-281.

- 
- Frey, S. D., Six, J., and Elliott, E. T., 2003. Reciprocal transfer of carbon and nitrogen by decomposer fungi at the soil-litter interface. *Soil Biol. Biochem.* **35**, 1001-1004.
- Fuller, L. G. and Goh, T. B., 1992. Stability-energy relationships and their application to aggregation studies. *Canadian Journal of Soil Science* **72**, 453-466.
- Gayler, S., Klier, C., Mueller, C. W., Weiss, W., Winkler, J. B., and Priesack, E., 2009. Analysing the role of soil properties, initial biomasses and ozone on observed plant growth variability in a lysimeter study. *Plant and Soil* **accepted**.
- Gerzabek, M. H., Antil, R. S., Kögel-Knabner, I., Knicker, H., Kirchmann, H., and Haberhauer, G., 2006. How are soil use and management reflected by soil organic matter characteristics: a spectroscopic approach. *European Journal of Soil Science* **57**, 485-494.
- Goebel, M. O., Bachmann, J., Woche, S. K., and Fischer, W. R., 2005. Soil wettability, aggregate stability, and the decomposition of soil organic matter. *Geoderma* **128**, 80-93.
- Golchin, A., Baldock, J. A., Clarke, P., Higashi, T., and Oades, J. M., 1997. The effects of vegetation and burning on the chemical composition of soil organic matter of a volcanic ash soil as shown by C-13 NMR spectroscopy .2. Density fractions. *Geoderma* **76**, 175-192.
- Golchin, A., Oades, J. M., Skjemstad, J. O., and Clarke, P., 1994. Study of free and occluded particulate organic matter in soils by solid state <sup>13</sup>C CP/MAS NMR spectroscopy and scanning electron microscopy. *Australian Journal of Soil Research* **32**, 285-309.
- Grandy, A. S. and Robertson, G. P., 2007. Land-use intensity effects on soil organic carbon accumulation rates and mechanisms. *Ecosystems* **10**, 58-73.
- Gregorich, E. G., Kachanoski, R. G., and Voroney, R. P., 1989. Carbon Mineralization in Soil Size Fractions after Various Amounts of Aggregate Disruption. *Journal of Soil Science* **40**, 649-659.

- 
- Guggenberger, G., Zech, W., Haumaier, L., and Christensen, B. T., 1995. Land-Use Effects on the Composition of Organic-Matter in Particle-Size Separates of Soils .2. Cpmas and Solution C-13 Nmr Analysis. *European Journal of Soil Science* **46**, 147-158.
- Guo, L. B. and Gifford, R. M., 2002. Soil carbon stocks and land use change: a meta analysis. *Global Change Biology* **8**, 345-360.
- Haynes, R. J., 1997. Fate and recovery of N-15 derived from grass/clover residues when incorporated into a soil and cropped with spring or winter wheat for two succeeding seasons. *Biology and Fertility of Soils* **25**, 130-135.
- Heinemeyer, O., Insam, H., Kaiser, E. A., and Walenzik, G., 1989. Soil microbial biomass and respiration measurements - an automated technique based on infrared gas-analysis. *Plant and Soil* **116**, 191-195.
- Helfrich, M., Ludwig, B., Buurman, P., and Flessa, H., 2006. Effect of land use on the composition of soil organic matter in density and aggregate fractions as revealed by solid-state C-13 NMR spectroscopy. *Geoderma* **136**, 331-341.
- Helfrich, M., Ludwig, B., Potthoff, M., and Flessa, H., 2008. Effect of litter quality and soil fungi on macroaggregate dynamics and associated partitioning of litter carbon and nitrogen. *Soil Biol. Biochem.* **40**, 1823-1835.
- Herrmann, A. and Witter, E., 2002. Sources of C and N contributing to the flush in mineralization upon freeze-thaw cycles in soils. *Soil Biol. Biochem.* **34**, 1495-1505.
- Herrmann, A. M. and Witter, E., 2008. Predictors of gross N mineralization and immobilization during decomposition of stabilized organic matter in agricultural soil. *European Journal of Soil Science* **59**, 653-664.
- Högberg, P., 1997. Tansley Review No. 95 15N natural abundance in soil-plant systems. *New Phytologist* **137**, 179 - 203.
- Hutchinson, J. J., Campbell, C. A., and Desjardins, R. L., 2007. Some perspectives on carbon sequestration in agriculture. *Agricultural and Forest Meteorology* **142**, 288-302.

- 
- Ingestad, T., Lund, A.-B., 1986. Theory and techniques for steady state mineral nutrition and growth of plants. *Scand. J. Forest Res.* **1**, 439-453.
- Jacobs, A., Rauber, R., and Ludwig, B., 2009. Impact of reduced tillage on carbon and nitrogen storage of two Haplic Luvisols after 40 years. *Soil Tillage Res.* **102**, 158-164.
- Jarecki, M. K. and Lal, R., 2003. Crop management for soil carbon sequestration. *Critical Reviews in Plant Sciences* **22**, 471-502.
- John, B., Yamashita, T., Ludwig, B., and Flessa, H., 2005. Storage of organic carbon in aggregate and density fractions of silty soils under different types of land use. *Geoderma* **128**, 63-79.
- Kaiser, K., Guggenberger, G., Haumaier, L., and Zech, W., 2001. Seasonal variations in the chemical composition of dissolved organic matter in organic forest floor layer leachates of old-growth Scots pine (*Pinus sylvestris* L.) and European beech (*Fagus sylvatica* L.) stands in northeastern Bavaria, Germany. *Biogeochemistry* **55**, 103-143.
- Kaiser, M., Ellerbrock, R. H., and Gerke, H. H., 2007. Long-term effects of crop rotation and fertilization on soil organic matter composition. *European Journal of Soil Science* **58**, 1460-1470.
- Kalbitz, K., Schmerwitz, J., Schwesig, D., Matzner, E., 2003. Biodegradation of soil-derived dissolved organic matter as related to its properties. *Geoderma* **113**, 273 - 291.
- Kalbitz, K., Solinger, S., Park, J. H., Michalzik, B., and Matzner, E., 2000. Controls on the dynamics of dissolved organic matter in soils: A review. *Soil Sci.* **165**, 277-304.
- Kawahigashi, M., Sumida, H., and Yamamoto, K., 2003. Seasonal changes in organic compounds in soil solutions obtained from volcanic ash soils under different land uses. *Geoderma* **113**, 381-396.
- Killham, K., Amato, M., and Ladd, J. N., 1993. Effect of substrate location in soil and soil pore water regime on carbon turnover. *Soil Biol. Biochem.* **25**, 57-62.

- Koba, K., Tokuchi, N., Yoshioka, T., Hobbie, E. A., and Iwatsubo, G., 1998. Natural abundance of nitrogen-15 in a forest soil. *Soil Science Society of America Journal* **62**, 778-781.
- Kögel-Knabner, I., 1997. C-13 and N-15 NMR spectroscopy as a tool in soil organic matter studies. *Geoderma* **80**, 243-270.
- Kögel-Knabner, I., 2002. The macromolecular organic composition of plant and microbial residues as inputs to soil organic matter. *Soil Biol. Biochem.* **34**, 139-162.
- Kögel-Knabner, I., Guggenberger, G., Kleber, M., Kandeler, E., Kalbitz, K., Scheu, S., Eusterhues, K., and Leinweber, P., 2008. Organo-mineral associations in temperate soils: integrating biology, mineralogy, and organic matter chemistry. *Journal of Plant Nutrition and Soil Science* **171**, 61-82.
- Kölbl, A., von Lützow, M., and Kögel-Knabner, I., 2006. Decomposition and distribution of 15N labelled mustard litter (*Sinapis alba*) in physical soil fractions of a cropland with high- and low-yield field areas. *Soil Biology and Biochemistry* **38**, 3292-3302.
- Kramer, M. G., Sollins, P., Sletten, R. S., and Swart, P. K., 2003. N isotope fractionation and measures of organic matter alteration during decomposition. *Ecology* **84**, 2021-2025.
- Langley-Turnbaugh, S. J. and Keirstead, D. R., 2005. Soil properties and land use history: A case study in New Hampshire. *Northeast. Nat* **12**, 391-402.
- Lundquist, E. J., Jackson, L. E., and Scow, K. M., 1999. Wet-dry cycles affect dissolved organic carbon in two California agricultural soils. *Soil Biol. Biochem.* **31**, 1031-1038.
- Macdonald, A. J., Murphy, D. V., Mahieu, N., and Fillery, I. R. P., 2007. Labile soil organic matter pools under a mixed grass/lucerne pasture and adjacent native bush in Western Australia. *Australian Journal of Soil Research* **45**, 333-343.

- 
- Marschner, B. and Bredow, A., 2002. Temperature effects on release and ecologically relevant properties of dissolved organic carbon in sterilised and biologically active soil samples. *Soil Biol. Biochem.* **34**, 459-466.
- North, P. F., 1976. Towards an absolute measurement of soil structural stability using ultrasound. *Journal of Soil Science* **27**, 451-459.
- Oades, J. M., 1984. Soil organic matter and structural stability - mechanisms and implications for management. *Plant and Soil* **76**, 319-337.
- Oorts, K., Bossuyt, H., Labreuche, J., Merckx, R., and Nicolardot, B., 2007. Carbon and nitrogen stocks in relation to organic matter fractions, aggregation and pore size distribution in no-tillage and conventional tillage in northern France. *European Journal of Soil Science* **58**, 248-259.
- Parfitt, R. L. and Newman, R. H., 2000. <sup>13</sup>C NMR study of pine needle decomposition. *Plant and Soil* **219**, 273-278.
- Paustian, K., Collins, H. P., and Paul, E. A., 1997. Management controls on soil carbon. In: Cole, C. V. (Ed.), *Soil organic matter in temperate agroecosystems: long-term experiments in North America*. CRC Press, New York.
- Plante, A. F. and McGill, W. B., 2002. Soil aggregate dynamics and the retention of organic matter in laboratory-incubated soil with differing simulated tillage frequencies. *Soil Tillage Res.* **66**, 79-92.
- Poertl, K., Zechmeister-Boltenstern, S., Wanek, W., Ambus, P., and Berger, T. W., 2007. Natural N-15 abundance of soil N pools and N<sub>2</sub>O reflect the nitrogen dynamics of forest soils. *Plant and Soil* **295**, 79-94.
- Preston, C. M., Trofymow JA, Niu J, and Fyfe CA, 1998. <sup>13</sup>CPMAS-NMR spectroscopy and chemical analysis of coarse woody debris in coastal forests of Vancouver Island. *Forest Ecology and Management* **111**, 51 - 68.
- Preston, C. M., Trofymow, J. A., Niu, J., and Fyfe, C. A., 2002. Harvesting and climate effects on organic matter characteristics in British Columbia coastal forests. *J. Environ. Qual.* **31**, 402-413.

- 
- Reth, S., Seyfarth, M., Gefke, O., and Friedrich, H., 2007. Lysimeter Soil Retriever (LSR) - a new technique for retrieving soil from lysimeters for analysis. *Journal of Plant Nutrition and Soil Science* **170**, 345-346.
- Rumpel, C. and Dignac, M. F., 2006. Chromatographic analysis of monosaccharides in a forest soil profile: Analysis by gas chromatography after trifluoroacetic acid hydrolysis and reduction-acetylation. *Soil Biol. Biochem.* **38**, 1478-1481.
- Sanchez, P. A., Palm, C. A., Szott, L. T., Chuevas, E., and R., L., 1989. Organic input management in tropical agroecosystems. In: Coleman, D. C., Oades, J. M., and Uehara, G. Eds.), *Dynamics of soil organic matter in tropical ecosystems*. NifTAL Project, University of Hawaii.
- Schimel, J. P. and Hättenschwiler, S., 2007. Nitrogen transfer between decomposing leaves of different N status. *Soil Biol. Biochem.* **39**, 1428-1436.
- Schmidt, M. W. I., Knicker, H., Hatcher, P. G., and Kögel-Knabner, I., 1997. Improvement of C-13 and N-15 CPMAS NMR spectra of bulk soils, particle size fractions and organic material by treatment with 10% hydrofluoric acid. *European Journal of Soil Science* **48**, 319-328.
- Schmitt, A., Glaser, B., Borken, W., and Matzner, E., 2008. Repeated freeze-thaw cycles changed organic matter quality in a temperate forest soil. *J. Plant Nutr. Soil Sci.-Z. Pflanzenernahr. Bodenkd.* **171**, 707-718.
- Schöning, I., Knicker, H., and Kögel-Knabner, I., 2005a. Intimate association between O/N-alkyl carbon and iron oxides in clay fractions of forest soils. *Organic Geochemistry* **36**, 1378-1390.
- Schöning, I. and Kögel-Knabner, I., 2006. Chemical composition of young and old carbon pools throughout Cambisol and Luvisol profiles under forests. *Soil Biol. Biochem.* **38**, 2411-2424.
- Schöning, I., Morgenroth, G., and Kögel-Knabner, I., 2005b. O/N-alkyl and alkyl C are stabilised in fine particle size fractions of forest soils. *Biogeochemistry* **73**, 475-497.



- 
- Setälä, H., Marshall, V. G., and Trofymow, J. A., 1996. Influence of body size of soil fauna on litter decomposition and 15N uptake by poplar in a pot trial. *Soil Biology and Biochemistry* **28**, 1661–1675.
- Sexstone, A. J., Revsbech, N. P., Parkin, T. B., and Tiedje, J. M., 1985. Direct measurement of oxygen profiles and denitrification rates in soil aggregates. *Soil Science Society of America Journal* **49**, 645-651.
- Shrestha, B. M., Singh, B. R., Sitaula, B. K., Lal, R., and Bajracharya, R. M., 2007. Soil aggregate- and particle-associated organic carbon under different land uses in Nepal. *Soil Science Society of America Journal* **71**, 1194-1203.
- Simpson, R. T., Frey, S. D., Six, J., and Thiet, R. K., 2004. Preferential accumulation of microbial carbon in aggregate structures of no-tillage soils. *Soil Science Society of America Journal* **68**, 1249-1255.
- Six, J., Bossuyt, H., Degryze, S., and Denef, K., 2004. A history of research on the link between (micro)aggregates, soil biota, and soil organic matter dynamics. *Soil Tillage Res.* **79**, 7-31.
- Six, J., Conant, R. T., Paul, E. A., and Paustian, K., 2002. Stabilization mechanisms of soil organic matter: Implications for C-saturation of soils. *Plant and Soil* **241**, 155-176.
- Six, J., Elliott, E. T., and Paustian, K., 1999. Aggregate and soil organic matter dynamics under conventional and no-tillage systems. *Soil Science Society of America Journal* **63**, 1350-1358.
- Six, J., Elliott, E. T., and Paustian, K., 2000. Soil macroaggregate turnover and microaggregate formation: a mechanism for C sequestration under no-tillage agriculture. *Soil Biol. and Biochem.* **32**, 2099 - 2103.
- Six, J., Elliott, E. T., Paustian, K., and Doran, J. W., 1998. Aggregation and soil organic matter accumulation in cultivated and native grassland soils. *Soil Science Society of America Journal* **62**, 1367-1377.
- Sollins, P., Homann, P., and Caldwell, B. A., 1996. Stabilization and destabilization of soil organic matter: Mechanisms and controls. *Geoderma* **74**, 65-105.

- 
- Spielvogel, S., Prietzel, J., and Kogel-Knabner, I., 2007. Changes of lignin phenols and neutral sugars in different soil types of a high-elevation forest ecosystem 25 years after forest dieback. *Soil Biol. Biochem.* **39**, 655-668.
- Stemmer, M., Gerzabek, M. H., and Kandeler, E., 1998. Organic matter and enzyme activity in particle-size fractions of soils obtained after low-energy sonication. *Soil Biol. Biochem.* **30**, 9-17.
- Strong, D. T., De Wever, H., Merckx, R., and Recous, S., 2004. Spatial location of carbon decomposition in the soil pore system. *European Journal of Soil Science* **55**, 739-750.
- Stuiver, M. and Polach, H. A., 1977. Reporting of C-14 Data - Discussion. *Radiocarbon* **19**, 355-363.
- Swanston, C. W. and Myrold, D. D., 1997. Incorporation of nitrogen from decomposing red alder leaves into plants and soil of a recent clearcut in Oregon. *Can J Forest Res* **27**, 1496-1502.
- Tan, Z., Lal, R., Owens, L., and Izaurrealde, R. C., 2007. Distribution of light and heavy fractions of soil organic carbon as related to land use and tillage practice. *Soil Tillage Res.* **92**, 53-59.
- Tate, K. R., Scott, N. A., Ross, D. J., Parshotam, A., and Claydon, J. J., 2000. Plant effects on soil carbon storage and turnover in a montane beech (*Nothofagus*) forest and adjacent tussock grassland in New Zealand. *Australian Journal of Soil Research* **38**, 685-698.
- Tisdall, J. M. and Oades, J. M., 1982. Organic matter and water-stable aggregates in soils. *Journal of Soil Science* **33**, 141-163.
- Trumbore, S., 2000. Age of soil organic matter and soil respiration: Radiocarbon constraints on belowground C dynamics. *Ecol. Appl.* **10**, 399-411.
- Van Reeuwijk, L. P., 2002. Procedures for soil analysis. 6th ed. *ISRIC, Wageningen, The Netherlands*.

- 
- Van Veen, J. A. and Kuikman, P. J., 1990. Soil structural aspects of decomposition of organic matter by microorganisms. *Biogeochemistry* **11**, 213-233.
- Vance, E. D., Brookes, P. C., and Jenkinson, D. S., 1987. An extraction method for measuring soil microbial biomass C. *Soil Biol. Biochem.* **19**, 703-707.
- von Lützow, M., Kögel-Knabner, I., Ludwig, B., Matzner, E., Flessa, H., Ekschmitt, K., Guggenberger, G., Marschner, B., and Kalbitz, K., 2008. Stabilization mechanisms of organic matter in four temperate soils: Development and application of a conceptual model. *Journal of Plant Nutrition and Soil Science* **171**, 111-124.
- Wall, A. and Hytonen, J., 2005. Soil fertility of afforested arable land compared to continuously forested sites. *Plant and Soil* **275**, 247-260.
- Weishaar, J. L., Aiken, G. R., Bergamaschi, B. A., Fram, M. S., Fujii, R., and Mopper, K., 2003. Evaluation of specific ultraviolet absorbance as an indicator of the chemical composition and reactivity of dissolved organic carbon. *Environmental Science & Technology* **37**, 4702-4708.
- Winkler, J. B., Lang, H., Graf, W., and Munch, J.-C., 2009. Experimental setup on field lysimeters for studying effects of elevated ozone and below-ground pathogen infection on a plant-soil-system of juvenile beech (*Fagus sylvatica* L.). *Plant and Soil* **accepted**.
- Woche, S. K., Goebel, M. O., Kirkham, M. B., Horton, R., Van der Ploeg, R. R., and Bachmann, J., 2005. Contact angle of soils as affected by depth, texture, and land management. *European Journal of Soil Science* **56**, 239-251.
- WRB, I. W. G., 2006. *World reference base for soil resources 2006 - A framework for international classification, correlation and communication*.
- Wu, J. and Brookes, P. C., 2005. The proportional mineralisation of microbial biomass and organic matter caused by air-drying and rewetting of a grassland soil. *Soil Biol. Biochem.* **37**, 507-515.

- Wynn, J. G., Harden, J. W., and Fries, T. L., 2006. Stable carbon isotope depth profiles and soil organic carbon dynamics in the lower Mississippi Basin. *Geoderma* **131**, 89-109.
- Zeller, B., Colin-Belgrand, M., Dambrine, E., Martin, F., and Bottner, P., 2000. Decomposition of N-15-labelled beech litter and fate of nitrogen derived from litter in a beech forest. *Oecologia* **123**, 550-559.
- Zsolnay, A., 1996. Dissolved humus in soil waters. In: Piccolo, A. (Ed.), *Humic Substances in Terrestrial Ecosystems*. Elsevier, Amsterdam.

## 9. Danksagung (Acknowledgements)

Mein besonderer Dank gilt meiner Betreuerin Frau Prof. Dr. Ingrid Kögel-Knabner für die Überlassung der Themen. Vielen Dank für die Freiheit eigene Wege gehen zu dürfen und die Motivation, die ich durch Sie in der zurückliegenden Zeit erfahren durfte. Ein wichtiges Element dabei ist die äußerst produktive Atmosphäre, die ich am Lehrstuhl erlebt habe. Bei Herrn Prof. Dr. Hans Papen und Herrn Prof. Dr. Axel Göttlein bedanke ich mich für die Übernahme des Zweitgutachtens sowie des Vorsitzes der Prüfungskommission.

Bei der Helmholtz Gemeinschaft, dem Bundesministerium für Bildung und Forschung und der Deutschen Forschungsgemeinschaft bedanke ich mich für die Finanzierung der Projekte.

Für die ausgezeichnete und mit besten Wiederfindungen versehene Unterstützung im Labor, ohne die ich wohl noch lange nicht fertig wäre, danke ich Livia Wissing, Maria Greiner, Gabriele Albert, Svetlana Schlund und Horst Fechter. Ohne die glänzenden mündsprachlichen Beziehungen von Josef Fischer zu lokalen Größen der Handwerkskunst wäre wohl so manches Brett ungesägt geblieben. Für die Pannenhilfe bei abgestürzten Rechnern, unmöglichen NMR Software Verbindungen und leeren Druckerpatronen bedanke ich mich bei Elfriede Schuhbauer, Brigitte Eberle und Florian Schmalzl. Mein Dank gilt hier auch all den anderen am Lehrstuhl!

For a huge bunch of great ideas and comments I want to thank Jeff Baldock, who showed me what is important when it comes to incubation and C mineralisation. Ebenso danke ich Herrn Helmut Erlenkeuser für seinen Anteil am Gelingen der Respirationsversuche.

In unermüdlicher Manier hat Rudolf Meier die Unmengen lysimetrischer Bodenfraktionen durch das Garmischer IRMS gejagt, vielen Dank für die hervorragende Zusammenarbeit. Danken möchte ich Nicolas Brüggemann, der bei vielen isotopischen Fragen eine Antwort wusste.

Für alles vom tagelangen Wurzeln ausgraben bis hin zum bunten allgegenwärtigen Lysimeterplan danke ich Gunda Stoelken, Karin Pritsch, Sebastian Gayler, J. Barbro Winkler und Sascha Reth für die Zeit und die Zusammenarbeit an den großen Stahlpöten.

Getting great radiocarbon data within a second and having great conversations about the whole  $^{14}\text{C}$  issue was possible with Xiaomei Xu and Susan Trumbore. Thank you for the fast processing of my samples and for hosting me in Irvine for the short course.

Ganz besonders möchte ich Angelika Kölbl danken, wemgleich sie eigentlich nichts mit meinen Baustellen zu tun hatte, so hatte sie immer ein offenes Ohr für meine vielen verqueren Fragen. Ich danke Heike Knicker, Jörg Prietzel und Peter Schad für all die regen Diskussionen und Hilfestellungen.

Mein Dank geht an Martin Gutsch für seine Führung in die Untiefen der Statistik und der Modelle (und der Curry-Würste). Meinen Mit-Doktoranden Britt Pagels, Josefine Beck, Pascale S. Naumann, Sandra Spielvogel, Alexander Dümig, Andreas Fritzsche, André Hilscher, Markus Steffens und Martin Wiesmeier gilt mein Dank für all die kleinen und großen Hilfen, willkommenen Ablenkungen und Hektoliter Maifestbier.

Dir – Lena – vielen Dank für Deine aufbauende Art und dafür das Du mir immer wieder gezeigt hast, dass es mehr und Wichtigeres gibt als berechnende Naturwissenschaft! Meinen Geschwistern Annett und Jörg danke ich für jahrelange Ermunterung und das geruhsame Erdulden der Macken eines kleinen Bruders. Uta Knappe danke ich für den glykämisch günstigsten Weg aus der Bequemlichkeitszone und die aufputschende Wirkung des Satzes „Du wirst verfolgt“ bei km 15.

Mein größter Dank gilt meinen Eltern Christine und Gotthard – Ihr habt mich all die Jahre unterstützt und habt mir somit all das hier ermöglicht!

Von ganzem Herzen – DANKE!

*Für glänzende Ideen, für all die neuen „Forschungs-Spielplätze“ danke ich Anke Herrmann, Katja Heister, Laura Sánchez García, Françoise Hillion, Gregor Grünz, Kevin Mueller und Marcus Schmid...und natürlich all den anderen...*